Rubidium Frequency Standard

Primer

W.J. Riley
Hamilton Technical Services
Beaufort, SC 29907

Copyright Notice

Rubidium Frequency Standard Primer

10/22/2011

Available from www.lulu.com as ID # 9559425

Hamilton Technical Services
650 Distant Island Drive
Beaufort, SC 29907-1580
USA

Phone: 843-525-6495
Fax: 843-525-0251
E-Mail: bill@wriley.com
Web: www@wriley.com

Cover photograph: Classic Efratom FRK and modern Symmetricom X72 rubidium frequency standards.

About the Author

William J. Riley, Jr.
Proprietor
Hamilton Technical Services
650 Distant Island Drive
Beaufort, SC 29907
Phone: 843-525-6495
Fax: 843-525-0251
E-Mail: bill@wriley.com
Web: www.wriley.com

Mr. Riley has worked in the area of frequency control his entire professional career. He is currently the Proprietor of Hamilton Technical Services, where he provides software and consulting services in that field, including the Stable program for the analysis of frequency stability. Bill collaborates with other experts in the time and frequency community to provide an up-to-date and practical tool for frequency stability analysis that has received wide acceptance within that community. From 1999 to 2004, he was Manager of Rubidium Technology at Symmetricom, Inc. (previously Datum), applying his extensive experience with atomic frequency standards to those products within that organization, including the early development of a chip-scale atomic clock (CSAC). From 1980-1998, Mr. Riley was the Engineering Manager of the Rubidium Department at EG&G (later PerkinElmer and now Excelitas), where his major responsibility was to direct the design of rubidium frequency standards, including high-performance rubidium clocks for the GPS navigational satellite program. Other activities there included the development of several tactical military and commercial rubidium frequency standards. As a Principal Engineer at Harris Corporation, RF Communications Division in 1978-1979, he designed communications frequency synthesizers. From 1962-1978, as a Senior Development Engineer at GenRad, Inc. (previously General Radio), Mr. Riley was responsible for the design of electronic instruments, primarily in the area of frequency control. He has a 1962 BSEE degree from Cornell University and a 1966 MSEE degree from Northeastern University. Mr. Riley holds six patents in the area of frequency control, and has published a number of papers and tutorials in that field. He is a Fellow of the IEEE, and a member of Eta Kappa Nu, the IEEE UFFC Society, and served on the Precise Time and Time Interval (PTTI) Advisory Board. He received the 2000 IEEE International Frequency Control Symposium I.I. Rabi Award for his work on atomic frequency standards and frequency stability analysis, and the 2011 Distinguished PTTI Service Award recognizing outstanding contributions related to PTTI systems.

Dedication

This handbook is dedicated to the memory Herbert P. Stratemeyer, my mentor, who introduced me to the time and frequency field and guided my early professional development. Together, we explored the world of rubidium frequency standards.

Herbert P. Stratemeyer

A Pioneer in Quartz and Atomic Frequency Standards

1931-2001

The frequency control community lost one of its pioneers in the field of quartz oscillators and rubidium atomic clocks when Herbert P. Stratemeyer died on November 20, 2001. Herb was born in 1931 in Mainz, Germany. Although too young to have participated actively in World War II, he nevertheless suffered along with the rest of the civilian population in its later days and aftermath. He received a Diplom Physik degree from the University of Mainz in 1954. During that time, he participated in early single sideband amateur radio experiments with Art Collins and others.

Herb began his career in frequency control in the quartz crystal industry in England. In 1954 he immigrated to the United States to accept a position as a Development Engineer at the General Radio Company in Cambridge Massachusetts. At that time, General Radio was the leading manufacturer of electronic instruments. He worked on quartz frequency standards and quartz crystals for filter applications. His first solid-state oscillator, the Model 1115, set new performance standards for low phase noise. Herb Stratemeyer became a U.S. citizen in 1962.

In the early 1960's, Herb's work turned to atomic clocks, specifically rubidium atomic frequency standards that were just becoming commercially available. Much basic investigation was necessary to develop these devices into practical products, and to devise the processes necessary for manufacturing their lamps and cells. His other contributions included work on frequency synthesizers and quartz crystal measuring systems.

The emphasis on rubidium frequency standards at General Radio soon shifted to military and space units. One such device was the NASA Spacecraft Atomic Timing System (SATS), which was the first rubidium clock developed and qualified for space. Another was the physics package for the Collins AFS-81 ruggedized rubidium frequency standard (RFS) used for many years by the U.S. Navy in the Verdin VLF communications system. Other projects included RFS designs for missile and tactical aircraft applications. Preliminary work was also done on rubidium clocks for the GPS program. Many of those units had performance equal to or better than most such devices today (although they were much larger and more expensive). In particular, the work at General Radio led to the eventual development of the ultra-stable rubidium clocks used in the Block IIR and IIF GPS satellites. Herb retired from General Radio (then GenRad) in 1975, but continued to consult in the field of atomic clocks at EG&G in the early 1980's. During his retirement, he became a computer "guru" in the 1980's and 1990's. His other interests included gunsmithing, hunting and photography.

Herb was an active participant in the frequency control community, regularly attending the Frequency Control Symposium during the Atlantic City era, and contributing to the watershed 1964 IEEE-NASA Symposium on Short-Term Frequency Stability. He was also a loyal IRE/IEEE member.

Throughout his career, Herb was a mentor to the next generation of "clock engineers", sharing both his knowledge and work ethic. Herb was an "engineer's engineer", displaying exceptional technical judgment and keen insight directed toward making things work. He was a man of great intellect with many talents who excelled in whatever he did. He was also a man of great professional and personal integrity who had a positive influence on all the people and programs he worked with. Those of us whose lives he touched will miss him greatly.

Note: This biography, written by the author, appears on the UFFC Memoriam web site.

Table of Contents

Table of Figures

List of Tables

INTRODUCTION

These primer sections introduce the subject of rubidium frequency standards, explain some of the terminology used in describing them, and tell a bit about their history.

Introduction

The rubidium gas cell atomic frequency standard is the most widely used type of atomic clock. Tens of thousands of those devices are manufactured each year and used in applications ranging from commercial telecommunications to global positioning satellites. They are the smallest, lightest, lowest power, least complex, least expensive, and longest lived such devices, offering excellent performance, stability and reliability. They are therefore the device of choice when better stability than a crystal oscillator is needed, providing lower aging, lower temperature sensitivity, faster warm-up, excellent retrace, lower acceleration and tip-over sensitivity, and better radiation tolerance. This primer provides an introduction to those devices, describing their physical basis, design, performance and applications.

Atomic frequency standards are named and distinguished by both the species (atom, ion, or molecule) and the physical structure (method of confinement, preparation, interrogation, and detection) used in their physics package (atomic resonator/discriminator). Three arrangements evolved as particularly effective in the early years of AFS development (1950's), the rubidium gas cell, the cesium beam tube, and the hydrogen maser. Before the availability of spectroscopic lasers, rubidium was the atom of choice for gas cell devices because of its unique ability to use isotopic hyperfine filtering of the pumping light from a Rb lamp. Now that suitable lasers are available, Cs can also be used for gas cells (e.g., CSAC). Cesium was (and still is) the atom of choice for a beam tube because of its single, abundant isotope and relatively high vapor pressure (thallium was once considered because of its lower magnetic sensitivity). Cesium is now the atom of choice by definition of the second. Hydrogen, the "atom with the fewest moving parts", was found to be the best choice for both wall-coated active and passive masers (rubidium has also been used). Today, over 50 years after the first practical atomic clocks, most commercially available units still either the "classic" lamp-pumped Rb gas cell or the magnetically state selected/detected Cs beam tube. Meanwhile, several new technologies (along with the availability of pumping/cooling spectroscopic lasers) have led to significant advances in primary standards (especially Cs and Rb fountains). At the other end of the performance spectrum, CPT and CSAC devices promise much smaller, lower power, lower cost, and more widely used atomic clocks.

Finally, please understand that the operation of atomic clocks does not depend upon radioactivity, and these devices do not present a nuclear radiation hazard. Nor do they depend on any "black magic" for their operation. A successful RFS design does, however, depend on close attention to many details.

Terminology

This primer uses the terms "frequency standard" and "clock" interchangeably even though "clock" implies the inclusion of counting circuits to keep time. One could also make that distinction on the basis of the intended application, or even that a unit runs continuously. A rubidium frequency standard is commonly abbreviated as RFS. We avoid the term "rubidium oscillator" because the Rb reference in an RFS is a passive discriminator that does not actively oscillate. That section of an RFS is commonly called the "physics package". Frequencies are usually expressed as dimensionless fractional frequency, a frequency deviation divided by its nominal value, written as either $1x10^{-11}$ or $1pp10^{11}$.

History

A summary of the early work leading to the development of today's rubidium gas cell atomic frequency standards is shown in Table I.

Table I. Early Contributors to Gas Cell Atomic Clock Technology

Persons	Year	Place	Work
A. Kastler	1950	Paris	Optical pumping
R.H. Dicke	1953	Princeton	Buffer gas
T.R. Carver	1957	Princeton	Microwave detection
H.G. Dehmelt	1957	Univ. Wash	Optical detection
M. Arditi & T.R. Carver	1958	ITT, Princeton	Optical detection, buffer gas effects, TC, light shift, etc.
P.L. Bender, E.C. Beaty & A.R. Chi	1958	NBS	
T.R. Carver & C.O. Alley	1958	Princeton, NBS	Isotopic filtering

References to papers by Bitter on optical pumping to enhance hyperfine state populations [13], Brossel and Kastler on optical pumping and detection [14], Dicke on the use of buffer gas to reduce Doppler broadening [15], and Bender, Beaty and Chi on hyperfine filtering and buffer gas mixtures [17] are included in the Bibliography.

Much of this work was described in papers at the 1958 Frequency Control Symposium. Prototype RFS units soon followed in the early 1960's as reported by Arditi & Carver, Carpenter, Packard & Swartz and others. Commercial units became available from Varian and General Technology soon thereafter. The January 1963 *Proc. IEEE* paper by M. Arditi and T.R. Carver is good overall reference to this early work [42].

The first type of atomic clock still being made today was the cesium beam tube device, based on the early work by Stern and Gerlach and I.I. Rabi. Development of optically-pumped gas cell devices followed later during a period of intense research in the late 1950's, work that can be followed by reading the Frequency Control Proceedings from that era. Robert Dicke's group at Princeton, which included Tom Carver and Carroll Alley, in collaboration with Maurice Arditi at ITT can probably be credited with building the first working devices that closely resemble modern rubidium frequency standards, but concurrent work at NBS also contributed importantly. The combination of optical pumping and detection along with vapor cells containing inert buffer gas, together with the isotopic filtering possible with Rb, led to the realization of the first RFS products in the early 1960's. These were produced by instrumentation companies like Varian, Hewlett Packard, General Radio and Rohde and Schwarz, as well as small aerospace organizations like Space Technology Laboratories, Clauser Technology (later General Technology). The final idea that led to the widespread availability of low cost RFS units was the integrated resonance cell developed by Ernst Jechart who founded Efratom in 1971 [305].

RFS applications gradually evolved from laboratory standards to avionics equipment and then to commercial telecommunications with yearly manufacturing volumes increasing from hundreds to tens of thousands, influenced greatly by the advent of GPS. The combination of a GPS time reference and a small Rb oscillator for short-term stability and holdover is essential to today's telecom networks. Meanwhile, several orders-of-magnitude improvements were realized in high-performance RFS units, particularly at EG&G (later PerkinElmer and Excelitas) for use on-board GPS satellites. The material in this primer comes, in large part, from the evolution of those units.

Today, RFS units are made by several companies in the U.S. and abroad, most with direct links to those early organizations and people. Their development and manufacturing remains the domain of small groups, not their much larger telecom and aerospace users, probably because their specialized nature. I find it ironic that ITT in Nutley, NJ, now the largest user of high performance space Rb clocks, and one of the main spawning grounds of that technology, announced in a 1958 news release a "lightweight atomic clock" as an "aid to space navigation in the future" but then, in 1965, declared "Dr. Arditi's atomic clock research has not been considered by ITT as worthy of continued financial support". He was clearly far ahead of his time.

PHYSICS

These primer sections cover the basic physics of rubidium frequency standards, and the design and implementation of their physics packages. Good general references to the physics of atomic frequency standards are [1], [6] and [9].

Rubidium

Rubidium (Rb) is an alkali element located between potassium and cesium at the left side of the periodic table. It is a soft silvery metal that melts at 39°C and is highly chemically reactive, oxidizing rapidly in air (see Figure 1). Natural rubidium contains two common isotopes, 72% stable ^{85}Rb and 28% slightly radioactive ^{87}Rb, a 0.28 MeV beta emitter whose 5x10^{10} year half-life is longer than the age of the universe.

Figure 1. Rb Ampoule

A rubidium frequency standard contains under a milligram of ^{87}Rb rubidium, and its radioactivity of about 20 pCi is less than that of a banana. No special precautions are needed for shipping or handling it. Rubidium is usually bought in the form of chloride, and isotopically-pure ^{85}RbCl and ^{87}RbCl can be bought from Oak Ridge National Laboratory where it was separated using now-decommissioned WWII era calutrons.

Rubidium is not particularly rare or valuable, and doesn't have much industrial use except as a getter and a dopant in glass. Interestingly it is the 16th most abundant element in the human body, ahead of most other metals. Foods high in Rb include coffee, black tea, fruits and vegetables (especially asparagus), and a typical daily dietary intake is 1-5 mg (more than used in several rubidium frequency standards). It has no negative environmental effects.

Rubidium is easily ionized, and its two strongest Rb optical emission lines are barely visible in the deep red at 780 and 795 nm.

Hyperfine Resonances

Atomic frequency standards use atomic resonances that are based on fundamental properties of nature.

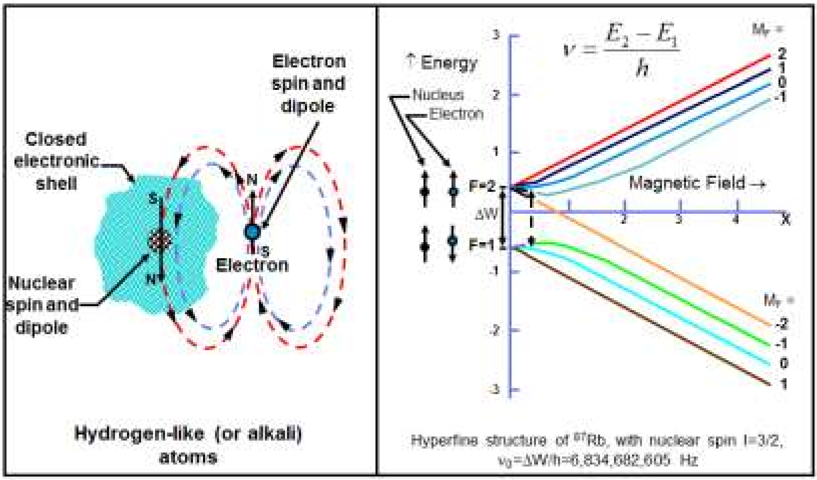

Figure 2. Hyperfine Structure of Alkali Atoms

Most atomic frequency standards use the quantized hyperfine energy level of hydrogen or hydrogen-like (alkali) atoms that have a single electron in their outer shell. The hyperfine structure is the result of the interaction between the electron and nuclear spins (magnetic dipoles) as shown in Figure 2 [355].

The lower-energy F=1 state corresponds to the case where the spins are opposite, and the higher-energy F=2 state where they are aligned. These hyperfine levels are separated by an energy difference corresponding to a microwave frequency (e.g. 6.834.6826109043 GHz for ^{87}Rb). The levels split in the presence of an external magnetic field (the Zeeman effect), and the ΔM_F=0 transitions with first-order (quadratic) field independence are used for clocks (magnetometers use the linearly-dependent ones). The ^{87}Rb energy levels are shown in Figure 3, and in more detail in Figures 4 and 5 [65].

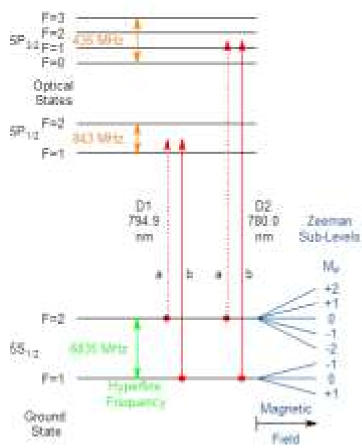

Figure 3. Energy Levels of ^{87}Rb

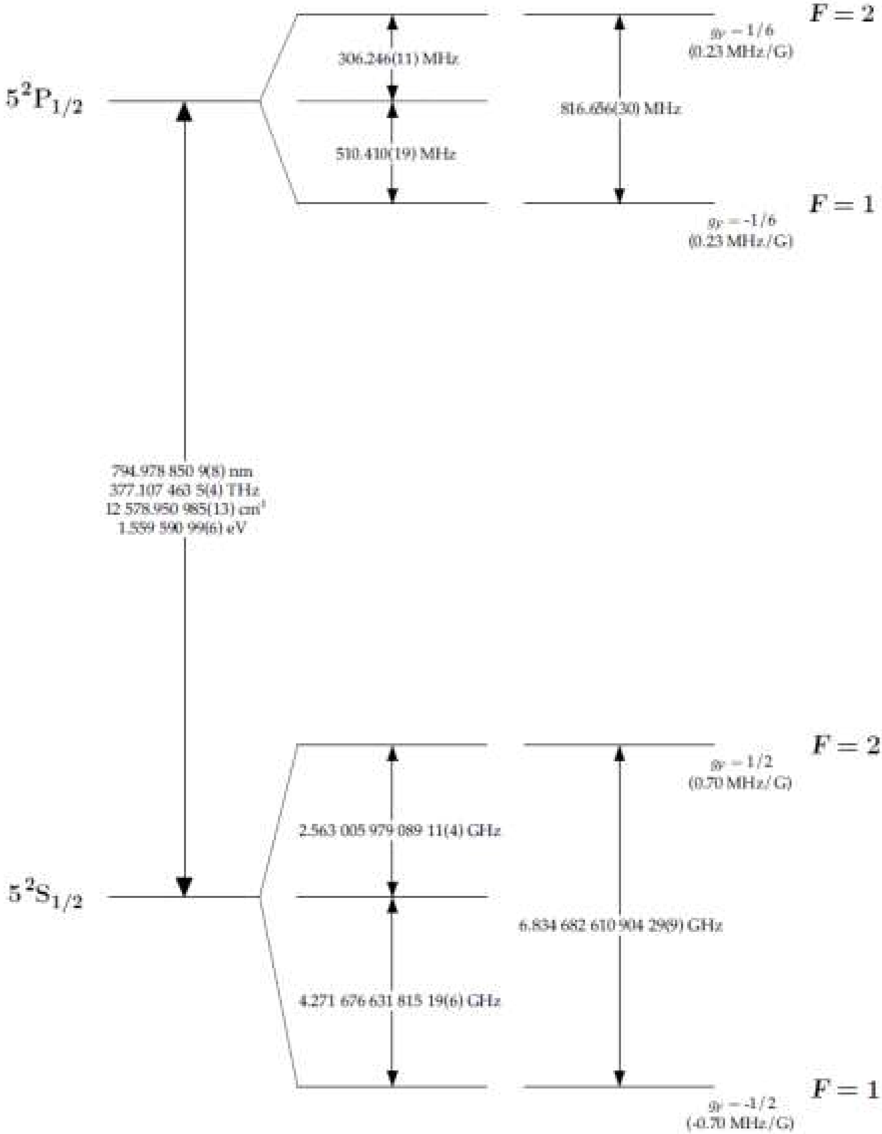

Figure 4. ^{87}Rb D_1 Hyperfine Structure

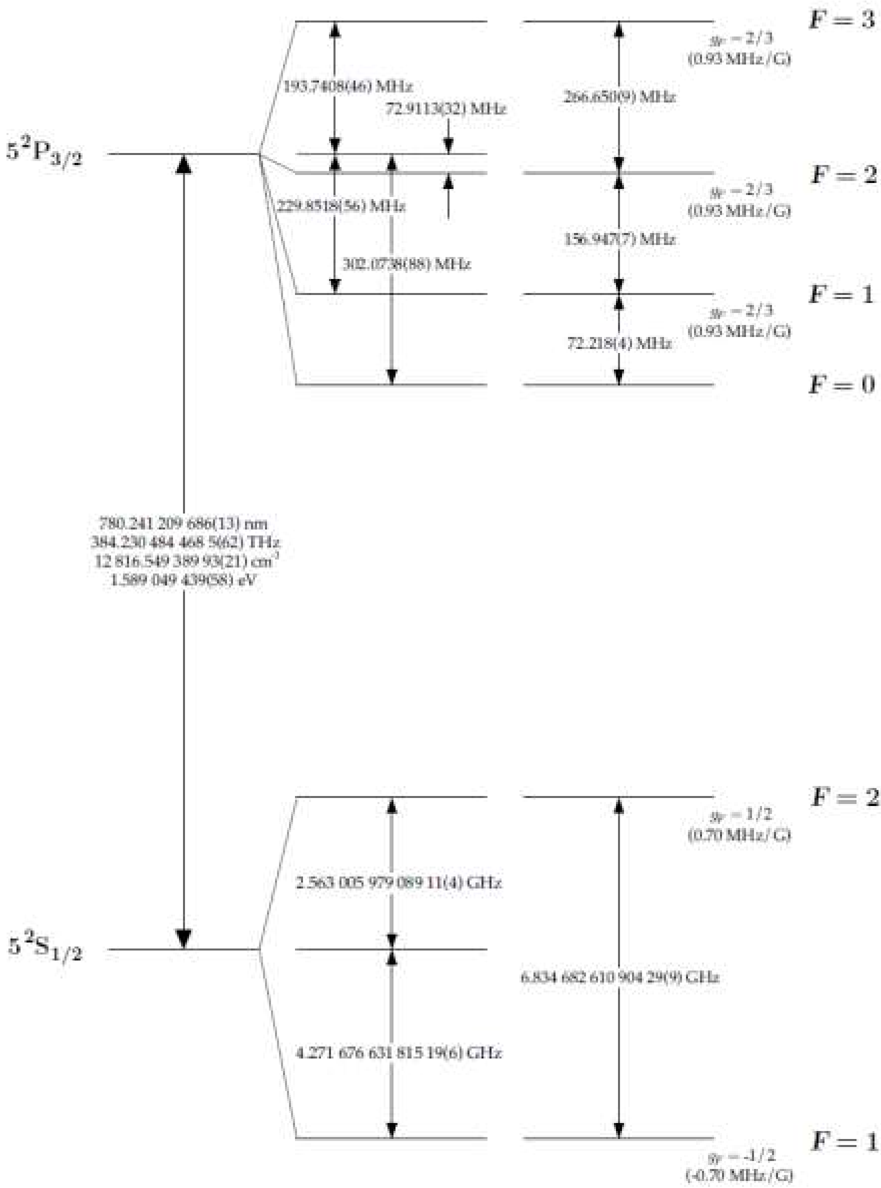

Figure 5. ^{87}Rb D_2 Hyperfine Structure

Optical Pumping

Most rubidium frequency standards use optical pumping by an Rb spectral lamp to create a non-equilibrium population difference between the two ground state hyperfine energy levels. This allows the hyperfine frequency to be measured by interrogating the atoms with microwave radiation and observing the change in light transmission through the cell.

More recently, some rubidium and cesium gas cell atomic frequency standards have used a diode laser for optical pumping. That technique, while offering the possibility of higher signal-to-noise ratio along with smaller size and lower power, has generally been unsuccessful because of noise and reliability problems with the laser diodes, and will not be discussed in detail herein. The reader is encouraged to keep abreast of new developments in this field, however, particularly regarding the use of coherent population trapping (CPT) and pulsed operation.

Optical pumping is one of the basic techniques used for atomic preparation/state selection, and is at the heart of several important atomic frequency standard technologies, including the Rb gas cell, the optically pumped/detected Cs beam tube, the trapped mercury ion standard, the Cs and Rb fountains, and (similar) coherent population trapping. The purpose of optical pumping is to move atoms (or ions) from one energy state to another. This can be done with either spectral lamps (classic Rb gas cell, and trapped Hg ion), or lasers (the others). Here we are considering optical pumping in a lamp pumped Rb gas cell device. In that case, it is desired to move Rb atoms from the lower (F=1) to the upper (F=2) hyperfine ground state by exciting atoms from the lower ground state to an optical state from which they will spontaneously decay to one of the ground states, thus creating a net overpopulation of the upper hyperfine ground level. To accomplish that, it is necessary to selectively apply optical energy at the component labeled “b” in Figure 3 from either or both of the Rb D-lines from a hyperfine-filtered Rb spectral lamp.

Hyperfine Filtration

The efficiency of the optical pumping process is enhanced by a fortuitous overlap between the optical absorption lines of the two naturally-occurring isotopes, ^{85}Rb and ^{87}Rb. This is the main reason that rubidium is used in most (non-laser pumped) gas cell atomic frequency standards. Rubidium is unique in that the ^{85}Rb isotope can serve as a hyperfine filter to remove one of the hyperfine components from the light emitted by an ^{87}Rb spectral lamp as shown in Figure 6.

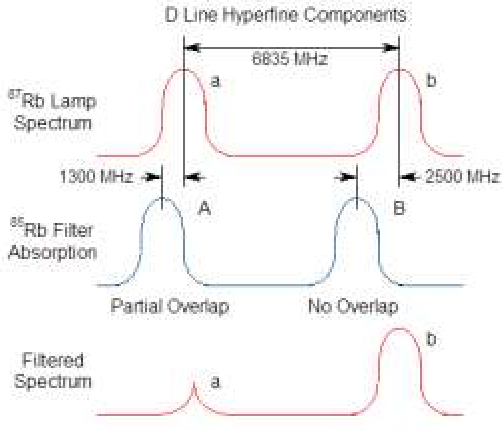

Figure 6. Isotopic Filtering of ^{87}Rb D Lines

In this cartoon figure (see Figure 7 for real spectra), the top plot shows the two hyperfine components in the optical spectrum of one of the ^{87}Rb D-lines. Because both hyperfine components are present at equal intensities, this light would be ineffective for the purpose of optical pumping. The middle plot shows the absorption spectrum of ^{85}Rb gas. Notice that the "a" and "A" components overlap while the "b" and "B" components do not. If the ^{87}Rb lamp spectrum is passed through the ^{85}Rb filter cell, the resulting filtered spectrum is shown in the bottom plot. The desired "b" component is now significantly larger than the "a" component, making the filtered spectrum more effective as an optical pumping source for an ^{87}Rb absorption cell. The filter cell can be separate or integrated with the absorption (resonance) cell by using natural Rb with both isotopes.

The D_1 line hyperfine spectrum of an actual unfiltered (A) and filtered (B) Rb lamp is shown in Figure 7 [120]. For optimum performance considering discriminator signal strength, light shift and temperature coefficient, the desired pumping component (labeled e,f) is only slightly enhanced.

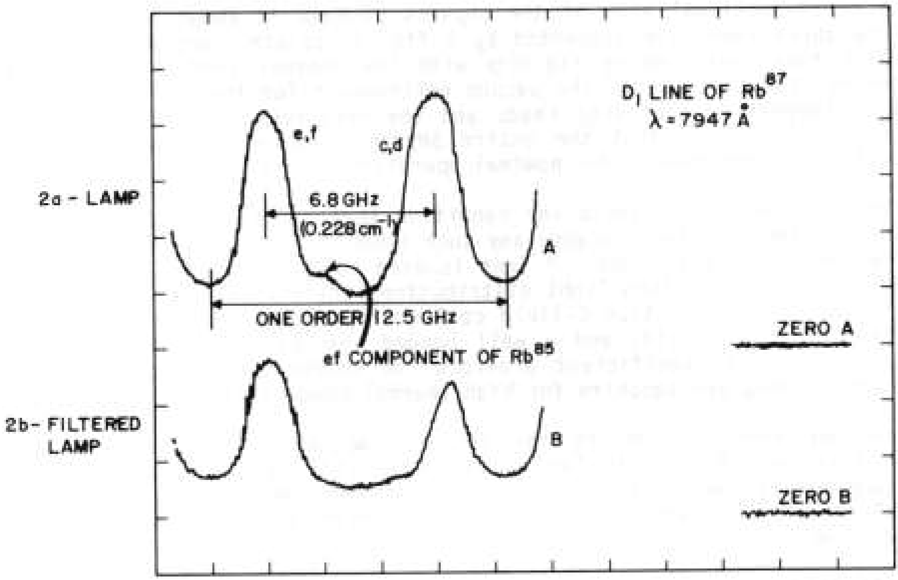

Figure 7. Unfiltered and Filtered Rb Lamp Spectrum

Passive Atomic Frequency Standards

A passive atomic frequency standard (AFS) is the most common type of atomic clock. It uses a crystal oscillator or other frequency source to excite a passive atomic discriminator that produces a correction signal for a frequency control loop to lock the oscillator to the atomic reference. The crystal oscillator provides the stable output frequency.

The other type of atomic clock is the active atomic frequency standard, which is an actual atomic oscillator. The active hydrogen maser is the most common of those, which excels as the atomic frequency source having the best short term stability. A passive device is preferred as a primary (absolute) standard (particularly the beam and fountain devices) because of the ability to evaluate and reduce their bias corrections and accuracy limitations.

Figure 8 shows the basic block diagram of a passive atomic frequency. The crystal oscillator excites the physics package through the RF chain, which synthesizes the nominal atomic frequency. The physics package acts as a passive atomic discriminator to produce an error signal that is processed by the servo amplifier to control the frequency of the crystal oscillator. The overall configuration is that of a frequency lock loop. The discriminator signal is the result of frequency modulation applied to the RF interrogation, which is synchronously detected by the servo amplifier to produce the crystal oscillator control voltage. The crystal oscillator provides the stable output frequency via an output amplifier.

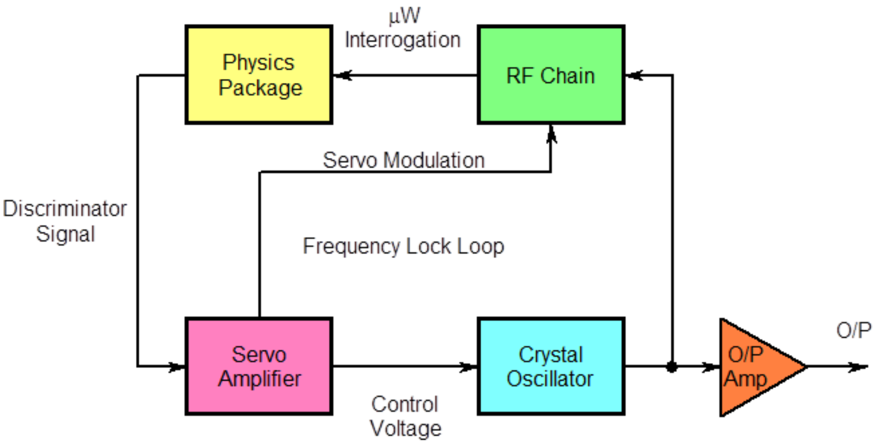

Figure 8. Block Diagram of a Passive Atomic Frequency Standard

Another way to categorize atomic clocks is as primary or secondary (working) standards. Primary standards can reproduce the frequency of their inherent atomic transition with high accuracy, have biases that can be well evaluated and corrected for, and show essentially no frequency drift. Among those are the cesium beam tube (both the classic magnetically selected and newer laser pumped/detected type), the trapped mercury ion, and (most importantly today) the Cs and Rb fountains. Secondary standards need calibration against a primary standard (perhaps via GPS), but can provide high stability thereafter, and are generally more practical (smaller, lighter, lower power, and less expensive). The Rb gas cell clock is, by far, the most commonly used secondary atomic frequency standard, but the chip-scale atomic clock (CSAC) has the potential to be deployed even more widely in the future.

Atomic frequency standards are sometimes used a frequency references along with a crystal oscillator that is loosely or intermittently syntonized (adjusted in frequency) using the atomic reference. This arrangement, a so-called "RbXO", can be effective to reduce average power, to optimize close-in phase noise, to achieve fast warm-up, to improve reliability, or to mitigate problems under transient radiation or vibration.

Rubidium Gas Cell Devices

The general requirements for implementing an atomic frequency standard are (1) confinement, (2) preparation/state selection, (3) interrogation, and (4) detection [2]. In the rubidium gas cell device, confinement is provided by means of a sealed cell containing buffer gas (a non-disorienting wall coating is a seldom-used alternative), state selection is done by optical pumping, interrogation is accomplished by interaction with a microwave field, and detection is implemented by a photodetector that senses the transmitted (or rarely the scattered) light.

Rb Physics Packages

The assembly comprising the atomic frequency reference of an atomic clock is traditionally called a "physics package", and a schematic diagram of a generic RFS physics package is shown in Figure 9.

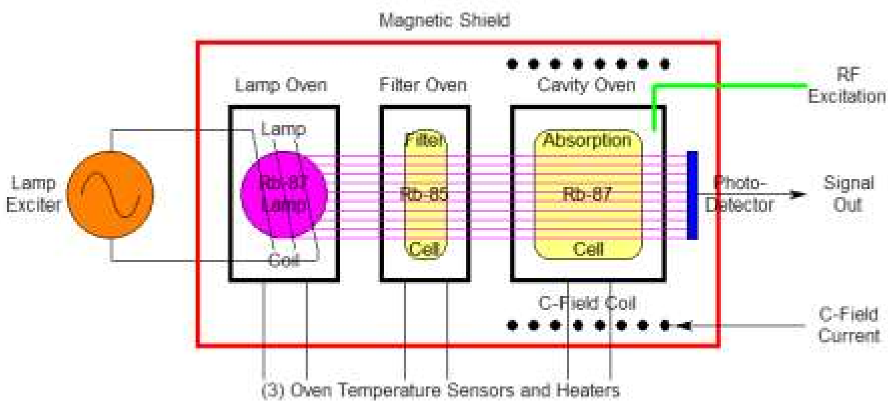

Figure 9. Schematic of a Classic RFS Physics Package

This figure shows the elements of a classic rubidium gas cell physics package. A lamp exciter (RF power oscillator) produces a plasma discharge in a small electrodeless lamp containing ^{87}Rb, possibly mixed with ^{85}Rb in a natural or custom ratio, and an inert buffer gas, usually Xe, sometimes Kr. The output from the lamp passes through a filter cell containing ^{85}Rb and another buffer gas, usually N_2, sometimes Ar or a mixture thereof. The filter cell works as a hyperfine optical filter to improve the optical pumping efficiency. The filtered light then passes through the ^{87}Rb absorption cell, which also contains a buffer gas, usually N_2 or a N_2-Ar mixture, and is located inside a microwave cavity and a C-field coil. The latter makes an axial DC magnetic field to orient the atoms, separate the Zeeman lines, and (perhaps) to make fine frequency adjustments. A silicon photodetector senses the light throughput, producing the output discriminator signal from the physics package, which is surrounded by one or more high-permeability magnetic shields. The light is a minimum when the RF excitation applied to the microwave cavity is at the center of the Rb atomic resonance at ≈ 6.835 GHz. The filter and absorption cells may be separate as shown or combined into a single integrated resonance cell, which contains a (usually natural) mixture of both Rb isotopes. The lamp, filter (if separate), and cavity ovens are temperature-controlled. Many aspects of this general arrangement have been optimized over the years to improve performance, reduce size, and reduce cost. In particular, the details of the cell sizes, cavity mode, isotopic and buffer gas mixtures, and oven operating temperatures can improve S/N ratio and short-term stability, and reduce sensitivity to temperature, light intensity, and RF power changes.

Again, the function of the Rb physics package is to produce a discriminator signal that indicates the frequency of the applied RF excitation. It contains a rubidium lamp, filter cell and absorption cell in their respective temperature-controlled ovens, enclosed inside a magnetic shield. The absorption cell oven is also a 6.835 GHz microwave cavity, and it has a coil to produce a DC magnetic bias field ("C-field"). The RF power oscillator that excites a plasma discharge in the lamp may be within or external to the physics package assembly, while a photodiode detects the light throughput, producing an output signal in response to the applied microwave power.

Rb Discriminator Signal

The Rb signal is generated as a change in the light transmission through the absorption cell in response to the application of resonant µW energy as shown in Figure 10. Optical pumping by the hyperfine-filtered Rb lamp excites atoms from the lower ground state to an optical state, from which they immediately decay to one of the ground states with equal probability, thus creating a higher population in the upper ground state. Equilibrium is restored by the resonant RF, which allows more light to be absorbed, reducing the light transmission.

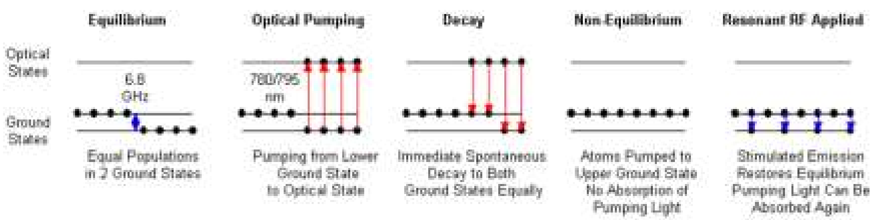

Figure 10. Rb Discriminator Signal

The Rb discriminator signal is the result of a dynamic process of optical pumping and microwave interrogation, which occurs together both spatially and temporally (a so-called "double resonance method"). That process is both simple and effective, producing a higher-energy optical photon for a microwave one, resulting in a high signal-to-noise (S/N) ratio. The disadvantage of this method, however, is that it causes a so-called "light shift" effect that can make the resonant frequency slightly dependent on the light intensity and spectrum. Much effort has been expended to reduce this effect by adjusting the lamp and filter cell parameters to achieve a nominal "zero light shift" operating condition.

Rb Resonance Line

The Rb resonance line (see Figure 11) is detected by a silicon photodetector as a (≈ 0.1% to 1%) dip in the light throughput with a typical linewidth of 150 Hz to 1 kHz between inflection points. Frequency modulation is applied to the microwave excitation to, in effect, measure the derivative of the line shape, the so-called "line dispersion". Near the center of the line, this produces a discriminator characteristic that is used to lock onto the atomic resonance. Because there is no discriminator signal far away from the line, when an RFS is turned on, its frequency usually must be swept to acquire lock. The light transmission is sensed by a photodetector whose response varies as a Lorentzian function of the applied microwave frequency. This resonance line has a width of a few 100 Hz ($Q \approx 10^7$). The line slope corresponds to the amplitude of the fundamental discriminator signal vs. frequency.

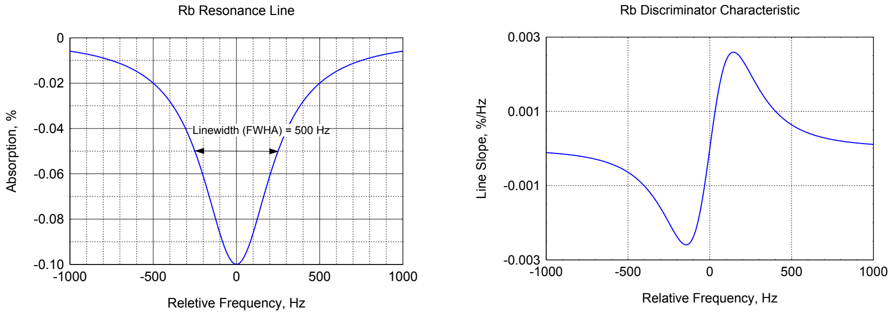

Rb Line — Rb Discriminator

Figure 11. Rb Resonance Line

An expression for the Lorentzian Rb resonance line is shown at the right. The resonance linewidth increases with modulation deviation, RF interrogation power and cell temperature, gradually at first and then more rapidly as those parameters are increased further.

$$I(f) = I_0 \left[1 - \frac{k}{1 + 4\frac{(f - f_0)^2}{\Delta f^2}} \right]$$

where: I = Photodetector current
I_0 = Off-resonance current
k = Absorption depth
f = Frequency
f_0 = Center frequency
Δf = Linewidth (FWHA)

Servo Modulation

The Rb resonance is interrogated by applying low frequency (≈150 Hz) FM to the microwave excitation and observing the resulting AC recovered signal, as shown in Figure 12. The sense of the fundamental component varies depending on whether the frequency is below or above the center of the line. At resonance, the fundamental component is a null, and a 2nd harmonic component is present.

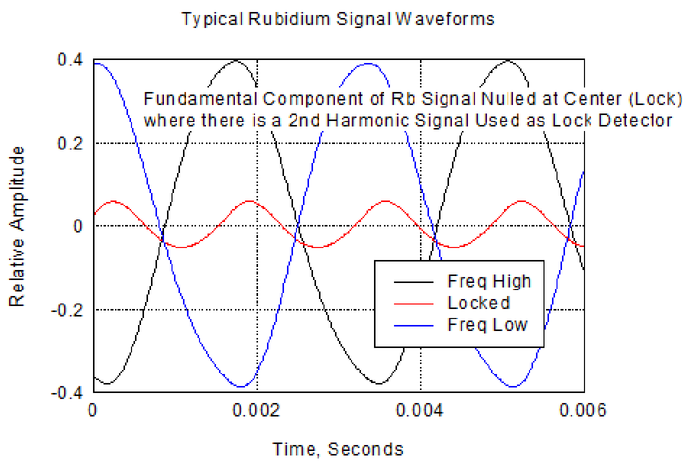

Figure 12. Rb Signal Waveforms

When the center frequency is below the center of the resonance line, the light throughput is higher on one half cycle of the modulation than the other, producing a fundamental recovered discriminator signal. When the center frequency is above the center of the resonance line, the light throughput is higher on the other half cycle, producing a fundamental signal having the opposite polarity. The frequency lock servo uses the discriminator signal by a process of synchronous detection to steer the center frequency to the exact center of the resonance line, where the fundamental component of the discriminator signal is null. At that condition, the square wave FM modulated RF excitation passes through the center of the resonance line twice per modulation cycle, producing a second harmonic component. Because the modulation rate is on the same order as the linewidth, the atomic discriminator acts like a low-pass filter, changing the square wave FM excitation waveform into a quasi-sine wave. The second harmonic signal is useful as a means of lock detection, for monitoring purposes, and to control lock acquisition.

Note that if the square wave FM rate were much lower than the linewidth, the recovered signal waveform would also be a fundamental square wave of alternating polarity on each side of resonance, and a null (with transients at the modulation switching points) at the center. This is the typical response of a cesium beam instrument.

The frequency lock servo must find the exact center of the atomic resonance with great precision, e.g., a 10 ppm or -100 dB fundamental null for an offset of 1.5×10^{-12} with a symmetric Rb linewidth of 1 kHz. This requires careful avoidance of even-order modulation distortion, fundamental pickup, and analog offsets.

Modulation Format

RFS designs nearly always use squarewave FM, although sinewave modulation is occasionally used (e.g., the Stanford Research PRS10, which uses a 12-bit DAC to synthesize 70 Hz sinusoidal PM), as is squarewave PM (e.g., the EG&G/PerkinElmer/Excelitas RFS-10, which uses a PLL to inject band-limited squarewave PM). Squarewave FM can be implemented by either a sawtooth signal to an analog phase modulator or (preferably) by switching the frequency of a DDS.

Modulation Rate

A relatively fast (in relation to the resonance linewidth) servo modulation rate is used in most RFS designs to support the fastest possible servo response and thus best transfer the stability of the Rb reference to locked crystal oscillator [32]. As mentioned above, this results in a quasi-sinusoidal 2nd harmonic component in the recovered signal when the system is in lock at the center of the Rb resonance.

The modulation rate is usually chosen as the highest convenient value that maintains a strong discriminator signal, as shown in Figure 13 where 146 Hz is used. The squarewave PM modulation format mentioned above extends that limit, an advantage for a tactical RFS in a vibratory environment. The particular modulation rate is often then selected on the basis of available values in its synthesizer that avoid power line frequencies and other interference.

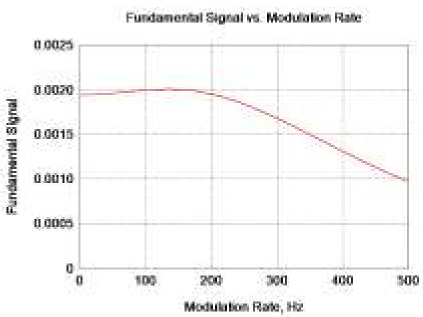

Figure 13. Signal vs. Modulation Rate

A slow modulation rate does not provide better performance unless a very high performance crystal oscillator is used, but may be an advantage for digital signal processing. Slow FM generates a squarewave fundamental signal, and, at the line center, there is no 2nd harmonic signal *per se* but rather transients in response to the frequency transitions. A DSP servo implementation would blank those out, and can also use a sampling technique that avoids power line interference. An example of RFS recovered signals for slow squarewave FM is shown in Figure 14.

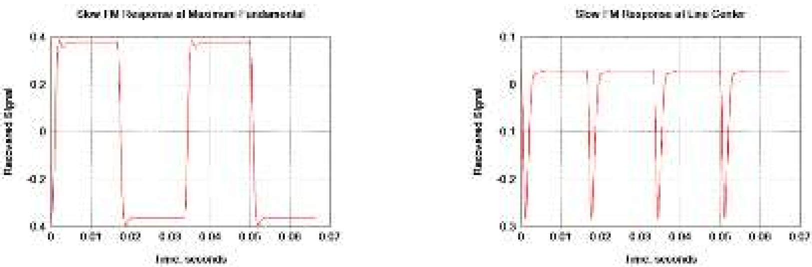

Off Line at Maximum Fundamental — At Resonance Line Center

Figure 14. Rb Recovered Signal Waveforms with Slow Squarewave FM

Modulation Deviation

The FM deviation is chosen to maximize the discriminator slope, and a typical setting is where the peak deviation, Δf, is equal to the linewidth between inflection points. Since the modulation rate is also chosen at about that value, the FM modulation index, $= \frac{\Delta f}{f_{mod}}$, is usually about 1.0. The deviation can be measured by observing the microwave interrogation spectrum and noting the difference between the amplitudes of the carrier and 1st sidebands (see Figure 15).

Figure 15. FM Modulation Sidebands

Modulation Distortion

Modulation distortion refers to even-order harmonic PM distortion or odd-order AM distortion applied to the RFS interrogation signal. Either of those results in a frequency offset and is an important cause of RFS frequency instability. It is easy to see how AM at the fundamental modulation rate causes a spurious fundamental error signal component that is synchronously detected like the desired discriminator signal and produces a frequency offset. The same thing happens to any odd-order AM component within the preamplifier bandwidth. A similar thing happens as a result of even-order PM distortion due to an intermodulation effect. For 2nd harmonic PM distortion, spurious sideband components are produced at $\pm 2 \cdot f_{mod}$ on the microwave excitation that mix with the normal f_{mod} modulation to generate a spurious fundamental recovered signal component that causes a fractional frequency offset given by

$$\frac{\Delta f}{f} = \frac{\delta_2}{2 \cdot Q_l}$$

where δ_2 is the relative amount of 2nd harmonic distortion and Q_l is the Rb line Q. For -70 dB 2nd harmonic distortion level and a 300 Hz Rb linewidth (Q_l = 23x10^6), the resulting frequency offset is 7x10^{-12}, and a 15% change in the distortion would cause a frequency deviation of 1x10^{-12}. This effect is clearly very important.

Modulation distortion can be caused in several ways: Distortion on the modulation waveform itself, distortion in the phase modulator, distortion caused by asymmetrical RF selectivity, and AM-to-PM conversion in the multiplier chain. The modulation signal itself can be made very pure by generating it from a precise squarewave followed by passive integration. A low-distortion analog phase modulator using an all-pass network is discussed below, and it should be applied at a relatively low RF frequency where the required deviation is small.

Ripple from the fundamental synchronous detector, can reach the VCXO control voltage even after attenuation by the servo integrator and loop filter. This is mainly at f_{mod}, which is significant only if it causes AM, but any leakage of $2 \cdot f_{mod}$ is another cause of even-order modulation distortion.

The Kenschaft Model

It is possible to simulate the discriminator signal of a rubidium gas cell atomic frequency standard with excellent fidelity using a model developed by R.P. Kenschaft [193]. This so-called "Kenschaft model", shown in Figure 16, produces a replica of the Rb optical absorption signal in response to a frequency control voltage input for tuning and modulation, and four parameters that describe the atomic resonance (Γ_1, Γ_2, A_{max}) and applied RF interrogation power (γH_1).

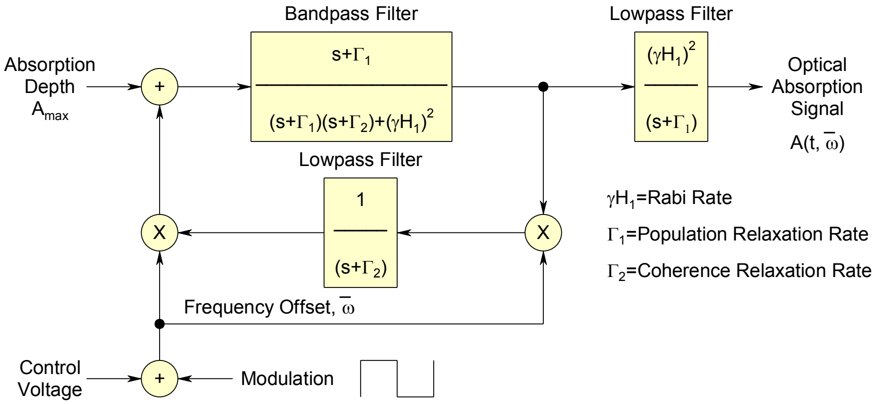

Figure 16. Kenschaft Model of the Rb Signal

This model has been implemented by a C-language dynamic link library (DLL), SPICE circuit simulation, MATLAB, and analog circuitry.

Examples of simulated and actual Rb 2nd harmonic and fundamental signal waveforms are shown in Figure 17 [194]. The Kenschaft model is able to very closely duplicate the actual response.

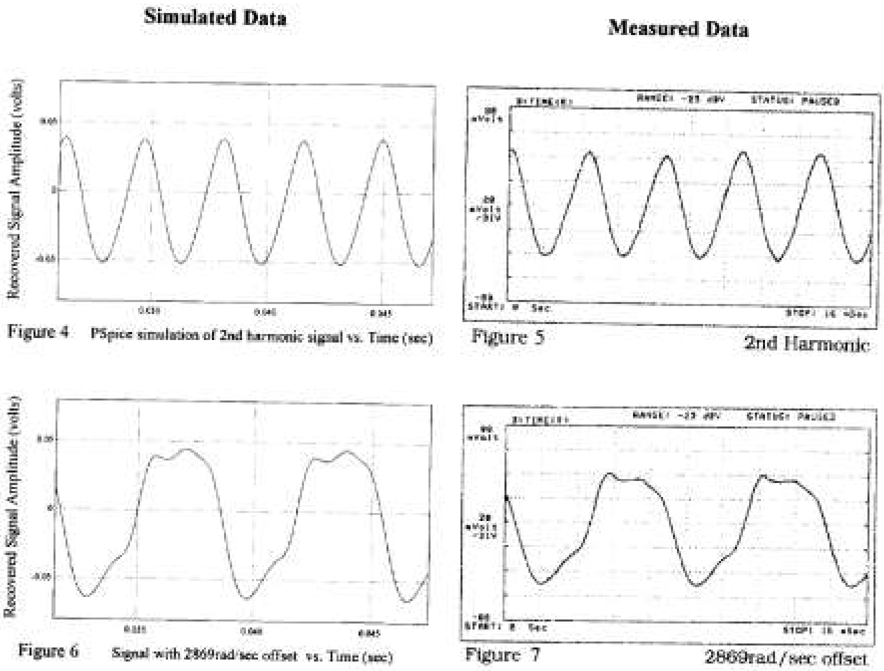

Figure 17. Simulated and Actual Rb Signal Waveforms

As another example of the utility of the Kenschaft model, it accurately predicts the magnitude and phase of the recovered 2nd harmonic signal as a function of the RF interrogation power (see Figure 18). The predicted sensitivity of the 2nd harmonic phase, 0.18° per percent change in RF power, was confirmed by laboratory measurements. Because it is difficult to directly measure the microwave magnetic field strength in an operating RFS, this relationship can be of interest for probing the applied RF power. The Kenschaft model can also be used to predict such parameters as the 2nd harmonic phase versus FM deviation, the magnitude and phase of the fundamental signal versus RF power and the fundamental phase versus FM deviation.

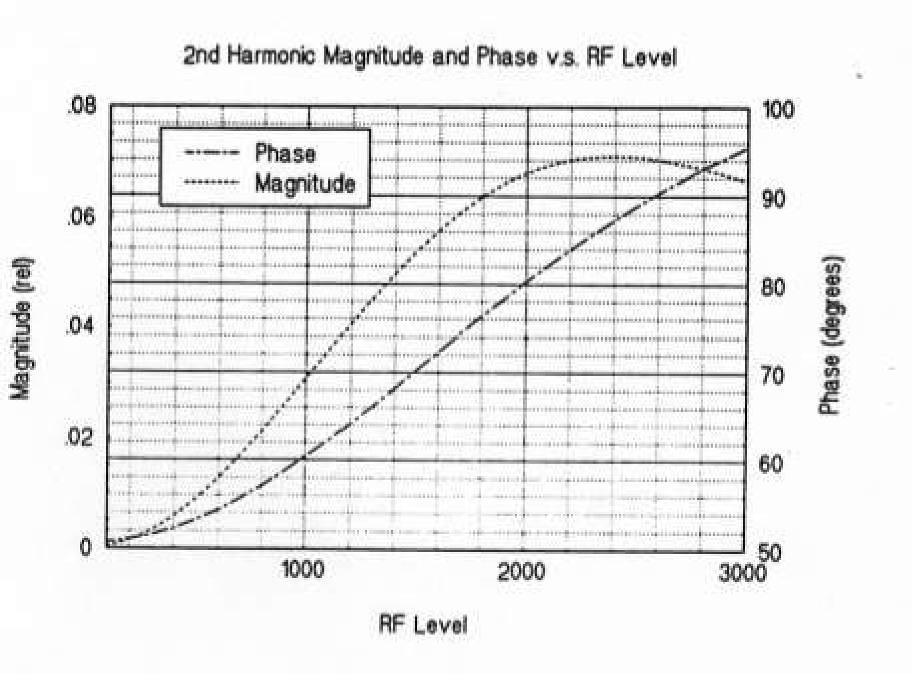

Figure 18. 2nd Harmonic Magnitude and Phase vs. RF Interrogation Power

The plots in Figure 19 show some of the other information about the Rb recovered signal that can be obtained from the Kenschaft model using these typical parameters:

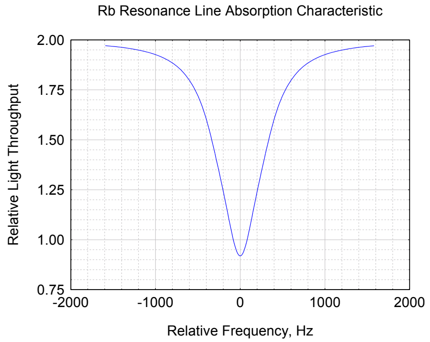

Gamma 1: 347.0 Hz
Gamma 2: 159.2 Hz
Modulation rate: 146.0 Hz
Modulation Deviation: 159.2 Hz peak
Discriminator Slope: 1.371 mV/1e-10
Relative µW Power: -12 dB
Relative µW Detuning: 1.00
Preamp Transimpedance: 5 MΩ
Low Pass Bandwidth: 796 Hz

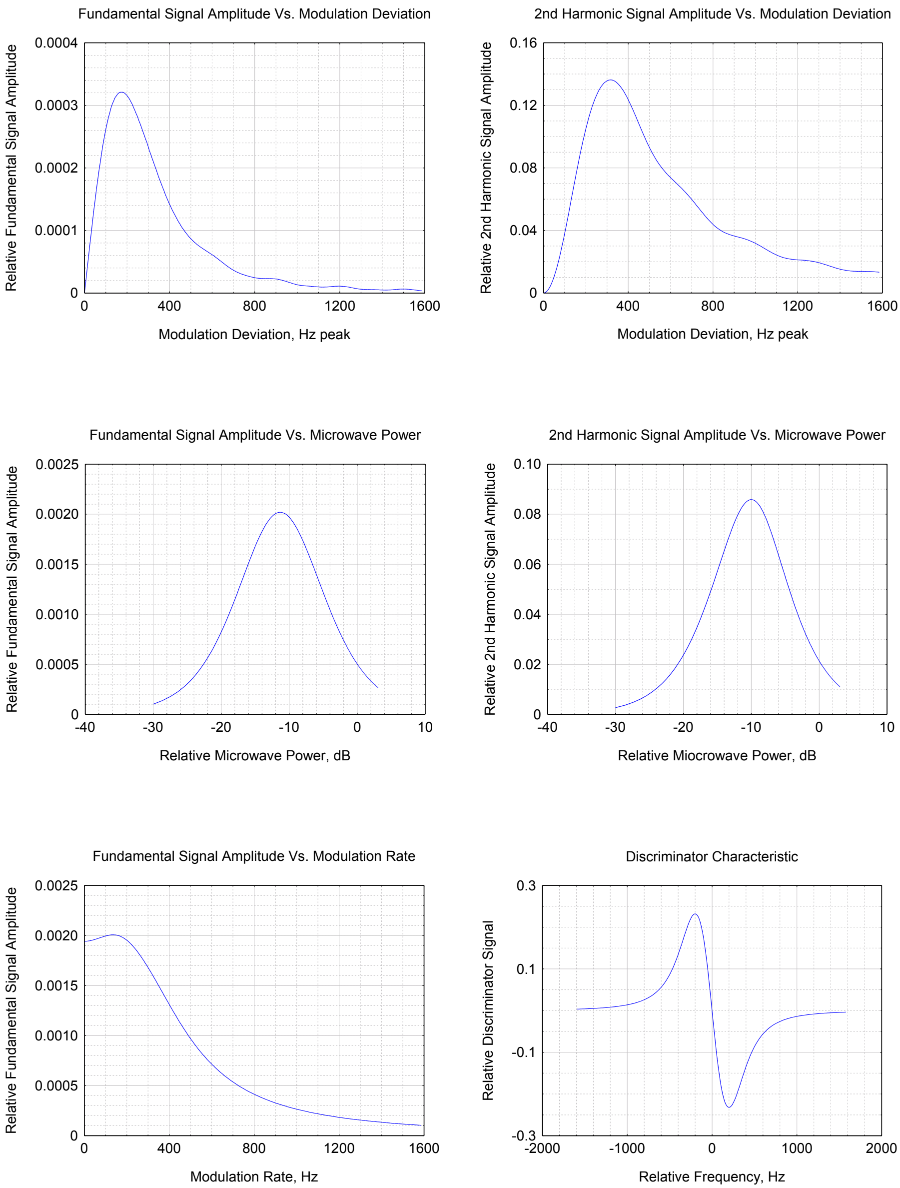

Figure 19. Rb Signal Plots from Kenschaft Model

Physics Package Recipes and Optimizations

Many successful rubidium frequency designs have been created and implemented, and it is somewhat presumptuous to declare any one of these "recipes" as the best. Nevertheless, it is reasonable to consider two such optimizations, one for a discrete filter cell and the other for an integrated cell, as examples of how to best implement those approaches.

In the case of a discrete filter cell, one can place it along with the absorption cell in a common cavity oven to achieve an overall optimization of temperature and light shift sensitivities (a so-called "tandem cell" approach as shown in Figure 17) [317]. That design usually uses a pure ^{87}Rb lamp and absorption cell, and a pure ^{85}Rb filter cell. In that case, the optical length of the filter cell is a design variable that will affect the nominal oven temperatures for optimized operation, and the length of the absorption cell is optimized for best signal under those conditions. An example of this design approach is shown in Figure 20. It is important, by the way, that the filter cell has a negligible amount of the ^{85}Rb isotope so that it does not produce a spurious resonance signal.

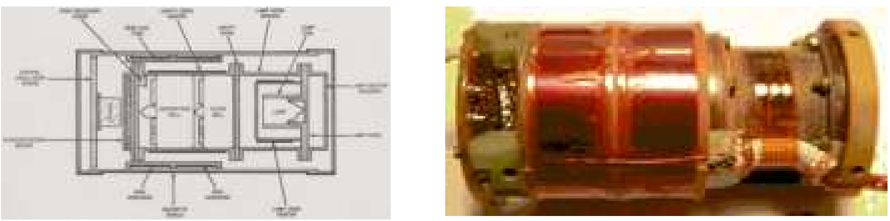

Cross Section Photograph

Figure 20. PerkinElmer RFS-10 Physics Package

Using the tandem cell approach, the temperature coefficient (TC) of the lamp oven, for the usual "mixed mode" of lamp operation, is mainly a light shift phenomenon that can be zeroed by adjusting the temperature of the filter cell in the cavity oven. Similarly, the TC of the cavity oven, which is determined mainly by that of the discrete filter cell since the absorption cell TC can be nulled by the buffer gas mixture, can be zeroed by adjusting the temperature of the lamp oven, because that affects the light intensity which in turn affects the filter cell TC, as shown in Figure 21.

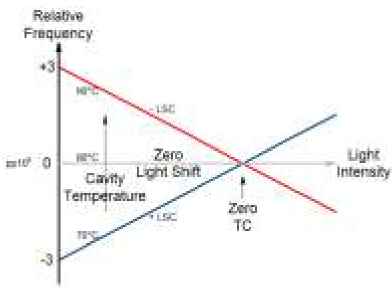

Figure 21. Characteristics of Tandem Cell RFS

Thus an RFS unit designed this way can be individually adjusted for overall zero TC and light shift by a simple adjustment of its lamp and cavity oven set points.

In the case of an integrated resonance cell, the filter and absorption cells necessarily share the same thermal environment inside the microwave cavity, and its buffer gas mixture can be chosen for an appropriate TC, which can be adjusted with the lamp oven temperature because that affects the light intensity and resonance cell TC. Likewise, the lamp oven TC can be zeroed by the cavity oven temperature. The nominal light shift condition can be set by adjusting the Rb isotopic ratio in the lamp [307]. The net result is another optimized design. The only significant disadvantage of the integrated cell design is that, because of resonance cell inhomogeneity, it has a significantly larger sensitivity to RF interrogation power than does the separate filter approach. An example of an integrated cell physics package is shown in Figure 22 [319].

It is worthwhile noting that other forms of inhomogeneity such as a non-uniform C-field or temperature gradient across the cell can also cause RF power sensitivity, all of which are aggravated by an uneven microwave interrogation H-field in the region of the absorption/resonance cell.

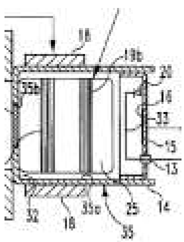

13=Feedthru C

14=Cavity & Inner Magnetic Shield

18=Heater Transistor

19b=C-Field Winding

25=Rb Cell

20=SRD

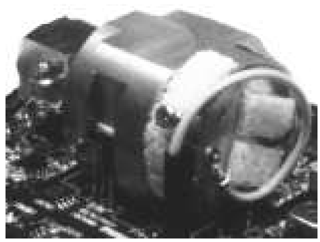

Cross Section Photograph

Figure 22. Symmetricom LPRO Physics Package

Interestingly, the highest performance RFS designs, a family of EG&G/PerkinElmer/Excelitas GPS satellite clocks, use discrete filter and absorption cells in separate ovens. In that case, the individual ovens, combined with overall chassis temperature control, have such high thermal stability that the relatively high filter cell TC ($\approx -6x10^{-11}$/ºC) is not a problem, and the separate filter oven set point allows precise independent nulling of the light shift.

So there is no single best recipe for an RFS physics package, but all successful designs have effective ways to minimize TC and light shift sensitivities. For example, in the GPS Rb clocks mentioned above, they utilize a total absorption cell buffer gas fill pressure that is chosen for minimum resonance linewidth (highest Q). In that case, the nominal frequency is a free variable that is adjusted for by the overall system. An alternative integrated cell space clock design, although not fully implemented, resulted in a somewhat smaller, lighter and lower physics package with similar signal parameters, except for an order-of-magnitude larger RF interrogation power sensitivity.

Rb Lamps

The Rb electrodeless discharge lamp and its RF exciter are important parts of a rubidium frequency standard. The lamp materials and processing are critical for long life under the conditions associated with its hot glass envelope and plasma. The exciter must provide reliable starting and stable running conditions.

Lamp envelope material and Rb fill affect lamp life and noise. Rubidium is lost by diffusion into the glass under lamp operating conditions, and the key parameters are glass type, temperature, and excitation power. Too little excess Rb will limit lamp life, while too much excess Rb can cause noise and instability. A breakthrough for Rb lamp life (the only important RFS wear-out mechanism) came in the early 1980's with T.J. Lynch's idea at EG&G to apply calorimetry to the Rb lamp filling process [100]. The lamp operates in a temperature-controlled oven at about 120 °C. An RF power oscillator supplies about 0.5 watt at 130 MHz to excite the lamp. It may be boosted to assure reliable starting, and must be well-regulated to provide a constant output spectrum and intensity to avoid frequency changes due to the light shift effect (frequency versus light intensity). The lamp output is a combination of Rb and buffer gas spectral lines. In the usual operating mode, the intensity of the Rb emissions is determined mainly by the Rb vapor pressure (lamp oven temperature), while the intensity of the buffer gas emissions depend mostly on the exciter RF power. Thus it is important that the lamp oven temperature be well-controlled to avoid light shift sensitivity. The lamp output may be passed through a thin-film optical interference filter to remove most of the useless buffer gas spectral lines so as to reduce shot noise at the photodetector.

The Rb lamp is the most critical element affecting the life of an RFS physics package, and it is also important to its frequency stability. Rb lamp life and reliability considerations are discussed in more detail in the following section. Here we wish to discuss some of the design considerations that affect successful lamp operation, particularly those associated with its noise and stability. A drawing [100] and photograph of a typical Rb lamp is shown in Figure 23.

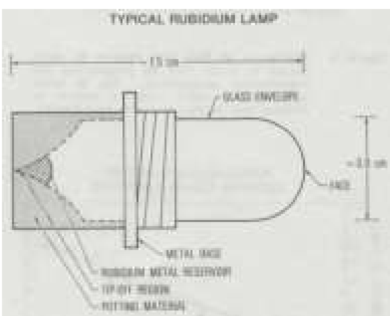

Drawing of Typical Rb Lamp

Photograph of PerkinElmer RAFS Lamp

Figure 23. Mounted RFS Rb Lamp

Perhaps the most remarkable characteristic of the small RF-excited electrodeless spectral lamps used in rubidium frequency standards is their intrinsically low noise. Lamp noise has negligible influence on the short-term stability of an RFS (in contrast to the visible flickering of a common neon lamp). Furthermore, the spectral width of the lamp emissions is ideal in the sense that it provides effective optical pumping without the need for elaborate wavelength stabilization.

The lamp noise power at the RFS physics package photodetector is effectively shot noise proportional to the overall light intensity, and recent improvements using optical filtration limit this noise to the useful Rb D-line emissions. The design issues related to the Rb lamp (excluding life, see below) therefore center on its reliable starting and stable running.

Stable lamp running mainly involves the thermal aspects of the Rb lamp, which can operate in two modes depending on its RF excitation power and temperature (see Figure 69J). A cold (room temperature) lamp is essentially a buffer gas lamp. The Rb emissions are small because its vapor pressure is low. As the lamp warms up, mainly because it is in a heated oven but also because of its excitation power, the Rb vapor pressure increases and so does the Rb spectral output, principally at the two deep red ^{87}Rb D-lines of 780 and 795 nm. That is the normal "mixed-mode" operating condition, where the lamp emits light at wavelengths associated with both its buffer gas and rubidium contents. The Rb output is mainly a function of the temperature (i.e., vapor pressure), while the buffer gas output is mainly a function of the RF excitation power.

That is the most desirable and stable operating condition, especially if the lamp is well heat sunk to its thermally-controlled oven. RF excitation power changes mainly affect the buffer gas output. If the temperature is raised higher, the lamp will enter a more-intense all-Rb "red mode", which can provide strong optical pumping and large signals, but is less stable and (unless attenuated) causes excessive light shift sensitivity. Furthermore, the region between the mixed and red modes is associated with gross instability cause by mode hopping and acoustic plasma oscillations (again, see Figure 69J). An RFS lamp is therefore almost always operated in the cooler, more stable mixed mode wherein it emits both Rb and buffer gas spectral lines. In this mode, the Rb light and discriminator signal both increase with a higher lamp oven temperature and Rb vapor pressure.

With Xe buffer gas, most of the unwanted buffer gas spectral lines can be blocked by a thin-film optical interference filter, reducing the total light intensity and shot noise and thereby improving the S/N ratio of the Rb discriminator signal and the overall short-term stability [154].

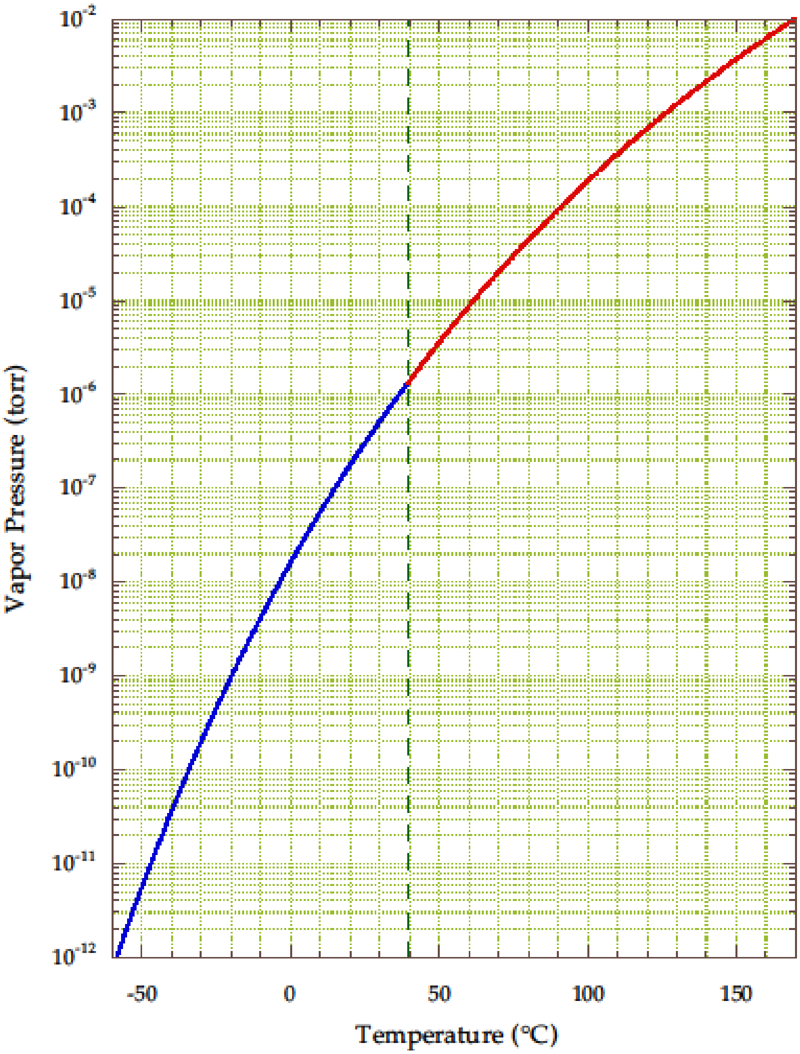

Figure 24. Rb Vapor Pressure vs. Temperature

A plot of the ^{87}Rb vapor pressure versus temperature is shown in Figure 24 [65]. The dashed line denotes the 39°C melting point. Only a very small amount of Rb metal is required to maintain a saturated vapor pressure, but excess Rb is needed to assure long lamp life as it diffuses into the glass lamp envelope. If the initial Rb fill is insufficient, the lamp will fail prematurely. If the lamp is over-filled, it can become noisy. Tight process control is therefore necessary on the initial Rb fill.

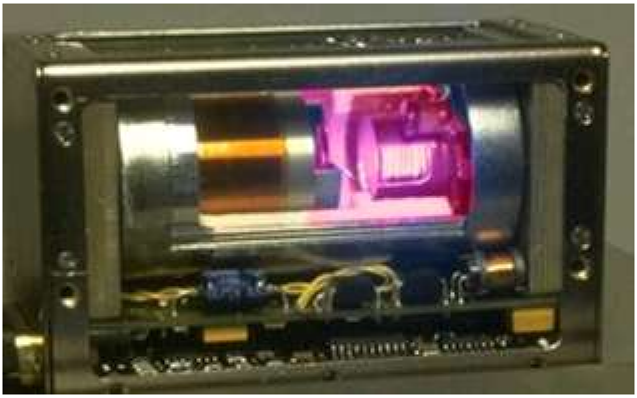

Figure 25. Photograph of Temex RFS with Cutaway Physics Package.

The back of the Rb lamp shown in Figure 23 is bonded into a metallic holder to assure good thermal contact with the lamp oven, and its front portion is inserted into a coil which couples RF power into it from its lamp exciter, producing a colorful plasma discharge as shown in Figure 25.

During normal operation, the Rb lamp temperature is well above the melting point of rubidium, and the molten rubidium must not be allowed to “slosh” around. Fortunately, for the small amount of excess Rb that is necessary for long lamp life, surface tension holds it in place under all but the most extreme conditions of shock, acceleration and vibration. Most importantly, the excess Rb must remain at the cooler tip of the lamp away from the active discharge region in order to avoid noisy behavior.

Lamp Life and Calorimetry

The critical factor determining lamp reliability is quantitative control of the lamp Rb fill and its depletion rate by diffusion into the glass envelope. Tom Lynch of EG&G effectively solved that problem in 1980 by devising the method of calorimetric Rb measurement that is now widely used by all organizations making rubidium frequency standards. By measuring the heat energy required to melt the rubidium in a lamp, and knowing its heat of fusion, calorimetry provides a nondestructive way to weigh the Rb in a lamp for manufacturing process control, assessing the initial “cleanup” due to chemical reactions when the lamp is first ignited, measuring the rate of Rb depletion as a function of materials (glass type and condition) and operating conditions (temperature, RF excitation power), and screening lamps for flight usage, as shown in Figure 26 [120]. Experience shows that it is possible, with the right design and manufacturing processes, to consistently obtain lamps that have both low noise and long life. More information about Rb lamp life and calorimetry will be found in Reference [100].

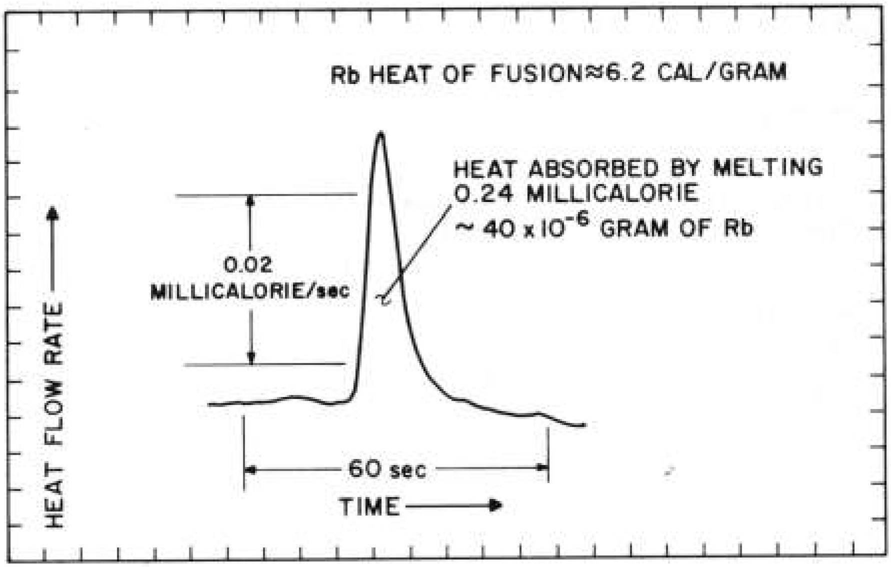

Figure 26. Lamp Calorimetry Plot

Rb Lamp Exciters

The lamp exciter is arguably the most unusual electronic circuit in a rubidium frequency standard. It is an RF power oscillator in the 100 MHz region that produces about 0.5 W of RF power to excite a plasma discharge in an electrodeless Rb spectral lamp.

Rb Spectral Lamps

The lamp itself is a small (≈1 cm diameter) glass bulb containing metallic Rb and a few Torr of inert xenon buffer gas whose purpose is to produce spectral lines at the Rb D-lines of 780 and 795 nm (deep red) to support optical pumping of the Rb atoms in the resonance cell. At room temperature, it works only as a buffer gas lamp and must be heated up to around 115 ºC to raise the Rb vapor pressure sufficiently so that it becomes an Rb lamp.

An Rb spectral lamp can be excited by either an RF magnetic field by operating it in a coil or an RF electric field by operating it between external electrodes [316]. While it is actually somewhat a combination of the two, the most common method is with the lamp located inside the coil of a high-Q resonant tank circuit (if you used electrodes to excite the lamp you'd need a shielded high-Q coil anyway, so you may as well use it to excite the lamp). The lamp is coupled to the exciter circuit by the coil, and it presents a complex load impedance that varies with its operating mode depending on its temperature and whether or not it is lit. When cold, it is a Xe lamp because there is negligible Rb vapor pressure. As the lamp heats, both because it is in a heated oven but also because of self-heating by the applied RF power, the Rb vapor pressure increases and the Rb atoms, having a lower ionization potential, absorb more and more of the RF energy, and the lamp enters a mixed Xe-Rb mode. At even higher temperatures, the lamp will change to a pure Rb mode. Most RFS operate in the mixed mode at a temperature chosen for optimum Rb spectral output. That output is controlled mainly by the Rb vapor pressure determined by the temperature of the well-controlled oven to which the rear of the lamp is thermally attached. Changes in the RF excitation mainly affect the Xe emission, an advantage for stable operation. Xe is chosen as the buffer gas for its easiest starting and because it is possible to remove its unwanted spectral lines by an optical interference filter [154].

More details about the acceleration of electrons and ions by electric and magnetic fields, energy gain within a mean free path to cause avalanche breakdown, plasma temperatures, ion densities and the like will be found in Reference [103].

Lamp Exciters

An RFS lamp exciter is nearly always an RF power oscillator rather than a master oscillator – power amplifier arrangement because it is essential that the excitation frequency be aligned with the lamp coil resonance.

There are many RF oscillator circuit configurations, and many of them have been used as lamp exciters (early RFS units used push-pull cross-coupled vacuum tube oscillators). One of the most popular is the series-tuned Colpitts configuration, shown in the basic schematic of Figure 27. The oscillator network comprises 150 and 30 pF capacitors along with the 0.7 μH lamp coil, series tuned to about 105 MHz by the 3.6 pF capacitor.

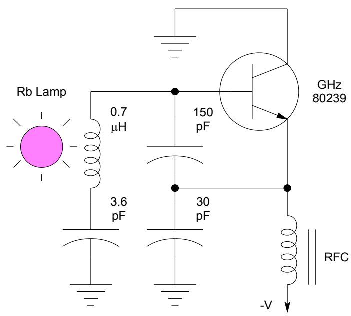

Figure 27. Basic Lamp Exciter Circuit

The exciter circuit has to (a) oscillate, (b) start the lamp, and (c) run the lamp. Item (a) requires that the circuit have sufficient gain to start oscillating at the proper frequency under all load conditions. Item (b) requires that sufficient RF voltage be produced to start the plasma discharge. Item (c) involves optimization of the lamp operating conditions (including its RF excitation power, temperature and temperature gradients) for best clock performance, and maintaining those conditions indefinitely.

Packaging

One important decision is whether to locate the exciter circuit inside or outside the lamp oven. The former has the advantages of short leads, smaller packaging, better

EMI containment, higher thermal efficiency and generally better behavior. But it requires that the exciter transistor operate at the lamp oven temperature. That factor, and its effect on derating and predicted reliability, can lead to the decision to locate the lamp exciter outside the lamp oven, connected to it by a short length of coax. That line is a performance disadvantage, but is an acceptable tradeoff against lower junction temperature, especially for space applications.

Components

The most important attribute in selecting the RF power transistor is its package. Not only does it determine its power rating and mounting (an isolated case is much preferred), but, most importantly it affects the RF circuit layout. More specifically, multiple low-inductance emitter leads result in better performance and behavior. The objective is to minimize the destabilizing effect of emitter inductance. No emitter degeneration resistors are used, both for that reason and to provide the most gain margin. A lamp exciter using a device with four wide emitter leads each connected by chip capacitors to adjacent base and collector leads results in excellent starting and running performance.

The choice between a BJT or MOSFET RF power transistor today is probably a matter of personal choice. A critical aspect of RF power transistor technology was the change to all gold metallization systems which solved a long-term metal migration problem associated with aluminum. A BJT is subject to two main considerations, base-emitter (B-E) junction breakdown and long-term DC bias stability. B-E breakdown can cause noisiness and eventual transistor degradation and failure. It is important therefore to make sure that the RF voltage swings are within bounds, accomplished mainly by using as large a B-E circuit capacitance as gain margin allows. The DC bias can be stabilized by an active current regulation loop [104].

The series capacitor in the lamp network also deserves mention because it must handle relatively a high RF circulating current and several hundred volts, especially under starting boost conditions. An ordinary lossy ceramic capacitor will literally glow cherry red in this circuit. A high quality porcelain RF chip capacitor should be used, one with a sufficiently high voltage rating.

Lamp Loading Measurements

It is quite easy to measure the load presented to the exciter circuit by an unlit lamp.

A test fixture can be constructed consisting of a lamp coil and resonating capacitor in series, with one end of the capacitor grounded and other lead from the coil going to a coaxial connector as shown in Figure 28. The resonant impedance of this network can be measured with a vector impedance meter or RF network analyzer.

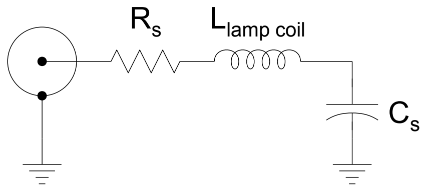

Figure 28. Lamp Test Circuit

Without a lamp, the Q is high and the equivalent series loss resistance is about 2.5 Ω, corresponding to a Q of about 170. When a lamp in inserted into the coil, the loss resistance increases, but normally only slightly because the dielectric loss of the glass is low and the excess Rb is all condensed in the tip of the lamp. The front lamp holder may be slotted to reduce its shorted-turn loading effect, as seen in Figure 23. This is the normal starting condition, and the exciter produces a high RF voltage at the high impedance point where the coil and capacitor connect at the top of the coil by virtue of the large RF circulating current in the resonant tank. In the case of a lamp where there is metallic Rb on the exposed inside surface of the lamp, this conductive layer de-Qs the coil and increases the series load resistance. That can also be measured in the test fixture, and the worst case loading results is an R_s of 25-50 Ω. Some loading is also caused by Rb that has diffused into the glass in a lamp that has operated a long time. This presents the worst case for lamp starting, and empirical tests are done with "bad" lamps (those that heavily load the coil) and/or by inserting a physical resistor in series with the coil.

The series LRC lamp network shown in Figure 28 with an added shunt capacitor (the connector in the test circuit, network capacitors in the oscillator circuit) is the same as the equivalent circuit for a quartz crystal resonator and many of the same analysis techniques can be applied, including the use of impedance and admittance circles.

Lamp Exciter Oscillation

A typical lamp exciter oscillates properly with a lamp equivalent resistance of ≈ 50 Ω, and produces a negative resistance of over 200 Ω, which provides a comfortable margin for its oscillation threshold. Excessive gain can cause spurious oscillation.

Lamp Starting

The details of lamp starting (like so many things when you dig deep enough) are only partially understood. Clearly electrons and ions are accelerated by the RF electric and magnetic field excitation until avalanche ionization occurs and the plasma is lit. But where do the original electrons and ions come from? Cosmic ray ionization is a leading contender, with natural background radioactivity and the high energy tail of the buffer gas kinetic distribution being other possibilities. The buffer gas pressure is optimized for easiest starting. Starting becomes easier as the lamp heats and the Rb vapor pressure increases because of its lower first ionization voltage. The coil geometry is another factor that can be optimized experimentally, as is the lamp position and the details of its holder. Photoionization is very effective in starting lamps (e.g., a photographic strobe flash or even an electrical spark), but is not normally necessary. The RF voltage is the most important exciter-related starting factor.

There isn't a lot of information available about long-term lamp starting behavior. One would assume that starting would become somewhat more difficult for a mature lamp, but Rb clocks seem to operate properly after years of dormancy without any problem. Commercial Rb oscillators do get turned on and off more frequently, and older lamps seem to start fine. The location of the excess Rb in the lamp is a much more important factor for lamp loading than its long term diffusion into the glass. Once "chased" into the lamp tip, the excess Rb stays there unless exposed to very high temperatures (something that does not occur inside a unit). A heavily Rb-loaded lamp starts if the exciter oscillates and delivers RF power to the lamp. That power "burns away" the Rb that is loading the exciter by RF induction heating, aided by the mobility provided by the elevated lamp oven temperature. Even with a well-chased lamp, a conductive Rb film forms on the inside surface of an unlit lamp that must be vaporized before it will start, a process that can take a few seconds when cool. The voltage across the lamp coil gradually increases as the loading decreases until the lamp starts.

Lamp Running

It is harder to measure the lamp load resistance for an operating lamp. The same test fixture can be used along with a source of RF power to start and run a lamp (which will self-heat even if it is not ovenized). But it is difficult to make impedance measurements in that setup. Passive directional couplers can measure the magnitude of the forward and reverse power flows. A classic General Radio 1602 passive UHF admittance meter (Thurston bridge) can provide some information. But the most practical way to obtain information about an operating lamp exciter is to calculate the RF current by measuring the RF voltage across a large grounded capacitor. A small RF current probe can also be used. Circuit voltages can be measured with built-in peak detector diodes.

Current Regulation

The lamp exciter circuit can includes a regulator that controls the transistor DC bias current at its nominal during normal operating and at a higher current for starting boost, controlled by detecting the light [321], [331]. This current regulation provides several important advantages by (a) stabilizing the lamp exciter DC current during normal operation, (b) providing a means for boosting the lamp exciter for starting, (c) maintaining (along with supply voltage regulation) constant DC power input and thus stabilizing the RF power delivered to the lamp, and (d) providing additional attenuation of power supply conducted EMI ripple. Experience from unregulated BJT lamp exciter circuits in the 1960's showed that the DC bias current decreases significantly over the long term for fixed bias because of transistor β falloff, causing a drop in lamp power. The current regulator solves that problem, as well as eliminating the need for individual adjustment. It also avoids changes in DC bias current caused by radiation exposure. Lamp starting can be aided by boosting either the exciter supply voltage or its current (or both).

Power Measurements

It is quite easy to measure the RF power delivered to a lamp assembly by a lamp exciter located outside the lamp oven. One simply uses the lamp oven temperature controller as a calorimeter by measuring the difference in heater power with the lamp exciter turned on and off.

Frequency Stability

The lamp exciter frequency is not particularly critical, and it is quite constant because it is determined mainly by a high quality RF capacitor and a high Q, temperature-controlled air inductor. The frequency changes several MHz between the lamp unlit and lit conditions because of non-linear transistor capacitance and plasma reactance, but that is of little consequence. Little information exists about long-term lamp exciter frequency change, but it does not appear to be important. Experience has shown that it is much better to use a tight-tolerance fixed capacitor in the lamp network rather than a trimmer to adjust the frequency because trimmer capacitors are very prone to failure, especially in this relatively high-voltage high-temperature application

Lamp Excitation Power

One would certainly expect that, after some initial stabilization, the lamp excitation power would naturally tend to decrease over the life of a clock. But most of the factors involved in such a change (e.g., transistor β falloff) are within the lamp exciter current regulatory control loop. Thanks to that control loop, most of the relevant factors can be modeled and analyzed. The main imponderable is the relationship between DC power input and RF power output delivered to the lamp. The RF power delivered to the lamp is not itself regulated *per se* but rather is determined by the saturation characteristics of the circuit (the supply voltage and current, transistor limiting, and the oscillator feedback network impedance ratio).

Light Shift

Light shift is the frequency deviation caused by a change in the optical pumping light intensity or spectrum. It is a fundamental sensitivity of an RFS using the "double-resonance" method whereby the Rb atoms are simultaneously exposed to pumping light and RF interrogation. It is easy to understand from a phenomenological standpoint, but its underlying physics is very complex. Normally one defines it as the frequency change due to light intensity (i.e., by inserting a neutral density filter in the light beam), but from a practical engineering standpoint the effect of changing the lamp oven temperature or the lamp exciter power is more important (those effects are not identical). Fortunately, the isotopic filter offers an effective way of nulling the light shift effect, especially if a discrete filter cell is used. In the integrated cell, light shift, even if nulled from an overall standpoint, causes significant inhomogeneity that then contributes to RF power sensitivity. In either case, light shift is a leading candidate for the cause of frequency aging as the properties of the pumping light change over time.

Pulsed Light

One way, in principle, to eliminate light shift is to operate an RFS in a pulsed mode whereby the pumping light and the RF interrogation signal are applied sequentially. Experiments have shown that this is effective to some extent [28] but it raises other problems having to do with the pulsed operation, and this technique has not found widespread use, particularly since the isotopic filter is so effective in reducing the light shift in a more straightforward way.

Isotopic Filter Cells

The ability to improve the optical pumping efficiency with isotopic filtering is a fundamental advantage of rubidium gas cell frequency standards, some of which use discrete filter cells for optimum performance. An RFS filter cell is a glass enclosure containing ^{85}Rb and an inert buffer gas (e.g., Ar) which is heated to the temperature where it provides not only enhanced pumping but also a first-order zero light shift (ZLS) condition.

Absorption Cells

A rubidium gas cell is a glass enclosure containing ^{87}Rb or natural Rb (72% ^{85}Rb, 28% ^{87}Rb) , and an inert buffer gas (e.g. N_2, Ar) or a mixture thereof. The cell may be used alone (a resonance cell) or as an absorption cell with a separate ^{85}Rb filter cell. The cell is operated at a stable elevated temperature to establish sufficient Rb vapor pressure, and the buffer gas prevents wall collisions that would broaden the resonance line. The cell is inside a microwave cavity and is surrounded by a coil to produce a static DC magnetic field (C-field). The rubidium inside the cell is not consumed, and lasts infinitely.

The absorption cell is the frequency-determining element in an RFS, and is therefore a critical aspect of its performance. Besides ^{87}Rb, it contains a buffer gas to avoid wall collisions that would otherwise broaden the resonance line (wall coating, a possible alternative, is seldom used). Two optimum "recipes" have evolved for RFS physics packages, one for the integrated cell (the more common arrangement), and another for separate filter and absorption cells. Nitrogen is almost always used (alone or mixed with argon) as an absorption cell buffer gas because its quenching effect improves the S/N ratio. Cell operating temperatures are set as cool as possible consistent with the unit's upper operating temperature range and the need to maintain oven temperature control. Cell length is determined by optimizing the discriminator signal at that operating temperature. Light shift is effectively the temperature coefficient of the lamp oven, while the absorption cell temperature coefficient is determined by its buffer gas.

For the integrated cell, natural Rb is used in the resonance cell, and light shift is minimized by adjusting the lamp Rb isotopic ratio [307]. The resonance cell buffer gas is pure N_2, or a N_2-Ar mix chosen to minimize its temperature coefficient.

For the separate filter cell, pure ^{87}Rb is used in the lamp, and light shift (lamp oven temperature coefficient) is minimized by adjusting the length and/or operating temperature of the filter cell. If the filter and absorption cells are both located in the cavity oven, their net temperature coefficient can be nulled by the absorption cell buffer gas ratio and/or the light intensity (set by the lamp oven temperature).

Before the advent of practical high-resolution DDS frequency synthesis, it was necessary to devise an integrated or absorption cell buffer gas mix and nominal fill pressure to match the nominal frequency of the fixed RF chain synthesizer. This also imposed very tight buffer gas fill tolerances. With an adjustable synthesizer, it can be used to calibrate the individual RFS frequency, and the manufacturing tolerances can be much wider.

A collection of Rb cells is shown in Figure 29.

Figure 29. Rb Cell Collection

L to R: Varian 4700 and R-20, HP 5065A, Tracor 304B or D, Efratom FRK and FRS, SRS PRS10, EG&G RFS-10, and Frequency Electronics FE5680A.

Early cells had long tubulations to keep condensed Rb out of the microwave cavity (General Radio did so for that reason and the HP 5065A used thermoelectric cooling of the cell tip). The Efratom FRK cell has indentations for cavity tuning screws.

The cells in the latest commercial RFS designs have, along with their cavities, gotten much smaller (see Figure 30). While this comes at the expense of a somewhat broader line, lower Q and poorer short-term stability, good performance (e.g. $\sigma_y(\tau)= 1x10^{-11}$ at 1 second) can still be realized. Shorter cells require a higher cell operating to maintain the same optical absorption and signal strength.

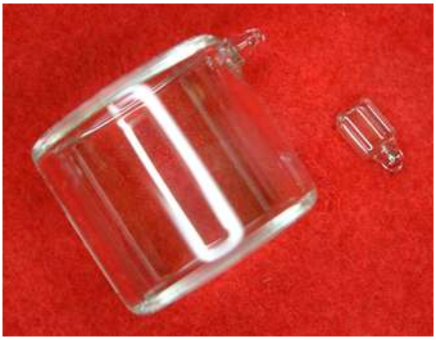

Left:
Symmetricom 8130A Resonance Cell.
Size: 1'' diameter x 1" long

Right:
Symmetricom X72 Resonance Cell
Size: About 0.3" long

Figure 30. Rb Resonance Cells

Cells can be made to operate at higher temperatures by depressing the rubidium vapor with potassium according to Raoult's law.

Cell volumetric change caused by atmospheric pressure variation causes a frequency deviation because of the buffer gas pressure shift coefficient [68]. This effect scales with the buffer gas frequency offset, and is primarily due to "oil-can" deflection of the cell windows. It has a typical value of about $1x10^{-10}$ per atmosphere, and can be an important error budget term for aircraft applications as well as a contributor to a unit's stability floor. Sealed RFS units or physics packages have been used to reduce or eliminate this effect [159].

All-metal cells have been proposed as a way to (a) eliminate Rb-glass reactions, (b) eliminate helium permeation, (c) allow high-temperature bakeout, (d) provide precise filling and sealing, (e) provide low thermal gradients, (f) integrate the cell, cavity and oven, and (g) support fast warm-up [349]. It is known that rubidium co-exists happily with copper, which is also an attractive cavity and oven material. Sapphire windows could be brazed into the cell ends to allow light transmission. The cavity could extend beyond the cell volume to allow integration of the microwave multiplier and photodetector. The assembly could use an integrated resonance cell or incorporate a separate filter cell, and they would be filled via copper tubulations that would then be pinch sealed. CSAC cells are fabricated from silicon [260].

Buffer Gas

The resonance cell of a gas cell atomic frequency standard contains a buffer gas to inhibit wall relaxation and reduce Doppler broadening. The use of buffer gas to reduce the linewidth of a microwave spectral line is one of the fundamental principles of these devices, based on a January 1953 paper by R.H. Dicke [15].

The following excerpt from the NIST web site describes the use of buffer gases:

> Buffer gases are commonly used to reduce the linewidth of microwave transitions in alkali atoms. The reason a buffer gas is important is that collisions of the alkali atoms with the cell walls reset the oscillating dipole moments of the atom. The lifetime of the oscillation determines the width of the resonance and hence the Q of the atomic system. Since a room-temperature atom traverses a 1 cm cell in about 3 microseconds, the collisional broadening of a pure vapor of alkali atoms is about 100 kHz, resulting in a Q of order 10^5. This Q is insufficient for most atomic clock applications.
>
> To improve the atomic Q-factor, several kPa of a gas such as Ne, Ar or N_2 is added to the cell with the alkali vapor. The alkali atoms collide frequently with the buffer gas atoms (the mean free path is of the order of a few micrometers) and therefore do not propagate ballistically to the walls of the cell. Instead they diffuse slowly throughout the cell, lengthening substantially the amount of time during which they can interact with the excitation field before collisional dephasing at the wall occurs. The buffer gas has a rather benign effect on the oscillation of the alkali atom: the alkali atom can undergo around 10^5 collisions with a buffer-gas atom before the alkali atom's coherence is destroyed (as opposed to a single collision with the cell wall). As a result, the oscillation lifetime can be increased to as much as 10 ms. The transition linewidth is reduced to around 100 Hz and the atomic Q-factor increased to near 10^8. This high Q for the atomic line results in a frequency reference with a frequency stability much better than could be achieved in a pure vapor alone.

Figure 31 shows the effect of buffer gas pressure on the width of the Rb resonance (i.e., the Q, as indicated by its transverse coherence relaxation rate). For this cell, the optimum buffer gas pressure is about 12 Torr.

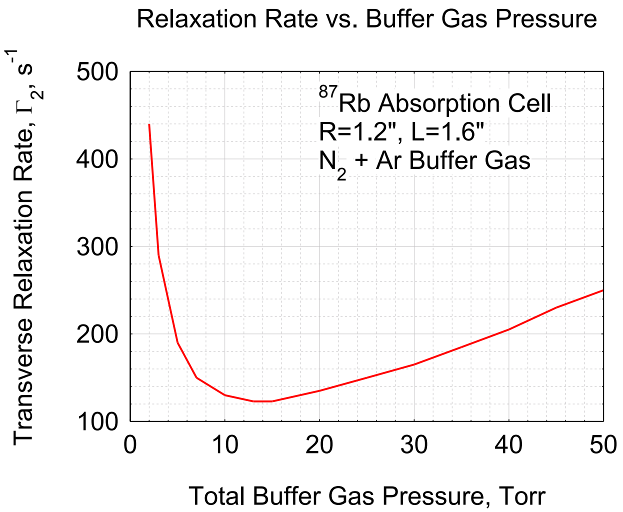

Figure 31. Linewidth versus Buffer Gas Pressure

The following excerpts from P. Bender, et al [220] and W. Stern and R. Novick [231] describe the effect of a buffer gas on the frequency:

> When a rubidium-87 atom collides with a foreign gas molecule, there is an instantaneous interaction between the dipole moments of the two species. This interaction can be explained in terms of the attractive van der Waals forces and the exchange forces and can be considered to cause either an expansion or contraction of the electronic charge clouds of the interacting species. The change in the density of the electronic-charge cloud causes a corresponding increase or decrease in the hyperfine splitting of the ground state of rubidium-87. The van der Waals forces are long-range attractive forces and always lead to decreases in the hyperfine separation. For collisions with light buffer gas atoms,, the shift in the rubidium-87 hyperfine levels is toward higher frequency while for heavy buffer gas atoms, it is toward lower frequency. The pressure shifts are temperature-dependent, and the sign of the temperature coefficient tends to be of the same as the sign of the pressure coefficient.

The buffer gas slightly changes the hyperfine resonance and the resulting frequency offset is somewhat temperature dependent. The buffer gas pressure shift and temperature coefficients are nonlinear (they vary with the cell operating temperature), and their values in the technical literature vary considerably because of that and other measurement factors. Those values do not appear to depend importantly on the alkali element (cesium or rubidium) used in the cell. The buffer gas partial pressure is usually specified at the temperature at which it is filled (typically +25°C), while the buffer gas pressure shift and temperature coefficients are usually specified at the temperature at which the cell is operated.

Each buffer gas has nominal values for its pressure shift, (PC in Hz/Torr) and temperature coefficients (TC in Hz/Torr/ºC). The lighter gases have positive pressure shifts. Specific values for those parameters that apply to the particular case should be used in synthesizing a buffer gas mixture. Some typical values are shown in Table II. Binary and tertiary buffer gas mixtures can be used to optimize performance by allowing independent adjustment of the frequency, fill pressure and temperature coefficient. In an RFS that produces a standard frequency with a fixed synthesizer, a particular buffer gas frequency offset is required, and a binary mixture can provide that offset with the desired temperature coefficient. A further optimization is to use a total buffer gas pressure that provides the narrowest resonance linewidth (highest Q). Another consideration is that a relatively small buffer gas offset provides lower barometric sensitivity.

Table II. Buffer Gas Coefficients

Buffer Gas	Pressure Shift Coefficient Hz/Torr	Temperature Coefficient Hz/Torr/°C
Nitrogen	+548	+0.46
Neon	+392	+0.26
Argon	-53	-0.24
Krypton	-590	-0.53
Helium	+718	+1.0
Hydrogen	+663	+1.0
Methane	-510	-0.61
Xenon	-2350	+3.68

An example of a buffer gas mixture is the one used in the original EG&G GPS Rb clock [120] which comprises an N_2/Ar = 0.728 ratio providing a frequency offset of +2800 Hz at a nominal fill pressure of 14.0 Torr with a TC of $+1.13 \times 10^{-10}$/°C. The fill pressure is chosen for best linewidth and the TC is slightly positive to partially compensate that of the filter cell.

Rb Cell Processing

RFS lamps and cells are small glass envelopes containing a low pressure buffer gas or gas mixture and a small amount of metallic rubidium. For lamps, the glass type is chosen primarily for high alkali resistance because gradual Rb loss by diffusion into the glass must be minimized for long life. The buffer gas, usually Xe or Kr, is necessary for the lamp to start, and its type is chosen for spectral considerations and its pressure for easiest starting.

For filter cells, the glass type is uncritical unless it is located inside the microwave cavity, in which case it is selected for low dielectric loss.

For absorption cells, the glass type is selected primarily for low He permeation and secondarily for low dielectric loss. The absorption cell geometry (dimensions and wall thicknesses), along with its buffer gas frequency offset, will determine its barometric sensitivity.

The best Rb ampoules, lamps and cells are processed on ultra-high vacuum systems and use special processing steps like plasma cleaning to assure the best results.

Ampoules of metallic rubidium are reduced from the chloride under vacuum by reacting it with barium azide according to the following:

$2\ RbCl + Ba(N_3)_2 \rightarrow 2\ Rb + BaCl_2 + 3\ N_2$

A typical cell processing setup is shown in Figure 32. The lamp or cell envelopes are attached to a glass manifold through short tubulations, and the manifold is connected to vacuum pumps through an isolation valve. The pumps can be a combination of a sorb pump for roughing and an ion pump for high vacuum. A previously-prepared Rb ampule is located in a side arm of the manifold along with a glass-coated magnetic slug used to break it. The system also has a bellows valve for adjusting its volume, leak and shutoff valves(s) for introducing buffer gas from a regulated gas bottle, and a high-resolution pressure gauge. The entire system can be covered with a bakeout hood.

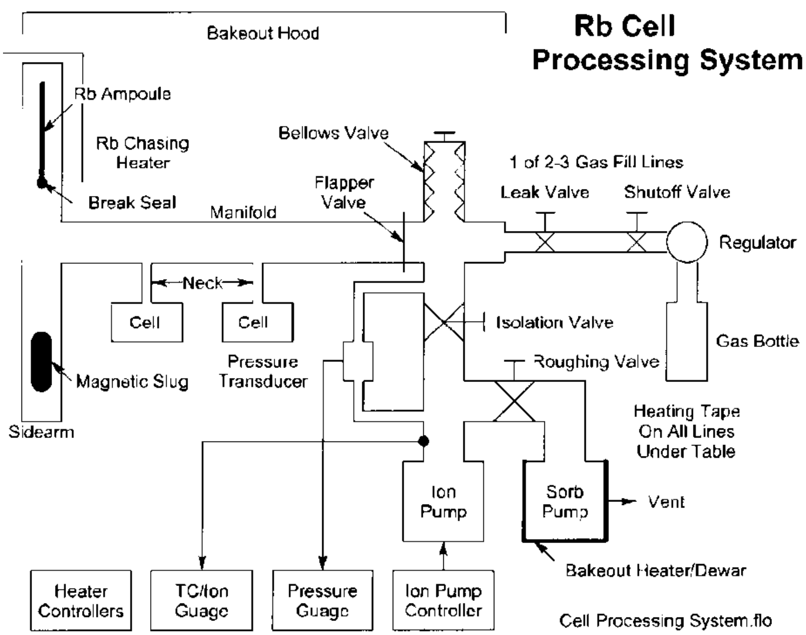

Figure 32. Typical Rb Cell Processing System

The processing begins by attaching the fabricated and chemically-cleaned lamp or cell envelopes to the side of the manifold by their tubulations, and attaching the sidearm with the Rb ampoule and slug to its end. After checking for gross leaks, plasma cleaning is performed by introducing a low pressure of inert gas into the system and exciting a glow discharge in the cells with a high-powered RF generator. The system is then baked out and pumped down to ultra-high vacuum.

After closing both the flapper and isolation valves, the Rb ampoule is broken and Rb metal is "chased" into the lamps or cells by heating the ampoule and allowing it to condense in them. Next, buffer gas is bled into the manifold and its pressure is adjusted with the bellows. Finally, the lamps or cells are pulled off the system by sealing and separating their tubulations (see Figure 33).

Figure 33. Pulling Lamps Off Vacuum System

Microwave Cavities

Essentially all RFS units use a cavity resonator to support the microwave magnetic field necessary to interrogate the Rb atoms in the absorption or resonance cell. Ideally the cavity would provide a uniform axial H field throughout its volume, and that condition is closely realized by a TE_{011} cavity with a cell at its center. That is what was used in early RFS units where miniaturization was not a primary concern. Since then, the trend has been toward the use of smaller cavities and other structures that, while having less ideal field patterns, allow the physics package to be smaller. To a large extent, the design of an RFS physics package (and the overall unit) begins with the selection of the microwave cavity, from which the entire design evolves.

The effect of cavity pulling on the frequency is quite small in a passive atomic frequency standard, it being proportional to the cavity mistuning, $\Delta f_c/f_0$, the small ratio (Q_c/Q_l) of the cavity and atomic line Qs, a factor α that depends on how close the system is to the maser oscillation threshold, and a saturation factor, S, that relates to the applied interrogation power [204]:

$$\frac{\Delta f}{f_0} = \frac{\Delta f_c}{f_0} \cdot \left(\frac{Q_c}{Q_l}\right) \cdot \frac{\alpha}{1+S}.$$

Typical values for an RFS are $(Q_c/Q_l) \approx 10^{-5}$, $\alpha \approx 0.01$ (1% of maser oscillation threshold) and $S \approx 1$ (for normal line broadening). The frequency of a cavity is proportional to its linear dimensions, and aluminum has a thermal expansion coefficient of about 20 ppm/ºC, leading to a cavity pulling effect of about 1×10^{-12}/°C. For a cavity oven stabilization factor of 100, this TC effect is negligible (as is the frequency offset compared with the buffer gas offset). Note that this does not consider the effect of cavity detuning on the interrogation power level along with the RF power shift coefficient. Nor does it consider the possibility of a stability floor due to oven temperature set point fluctuations.

The H-field distributions of the near-ideal TE_{011} and smaller TE_{111} cavity modes are shown in Figure 34 (a) and (b) respectively [6]. Note that the optimum position for the resonance cell is at the center of a TE_{011} cavity.

The 6.8 GHz microwave cavity of a RFS, more than any other item, determines the size of the physics package, and much effort has been devoted toward devising small microwave cavities/resonators having a suitable H-field distribution. The classic TE_{011} has an ideal field pattern, but is quite large (the size of a coffee mug) even if dielectrically loaded, and various smaller TE_{111} and "magnetron" configurations have been used. More recently, a significantly smaller capacitively-tuned re-entrant resonator has been developed for a very small commercial RFS.

The 6.8 GHz microwave cavity of an RFS must provide a reasonably linear and uniform H-field pattern parallel to the DC magnetic bias (C-field), generally, but not necessarily, along the optical axis. For a TE_{011} cavity, the cell is positioned at the center. For a TE_{111} cavity, it fills the entire cavity. Only moderate Q ($\approx$100) is wanted, to reduce the microwave power requirement without making the tuning critical. Microwave power is applied to the cavity via an E-probe or H-loop. Non-uniform microwave magnetic field strength causes signal loss and spatial frequency differences that produce line broadening and RF power sensitivity. RF power sensitivity (frequency versus microwave power) is especially important for an integrated cell, where the frequency has a relatively large spatial variation due to light shift as hyperfine filtering occurs along the optical path.

The microwave cavity is also a temperature-controlled oven for the resonance/absorption cell, and it often houses a step recovery diode (SRD) microwave multiplier. Residual magnetic field from the oven heater must be minimized to avoid a pseudo temperature coefficient. The C-field coil is generally wound either on the outside of the cavity or, in the case of a TE_{111} cavity, directly on the cell. A temperature gradient is needed to keep the optical path free of condensed rubidium, but must not be so large as to cause line broadening.

It should be noted that, because of the field reversal in a TE_{111} cavity, it must be used either with a buffer gas or a septum to confine the Rb atoms to one region during the time of an interrogation cycle.

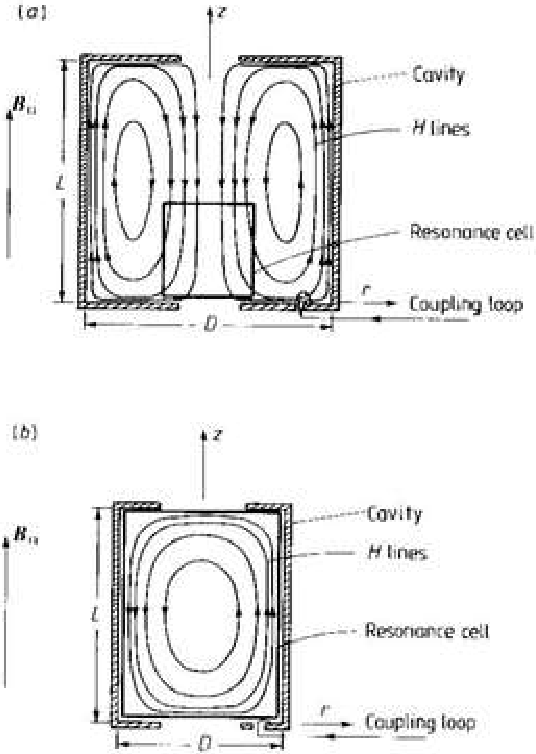

TE_{011} Cavity H-Field Lines

TE_{111} Cavity H-Field Lines

Figure 34. Cavity Modes

At 6.8 GHz, a TE_{011} cavity is about the size of a coffee mug, while a TE_{111} cavity resembles a “C-size” flashlight battery. Either can hold a 1” diameter by 1” long typical full-sized cell that operates at around +65°C, in the center of the TE011 cavity or filling the TE_{111} cavity. The H-field of the TE_{011} mode is radially symmetric, but it is asymmetric for the TE_{111} mode, having two regions of higher H-field intensity whose orientation is determined by the way the RF current flows across the ends. A slotted end cap can be used to let light to pass through while allowing the current to flow. The resonant frequency of an unloaded TE_{111} cavity is given by [113]:

$$f = \sqrt{\frac{0.478x10^8}{D^2} + \frac{0.348x10^8}{L^2}}$$

where f is the frequency in MHz, and D and L are the diameter and length of the cavity in inches. Some dielectric loading is provided by the cell, and more can be added to make the cavity smaller.

The RF current flows in concentric circles around the end cap of a TE_{011} cavity, and a central opening for the light does not have much effect on it. No current flows laterally from the end cap to the cylindrical portion, and gaps can be inserted at the ends to suppress the nearby TM mode. A waveguide beyond cutoff can be added to the end of the cavity to isolate the light path to the photodetector.

The cavity Q is not particularly critical. High Q is not needed as much as H-field uniformity. Low Q reduces frequency pulling in a passive atomic frequency standard, while higher Q reduces the required RF power to achieve the optimum microwave H-field strength. Lower Q also reduces the need for precise tuning, and the effect of subsequent de-tuning. A Q of about 100 is a reasonable value. Energy may be coupled into a microwave cavity by either an H-field loop or an E-field probe, often associated with a SRD microwave multiplier.

Condensed rubidium in the absorption/resonance cell can de-Q the cavity and can also obscure the light path. In a very clean cell, a highly-conductive but invisible film can form on the cell surface when it cools. Cavity de-Qing is a much more important consideration when TE_{011} cavity is used because the cell walls are within microwave field rather than at the wall of a TE_{111} cavity. Early RFS units that used TE_{011} cavities often had cells with long tubulations that protruded outside the cavity where the excess Rb condensed at a cooler location (thermoelectric cooling was also used for that purpose). That had the undesirable effect of producing long stabilization times, and is unnecessary for TE_{111} cavities where the excess Rb is driven from the optical path by the small thermal gradient created by heat (IR radiation) from the hotter lamp oven. The thermal transfer from the cavity oven to the cell is an important factor for fast RFS warm-up.

Jin Resonator

The Jin Resonator (see Figure 35) is the enabling technology for making the Symmetricom X72 so small [208], [347]. It can be understood as the progression from a lumped LC resonant circuit to two small inductances formed by the box in parallel with an off-center capacitive tuning post.

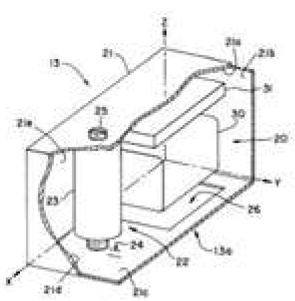

13=Resonator Assembly
23=Tuning Rod
26=Hole for Light
30=Rb Cell
31=Photodetector
Volume ≈ 1 cm^3

Figure 35. Jin Resonator

C-Field

An RFS physics package always includes a coil around the absorption or resonance cell or its microwave cavity to produce a DC magnetic field along the axis of the microwave H-field that orients the Rb atoms and separates the Zeeman lines so that the unit locks up on the $M_F=0$, $\Delta M_F=0$ transitions with a small quadratic field dependence. The C-field also provides a means for adjusting the RFS frequency to correct for cell fill tolerances and frequency drift. Figure 36 shows the RFS C-field characteristic, $f = 573 \cdot H^2$, where f is the frequency offset in Hz and H is the magnetic field in Gauss. A typical C-field coil has a coefficient of 30 mG/mA and is operated from 50 mG to 300 mG, providing a tuning range of about 7.3×10^{-9}. It can, of course, only raise the frequency.

There are several important advantages of operating an RFS at a minimum C-field setting of 50 mG, including a relaxation of the magnetic shielding and C-field stability requirements. That can be made feasible by including provisions for boosting the C-field during lock acquisition and by using an adjustable synthesizer to correct for absorption/resonance cell fill tolerances and subsequent frequency drift.

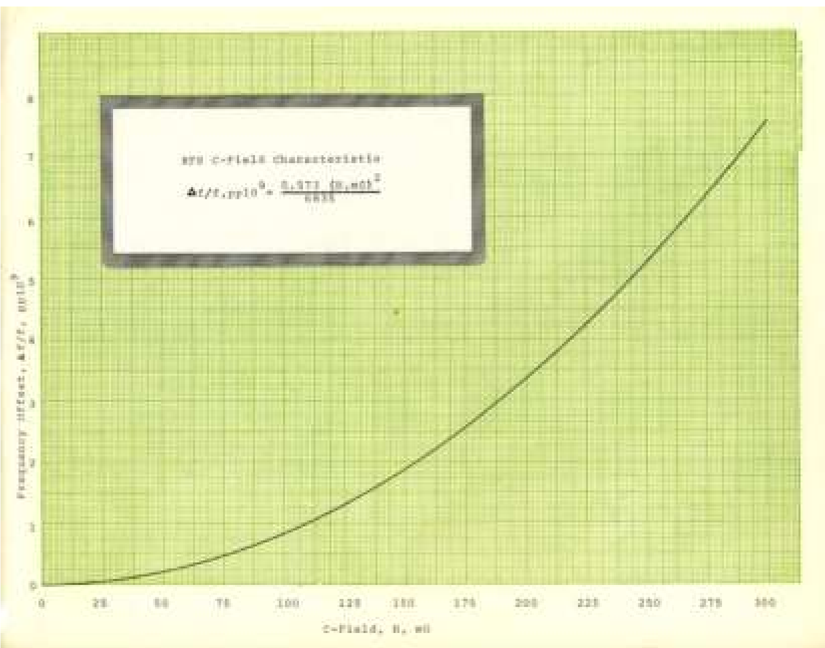

Figure 36. RFS C-Field Characteristic

Advantages of Fixed Minimum C-Field

The quadratic RFS C-field dependence means that the incremental C-field dependence varies linearly with its nominal value according to the expression (where H is C-field in Gauss in this and the following equations):

$\Delta f/f = 1.68\text{x}10^{-7} \cdot H \cdot \Delta H$

and the fractional C-field sensitivity therefore varies as H^2:

$\Delta f/f = 1.68\text{x}10^{-7} \cdot H^2 \cdot \Delta H/H.$

The first equation applies to the case of a small field change (perhaps caused by an external field), while the second equation describes a fractional C-field change (perhaps due the TC of the C-field source reference zener). At a nominal C-field of 250 mG, those sensitivities are:

$\Delta f/f = 4.19\text{x}10^{-8} \cdot \Delta H = 1.05\text{x}10^{-8} \cdot \Delta H/H.$

For example, if an RFS has a magnetic sensitivity specification of $1\text{x}10^{-12}$/Gauss, the C-field can change by no more than $1\text{x}10^{-12}/4.19\text{x}10^{-8}$ = 24 µG/G, which requires a shielding factor of about 42,000. Similarly, for a fractional frequency change of $1\text{x}10^{-13}$, the C-field must be stable to a factor of at least $1\text{x}10^{-13}/1.05\text{x}10^{-8}$ = 9.5 ppm.

These requirements can be relaxed by factors of 5 for the shielding factor and 25 for the C-field stability by operating at the minimum 50 mG C-field value.

C-Field Commutation

The sensitivity of a rubidium frequency standard to external DC magnetic field is always reduced by surrounding its physics package with magnetic shielding. That sensitivity can, in principle, be reduced further by symmetrically commutating the C-field to provide first-order cancellation of the effect of the external field [322].

As stated above, the Rb hyperfine frequency magnetic field dependency is quadratic according to the relationship:

$f = 573 \cdot H^2$

where f is the frequency offset in Hz, and H is the magnetic field strength in Gauss. If H is the sum of the applied C-field, H_C, and the residual external (or Earth's) field, H_E, then the frequency offsets for the two directions of the commutated C-field are:

$f_1 = 573 \cdot (H_E + H_C)^2 = 573 \cdot (H_E^2 + 2H_E H_C + H_C^2)$, and

$f_2 = 573 \cdot (H_E - H_C)^2 = 573 \cdot (H_E^2 - 2H_E H_C + H_C^2)$, and their average is $\overline{f} = (H_E^2 + H_C^2)$.

For the case where the residual external field is small compared with the C-field, $H_E \ll H_C$, the H_E^2 term is very small, and the commutated average frequency offset is approximately equal to the desired undisturbed value:

$$\overline{f} \approx 573 \cdot H_C^2$$

instead of non-commutated values of

$$f_1 = 573 \cdot (H_C^2 + 2H_E H_C) \text{ or } f_2 = 573 \cdot (H_C^2 - 2H_E H_C).$$

For example, for $H_E = 0.1 \cdot H_C$, the additive non-commutated field is 1.21 while the commutated field is 1.01. Commutation thus provides a significant reduction in the effect of the external field disturbance (1% versus 21%, in this example).

Unfortunately, it is hard to successfully implement C-field commutation because of the difficulty of gracefully reversing the direction of current flow through an inductor (the C-field coil). Transients are produced that degrade the speed and symmetry of the commutation, and, even more importantly, create unwanted modulation and interference that impairs RFS operation. Slow commutation produces unacceptable FM equal to the difference between the two commutated frequencies, $\Delta f = 4 \cdot H_E H_C$, commutation near or synchronous with the servo modulation rate produces unacceptable interference with the frequency lock loop, and fast commutation aggravates the switching transient problems.

Active C-field commutation may have merit in special situations, but it is not a viable general substitute for adequate passive magnetic shielding in a rubidium frequency standard.

C-Field Boost During Lock Acquisition

The minimum allowable C-field during lock acquisition is dictated by the accuracy and tuning range of the crystal oscillator as it is swept to find the Rb resonance. It is necessary that the C-field be sufficient to prevent lockup on a Zeeman line. The first order Zeeman lines occur at a separation of ±700 kHz/Gauss, so, for a VCXO with a tuning range of ±10 ppm, the minimum C-field to assure proper lock acquisition is:

$$H_{\text{min}} = 10\text{x}10^{-6} \cdot 6835\text{x}10^{6} / 700\text{x}10^{3} = 100 \text{ mG}$$

If a lower C-field value is desired during normal operation (say 50 mG), then the C-field should be boosted during lock acquisition.

Magnetic Shielding

An RFS physics package must include magnetic shielding to provide a clean C-field and to avoid frequency sensitivity from external DC magnetic fields, including the Earth's field of about 0.5 Gauss.

Calculations of magnetic shielding factor are only approximate at best because the actual geometry is different from that of common equations for the radial attenuation of infinite nested cylindrical shields. Formulae do exist for calculating the axial (longitudinal) shielding factor for one or two nested cylindrical shields, but not for three or more, where only approximate expressions are available. That shielding factor is higher smaller values of length/radius (L/R). Real RFS shields, even if nested cylinders, must provide axial attenuation, and are subject to fringing effects at their ends. They may also have holes and more complex shapes. Shielding formulae are therefore useful for only first approximations, which can provide insight into important design variables (e.g., L/R, permeability, annealing process, thickness and spacing), must yield to empirical measurements to obtain accurate values. An axial shielding factor of 200,000 is possible with three shields, especially if one of them is a larger outer case. Modern electromagnetics modeling software may be of some help. Large shielding factor measurements are often made using low-frequency AC excitation using a Helmholtz coil to produce a uniform external field and a multi-turn pickup coil the size and shape of the absorption/resonance cell, perhaps using a lock-in amplifier as the detector. Those measurements generally correlate well with actual frequency sensitivity. It is important to measure the shielding at the specified level external field. RFS magnetic sensitivity is generally measured by observing the frequency change caused by a reversal of the largest specified field. Besides shield permeability and thickness, end spacing is particularly critical to avoid reduced shielding due to fringing. Removable end caps must fit tightly and have generous overlap, and holes should preferably be at the sides or off-axis. Shields should be carefully heat treated (annealed) after any machining is done, and handled with care afterwards. In critical applications, each manufacturing lot should be tested.

Magnetic shield saturation is seldom a problem, but may favor using a lower-permeability, higher saturation flux material for the outer shield. As its permeability decreases in a high external field, the inner shields are biased higher and have higher permeability than their initial value. Obtaining adequate magnetic shielding becomes increasingly difficult as the overall physics package is made smaller, and it becomes necessary to use the outer case for that purpose. On the positive side, that material also serves well to shield against EMI and nuclear radiation. High permeability tape is sometimes a useful supplement to thicker shields.

Besides passive magnetic shielding, the magnetic field sensitivity of an RFS can be reduced by (a) operating the unit at low C-field, (b) orienting it that its C-field axis is orthogonal to the external DC magnetic field, (c) by measuring and compensating for the external magnetic field by using a magnetic sensor, (d) by occasionally operating the unit on a Zeeman transition to measure and correct the C-field, or (e) by periodically reversing the polarity of the applied C-field (commutation) to eliminate the quadratic dependence to first order. Method (a) is facilitated by having a high-resolution synthesizer to make frequency adjustments, method (b) is feasible only in certain specific cases, method (c) has been implemented with limited success using Hall-effect magnetic sensors, method (d) has been proven highly effective for a unit that has microprocessor control and high-resolution frequency synthesis, and method (e) has also been used, but with limited success.

The innermost RFS magnetic shield is usually close to the C-field winding to improve its magnetic field uniformity. Any effort to optimize C-field uniformity must include the effect of magnetic materials in close proximity, including hardware, electronic devices and heater currents. The latter vary with ambient temperature and can contribute toward a unit's temperature coefficient. A useful diagnostic is to compare the TC for both C-field polarities. Double-layer, meander-pattern metal foil heaters with twisted leads have much lower residual field than transistor heaters.

RFS magnetic shields should be degaussed *in situ* before being used. This can be done by placing the entire RFS in a solenoidal coil with a series-resonating capacitor and driving it from the power line via an adjustable autotransformer. The excitation should be sufficient to saturate the innermost shield and then be slowly reduced to zero, thereby eliminating residual magnetism.

Photodetectors

Rubidium frequency standards use large area silicon photodiodes to detect the light transmission through their physics packages. A smaller photodetector would require bulky focusing optics. Silicon photodiodes have excellent responsivity at the Rb 780 and 795 nm wavelengths (see Figure 37), and should have high shunt resistance (low dark current) at their operating temperature to minimize noise, as well as reasonably low zero-bias capacitance.

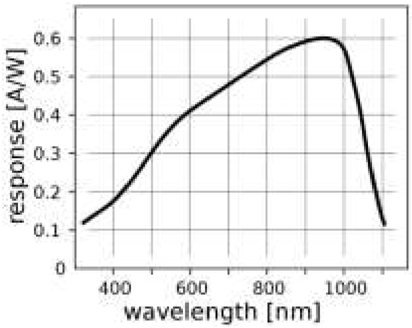

Figure 37. Si Photodiode Responsivity

The photodetector shunt resistance determines the amount of noise current that flows as a result of voltage noise at the input of the preamplifier op amp. It is measured as the leakage (dark) current that flows when a small reverse voltage is applied across the junction.

Radiation hardness, particularly responsivity loss in a neutron environment, can also be a consideration. Neutron bombardment creates lattice defects that cause loss of photo carriers due to recombination before they can diffuse out of the junction.

ELECTRONICS

These primer sections cover the electronics of rubidium frequency standards, and the design and implementation of their circuits.

Preamplifier

The function of an RFS preamplifier is to convert the photodetector current into an amplified output voltage. The DC preamplifier output indicates the light level of the Rb lamp, and the AC output provides the discriminator signal to the servo amplifier. A typical basic preamplifier circuit is shown in Figure 38. It is a single-stage op amp transimpedance amplifier that converts the photodetector current into an output voltage. The photodetector operates at zero bias across the op amp input terminals, which presents low input impedance (determined by the transimpedance divided by the op amp open-loop gain at any particular frequency) which reduces the effect of the photodetector capacitance. The DC transresistance is determined by the sum of the resistors between the non-inverting input and ground, and between the inverting input and op-amp output. The much higher AC transimpedance is determined by those resistors and the shunt resistor of the "T" feedback network. The capacitors shape the AC frequency response, which is broadly peaked at the fundamental modulation rate.

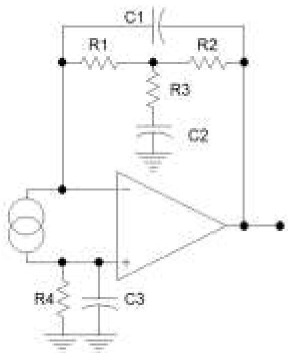

DC Transresistance:

$R_T = R_1+R_2+R_4$

Peak AC Transimpedance:

$Z_T(max) = R_1+R_2+R_4 + R_2/R_3 \cdot (R_1+R_4)$

Transfer Function:

$$F(s) = R_T \cdot \frac{s^2 C_1 C_2 [R_1 R_2 + R_3(R_1 + R_2)] + s[C_1(R_1 + R_2) + C_2(R_2 + R_3)] + 1}{\{s^2 C_1 C_2 [R_1 R_2 + R_3(R_1 + R_2)] + s[C_2 R_3 + C_1(R_1 + R_2)] + 1\} \cdot (sC_3 R_4 + 1)}$$

Figure 38. Basic Preamp Circuit

Noise at the fundamental servo modulation frequency is the main consideration for the preamplifier circuit. Excluding photodetector shot noise, the largest noise contributor is usually the noise current due to op amp input voltage noise that flows through the photodetector shunt resistance. Other noise sources are the op amp input current noise and the Johnson noise of the resistors.

S/N Ratio

The dominant noise source in a rubidium gas cell passive atomic frequency standard is shot noise at the photodetector. Shot noise has a white power spectral density, and the discriminator signal at the photodetector represents the frequency error, so this noise corresponds to white FM, and it therefore results in a frequency instability (Allan deviation) that varies inversely with the square root of the averaging time [191]. In addition, it is necessary to include a term that represents the contribution of the phase noise of the RF interrogation signal at twice the servo modulation frequency that causes additional white FM noise due to an intermodulation effect [189]. RFS stability is therefore determined by a combination of the signal-to-noise ratio (S/N), rubidium line Q, and the phase noise of its crystal oscillator according to the following expression:

$$\sigma_y(\tau) = \frac{0.11}{Q_l \cdot (S/N) \cdot \sqrt{\tau}}$$

where Q_l = Rubidium line Q, full width measured at half amplitude (FWHA).

Rubidium linewidth, maximum signal power, and the photodetector bias current can all be measured in the laboratory. The signal-to-noise ratio at the output of the photodetector is defined in a 1-Hz bandwidth as:

(S/N) = (maximum signal power / shot noise power)$^{1/2}$
= [(rubidium signal current)^2/ $(2eI_0)$]$^{1/2}$

where

I_0 = photodetector bias current
e = electron charge = $1.6\text{x}10^{-19}$ coulomb.

Q_l is usually measured at normal microwave interrogation power and line broadening, and a typical value is about 10 million.

The shot noise is caused by the photodetector DC current, which can be calculated from the preamplifier DC output level and its DC transresistance. A typical value is 50 to 100 μA.

The maximum signal current is calculated based on the peak fundamental rms signal at the output of the preamplifier and its transimpedance gain at fundamental frequency.

The contribution to stability due to the VCXO phase noise is discussed in References [213] and [214]. The second paper indicates that a good estimate of the stability limit can be made by using the following equation:

$$\sigma_y(\tau) = \frac{\left[S_y(2f_M)\right]^{1/2}}{2\sqrt{\tau}}$$

where:

$S_y(2f_M)$ = Power spectral density of fractional frequency fluctuations at twice the modulation frequency (f_M)

$S_y(2f_M)$ is related to the phase noise of the primary loop oscillator by the following equation:

$$S_y(2f_M) = \frac{(2f_M)^2}{f_0^2} S_\phi(2f_M) = 2\frac{(2f_M)^2}{f_0^2} 10^{\mathcal{L}(2f_M)/10}$$

where:

$\mathcal{L}(2f_M)$ = Phase noise of the primary loop oscillator at twice the modulation rate
f_M = Modulation rate
f_0 = Nominal VCXO frequency

The two effects combine as the square root of the sum of their squares.

Analog Servo Amplifiers

A typical analog RFS frequency lock servo is shown in Figure 39. The upper channel processes the fundamental discriminator signal to produce a control voltage for a VCXO, while the lower channel detects the 2nd harmonic signal and serves as a lock detector. A sweep circuit aids lock acquisition.

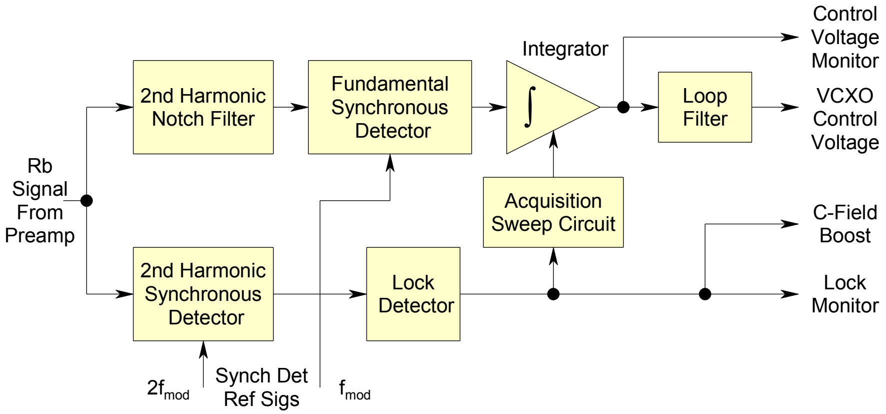

Figure 39. Typical Analog Servo Amplifier Block Diagram

Another way to efficiently configure an RFS servo amplifier is to pass the recovered signal serially through the 2nd harmonic detector and then the fundamental detector. The first stage not only detects the 2nd harmonic level, but it also converts it to a 4th harmonic signal that is more easily low-pass filtered ahead of the fundamental detector, while the fundamental signal is folded back to its fundamental frequency for detection in the second stage.

Low Pass or Notch Filtration

It is desirable to reduce the relatively high level of 2nd harmonic signal that reaches the fundamental synchronous detector in order to improve its dynamic range and ability to null the fundamental component. This can be accomplished by low pass or notch filtration. Notch filtration has the advantage of providing large 2nd harmonic attenuation without significant fundamental phase shift. The Hall notch filter circuit shown in Figure 40 is particularly effective.

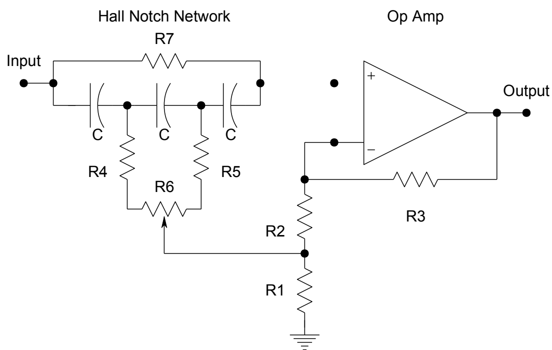

Design Equations:

$$Q = \frac{1}{4(1-\alpha)}\ ;\ \alpha = \frac{R1}{R1+R2}$$

$$R7 = 6 \cdot (R4 + R5 + R6)$$

$$f_{notch} =$$

$$\left[2\sqrt{3} \cdot \pi \cdot C \cdot (R4 + R6/2)\right]^{-1}$$

$$\text{Gain} = \frac{R3}{R1+R2} + 1$$

Figure 40. Hall Notch Filter

Synchronous Detection

Synchronous detection is a signal processing technique that provides optimum detection of a signal whose frequency and phase is known. Also known as a lock-in amplifier, it was invented by Robert Dicke in 1946, and has become a common means for processing weak signals in scientific instruments. Functionally, it can be considered a rectifier (AC to DC converter) that responds only to an AC signal at the frequency and phase of its reference signal. In the context of rubidium frequency standard technology (to which Dicke also made important early contributions), synchronous detection is the means employed to precisely null the discriminator signal from the Rb physics package, thereby locking a crystal oscillator to the exact center of the Rb atomic resonance. This process is enabled by applying AC modulation to the RF interrogation and using the same modulation source as the reference for the synchronous detector. An analog full-wave synchronous detector is generally implemented by a pair of switches driven by bi-phase reference signals, and it is sensitive only to an AC input signal at the reference frequency (and its odd harmonics) having the same phase.

It is important to realize how extremely well the line center must be found. Consider a GPS Rb clock having a linewidth of 150 Hz at 6835 MHz that realizes a stability of 1×10^{-14}. The frequency lock loop, and in particular, the fundamental synchronous detector of the servo amplifier must therefore locate and maintain the frequency to within 68 μHz, thus "splitting" the resonance line by a factor of about 2 million.

An example of a basic analog synchronous detector circuit is shown in Figure 41.

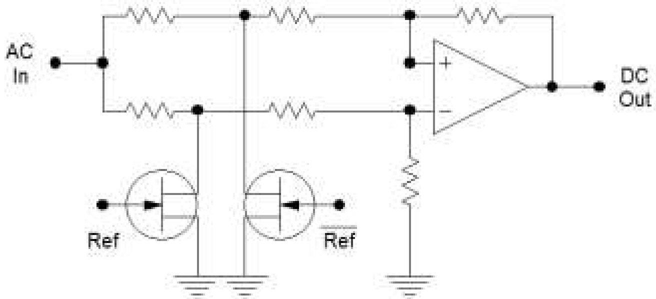

Figure 41. Basic Synchronous Detector Circuit

This configuration uses shunt FET switches to switch a differential amplifier from an inverting to a non-inverting configuration in response to the bi-phase reference signals. Other configurations using series switches and other switch types are obviously possible. It is critical to keep the reference signals from the synchronous detector input, and to maintain circuit symmetry in order to avoid offsets and maintain high quadrature and even harmonic rejection.

A numerical implementation of (perfect) synchronous detection is obviously possible by appropriately multiplying the signal waveform by +1 or -1.

In an RFS servo, the synchronous detector operates with an integrator to null the fundamental component of the recovered physics package discriminator signal, the condition at the center of the Rb resonance line.

Frequency Lock Loop

The frequency lock loop is an essential part of any RFS, and its transfer function affects its overall stability as described in Reference [213], reproduced in part as Figure 42 below.

Passive atomic frequency standards

In the case of passive atomic frequency standards, a frequency-lock loop is used. A block diagram of such a system is shown in figure 7. In order to reduce the effect of frequency drifts of the quartz crystal oscillator, it is general practice to use for F(p) an integrator with transfer function,

$$F(p) = \frac{1}{p t_1}, \quad (13)$$

where t_1 = RC is the time constant of the integrator. In this case, the spectral density of the locked quartz crystal oscillator is given through simple analysis by,

$$S_{yq}^{L}(f) = \left[\frac{(f/f_n)^2}{(1+(f/f_n)^2)}\right] S_{yq}^{f}(f) + \left[\frac{1}{1+(f/f_n)^2}\right] S_{yr}(f), \quad (14)$$

where

$$f_n = \frac{n K_v K_I}{2\pi t_1} \quad (15)$$

which defines f_n. Here K_I is the equivalent frequency discriminator sensitivity of the atomic ensemble coupled to the phase sensitive detector, in volts per radian per second. K_v has the same meaning as in the case of the phase-lock loop.

Figure 42. PSD of Passive Atomic Frequency Standard with Pure Integrator Frequency Lock Loop

Here, a simple pure integrator is assumed, and the power spectral density (PSD) of the fractional frequency fluctuations of the locked quartz oscillator that produces the output signal, $S_{yq}^{l}(f)$, 1/Hz, is determined by the PSD of the oscillator, $S_{yq}^{f}(f)$ and the PSD of the atomic reference, $S_{yr}(f)$. In addition, it is necessary to include a term that represents the contribution of the crystal oscillator phase noise at twice the servo modulation frequency that adds a white FM noise due to an intermodulation effect. Those factors are analyzed in Reference [214] as excerpted in Figure 43 below:

$$S_y(f) = \left[\frac{G(f)}{G(f)+1}\right]^2 \left[S_y^{R} + \frac{S_y^{o}(f)}{G^2(f)}\right] + S_y^{N}(f) \quad (1)$$

where $Sy^{o}(f)$ is the open-loop spectral density of fractional frequency fluctuations of the probe source, $Sy^{R}(f)$ is that of the reference, and $Sy^{N}(f)$ is that of the detector and interrogation noise referred to the demodulator output. Cutler [10] has pointed out that noise in the local oscillator at the 2nd harmonic of the modulation frequency, which is usually ignored, causes a time varying frequency offset that is undistinguishable from reference noise. This sets the lower limit to the interrogation noise and often sets the lower limit of the noise performance of the local oscillator necessary not to degrade the overall performance. The magnitude of the 2nd harmonic noise modulation in radians/s is estimated in appendix B of [1] to be $k_2 = 2\pi\nu_0 (S_y(\Omega/\pi))^{1/2}$, where $\Omega/(2\pi)$ is the modulation frequency. This leads to an interrogation noise term which is of order [1,4,10] $S_y^{N}(f) = 1/(16\pi)\, S_y^{o}(\Omega/\pi)$. For large values of G(f), $S_y(f)$ of the probe source reflects that of the reference plus the added noise of the detection system [1-6].

Figure 43. PSD of Passive Atomic Frequency Standard with General Frequency Lock Loop

Here the frequency lock servo is characterized by its open-loop (OL) transfer function, G(s), a typical example of which is shown below, whose configuration includes a lag-lead filter which is commonly used to allow higher gain at low frequencies.

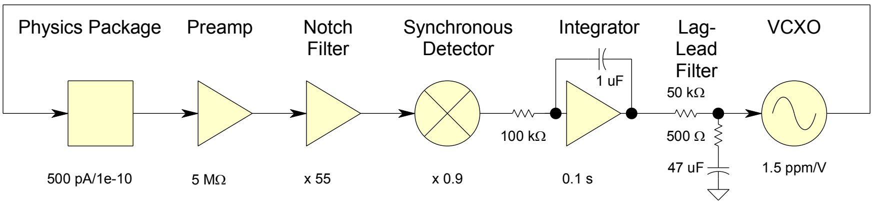

Figure 44. Model of RAFS Servo

Figure 44 shows the model for the frequency lock servo. The combination of the gain blocks is x1860 and the integrator block has a time constant of 0.1 seconds, resulting in an overall integration characteristic having 0 dB gain at 2960 Hz and a transfer function $G_1(s)=18600/s$. The lag-lead network with R1=50k, R2=500 and C=47 μF has a transfer function $G_2 = (1+Ts)/(1+\alpha Ts)$ where $T = R_2C = 0.0235$ seconds and $\alpha = (R1+R2)/R2 = 101$, with $\alpha T = 2.37$ seconds. This leads to the overall OL servo transfer function shown in Figure 45.

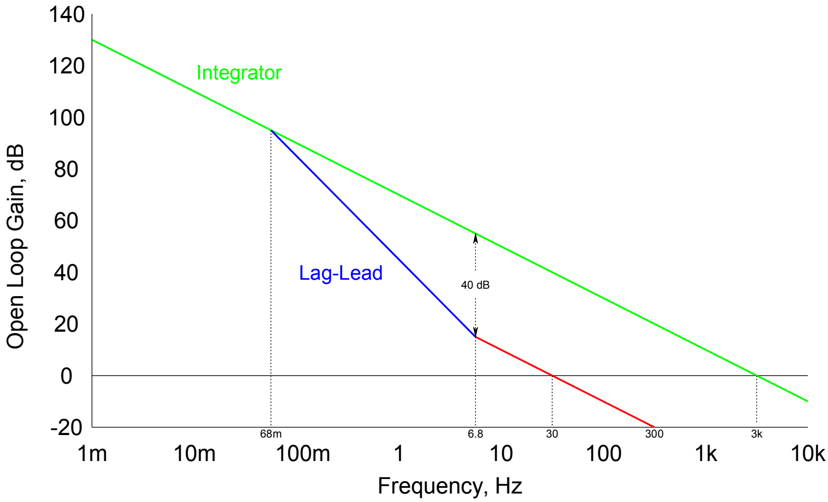

Figure 45. RAFS Servo Open Loop Gain (Log Approximation)

For good loop stability, the OL servo gain characteristic slope at 0 dB must be about -6 dB/octave. Thus the overall characteristic is a (not quite pure) integrator with a -20 dB/decade roll-off plus a lag-lead network seen at the central frequencies as an increase in the roll-off rate to -40 dB/decade between about 68 mHz and 6.8 Hz that provides an additional attenuation of -40 dB to stabilize the loop. The closed-loop (CL) bandwidth is at about 30 Hz and the resulting phase margin is a comfortable 80º.

Lock Acquisition

An RFS frequency lock loop does not necessarily lock-up on its own, and may need a specific means of lock acquisition. If the initial VCXO frequency is too far away from the Rb resonance there may not be sufficient discriminator signal to drive servo loop into lock. In that case, it is necessary to sweep the frequency until a signal is detected. Fortunately, that process is quite simple because the servo integrator is easily made to sweep the VCXO control voltage by injecting an offset current into it, and the 2^{nd} harmonic synchronous detector provides a means for indicating lock. When an RFS is turned on, the VCXO control voltage sweeps until it warms up sufficiently to produce a discriminator signal. That signal then drives the servo loop into lock with a frequency offset caused by the integrator sweep injection. Then, when the signal reaches the lock detector threshold, the sweep is turned off and the unit operates normally. The whole process is very graceful. In some designs, especially when fast lockup is required, information from the fundamental detector is also used to control lock acquisition.

Digital Signal Processing

Digital signal processing (DSP) is increasingly an attractive alternative to an analog implementation of an RFS servo amplifier [346]. By converting the Rb recovered signal to numeric form with an analog-to-digital converter, it can be processed digitally to produce either a VCXO control voltage via a digital-to-analog converter, or, even better, to directly steer a numerically-controlled oscillator such as a DDS. Although these techniques are still evolving, they offer the advantage of eliminating analog errors, better reproducibility, simpler hardware and near-infinite DC gain since the processing is performed with software rather than analog circuits.

Several hybrid approaches can be taken to evolve from a purely analog to a purely digital servo amplifier. For example, Figure 46 shows a DSP servo whose front end uses an analog integrate and dump circuit that acquires information during each half-cycle of the modulation that is digitized, processed and converted into an analog control voltage. An important consideration is the need for a high-resolution (e.g., 20 to 24 bit) DAC. This technique is best applied for relatively slow modulation rates where there is no large 2^{nd} harmonic content and the modulation transients can be suppressed by the reset interval.

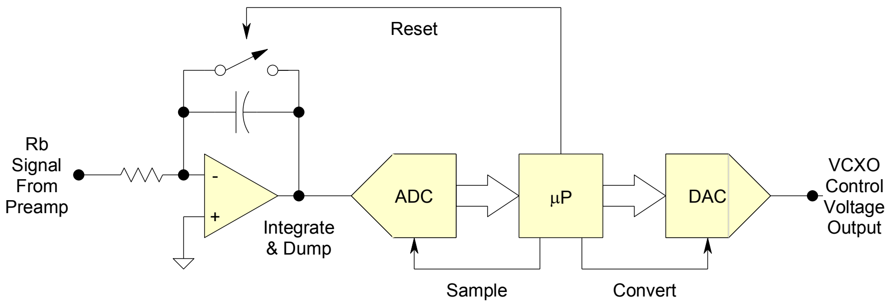

Figure 46. Integrate and Dump DSP Servo

Figure 47 shows the next step toward DSP where the inputs signal is digitized directly. In this case, the ADC will acquire multiple samples during each modulation cycle that are then averaged before further processing. The same high-resolution DAC requirement applies.

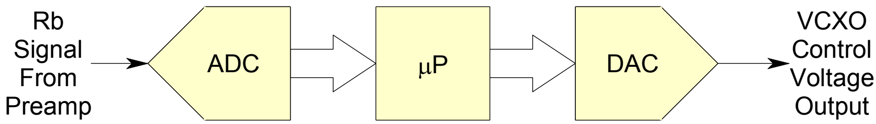

Figure 47. ADC and DAC DSP Servo

The final step toward an all-digital approach is shown in Figure 48. Here the oscillator is controlled numerically, eliminating the need for a high-resolution DAC. The NCO is probably part of a DDS synthesizer.

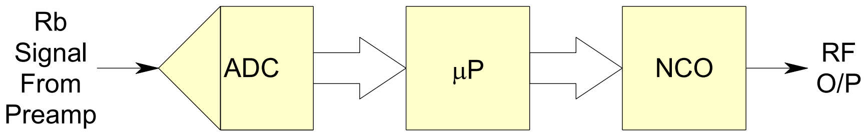

Figure 48. All Digital DSP Servo

An important consideration in implementing a DSP servo is the modulation rate, i.e., whether the recovered signal has a large 2nd harmonic component due to fast interrogation (in relation to the atomic resonance linewidth), or whether it more closely resembles a slower squarewave with a switching transient. Most analog RFS servos are the former type, and endeavor to implement a fast loop that tightly locks a VCXO to the atomic resonance. That has important advantages, especially when the stability of the atomic reference is better than that of the VCXO, and the latter two

DSP servo schemes are therefore preferred. The DSP software can quite easily implement signal averaging, synchronous detection and integration, and shaping of the overall loop response. It can also handle lock acquisition and monitoring, as well as supporting other more sophisticated processing tasks such as control of the RF interrogation power and C-field stabilization. Quadrature detection is also quite easily implemented, which can be used to determine and adjust the detector phasing.

An intermediate implementation can also be effective wherein an analog servo is controlled by a microcontroller. Digital signal processing can also be employed for other tasks in an RFS design, including adaptive oven temperature control.

Crystal Oscillators

The crystal oscillator is a key element in an RFS design, particularly since it determines the unit's output phase noise performance beyond the Rb loop bandwidth and it must also have sufficiently low phase noise, especially at $2 \cdot f_{mod}$ from the carrier, to drive the internal RF interrogation chain. Its vibration sensitivity is critical in tactical applications where the combination of passive vibration isolation along with a fast Rb loop can be an effective solution.

An especially challenging requirement is when the specified phase noise close to the carrier is better than can be provided by the Rb reference. In that case, a high performance OCVCXO is necessary along with a slow frequency lock loop. If also exposed to vibration, a special low g sensitivity crystal oscillator may be required.

RFS crystal oscillators therefore can take several forms. A high stability Rb reference with a fast servo may use a simple non-ovenized VCXO. More commonly, a simple VCXO with a temperature-controlled crystal is used, or perhaps the VCXO shares the physics package cavity oven. Often, the RFS oscillator is at a higher frequency than its output, which is obtained via frequency dividers. And, as described above, a high quality OCVCXO may be necessary to provide a low phase noise output, either as the main RFS source or as separate unit in a secondary phase-locked loop. In the limit, the overall system may be considered to be an OCVCXO loosely-coupled to an Rb reference to improve its aging.

Other Oscillators

Some RFS designs use additional oscillators. For example, the RF chain may include another phase-locked crystal, SAW or DRO VCO to reduce the phase noise of the microwave interrogation signal.

Transient Response

It must be expected that the quartz crystal resonator of an RFS VCXO will experience an occasional frequency jump, which will cause a permanent phase error. For example, a 1×10^{-9} VCXO frequency jump would cause a phase error that grows at the rate of 1 ns per second. For an RFS frequency lock loop that responds within

16 ms (a loop bandwidth of 10 Hz), that would cause a time error of only 0.016 ns. A transient upset of the frequency lock loop itself, without a VCXO or Rb reference frequency change, will not cause a permanent phase error since the input to the servo integrator represents frequency, and its VCXO control voltage output represents time (the integral of frequency), which does not change as long as the loop remains within its linear range. This is true even if the VCXO frequency requires some finite amount of time to recover [240]. In contrast, a jump in the Rb reference frequency causes a permanent frequency change and a corresponding time error that grows with time.

RF Chains

Many RFS RF chain designs have been successfully implemented as different RF components have become available. Most start with a requirement to produce a standard (e.g., 10 MHz) unmodulated RF output, thus requiring some form of frequency synthesis. Generally, the output signal is derived directly from a VCXO that is locked to the Rb atomic resonance and determines the phase noise and spectral purity outside the loop bandwidth. Early RFS RF chain designs were constrained by the need to use a relatively simple fixed integer (A/B) relationship between the Rb and output frequencies, thereby determining the absorption buffer gas offset, and requiring a variable C-field to make frequency adjustments. An important consideration is the way that their servo modulation is applied, generally by some form of analog phase modulator. Occasionally, the application does not require a standard output frequency, and in that case a simpler non-synthesized approach can be used. More rarely, it is acceptable for the output signal to contain the servo modulation, which also allows simplification. Modern RF chain designs can benefit from the availability of direct-digital synthesis (DDS) to support high-resolution digital frequency adjustment and near-perfect servo modulation. They can also benefit from the availability of RF components developed for wireless applications. Note that, as a general principle, one should not use the output of a DDS as the main source that is multiplied to the Rb frequency, but only as an offset that is mixed with a pure signal from a crystal oscillator because its phase noise is relatively high. The following examples show some of the RF chain configurations that have been used in RFS designs.

Figure 49 shows an example of an RF chain configuration that was popular during the age of discrete components. It utilizes a simple synthesizer scheme whereby the Rb frequency is generated by mixing a multiple of 60 MHz (x114 = 6840 MHz) with 5.3125 MHz, which can easily be obtained by mixing 5 MHz with 312.5 kHz (1/16th of 5 MHz, a particularly favorable binary divisor). The arrangement is further simplified by using a step recovery diode (SRD) multiplier as the final mixer. Modulation is applied with an analog phase-shifter near the bottom of the multiplier chain, and the power of the microwave interrogation signal can be conveniently adjusted by the level of the 5.3125 MHz component that is simply added to the 60 MHz SRD drive. The disadvantages of this approach are (a) a rather large 4.9 kHz buffer gas offset, and (b) a microwave spectrum containing many spurious components. It is important that the multiplicative contribution to the phase noise on the interrogation signal comes directly from the pure crystal oscillator. Other early RFS RF chain designs used a similar arrangement, but incorporated a complex ≈ 5.3125 MHz discrete-component synthesizer to allow frequency adjustments and a lower buffer gas offset. Still other designs of that era used separate multiplier and balanced mixer assemblies which allowed suppression of the otherwise stronger carrier component.

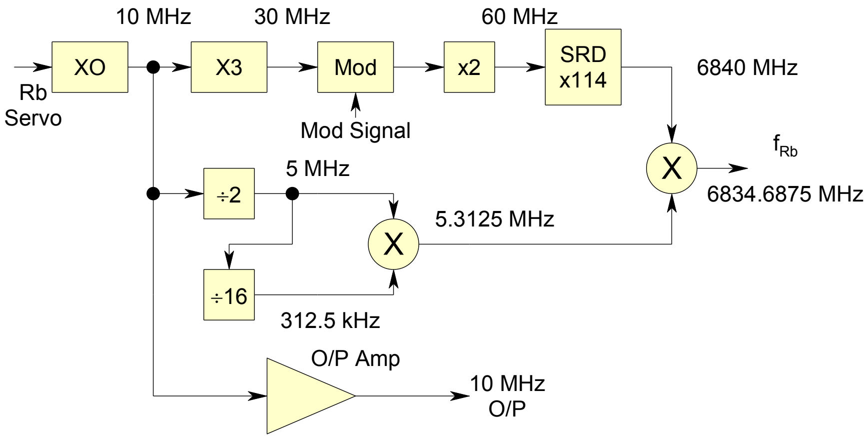

Figure 49 Classic RFS RF Chain

A modern version of that RF chain is shown in Figure 50, where the fixed 5.3125 MHz section is replaced by a high-resolution DDS that allows fine frequency adjustments and ideal squarewave FM. Additional advantages of the DDS are that it can correct for absorption cell frequency tolerances, and that it supports a simple means for temperature compensation.

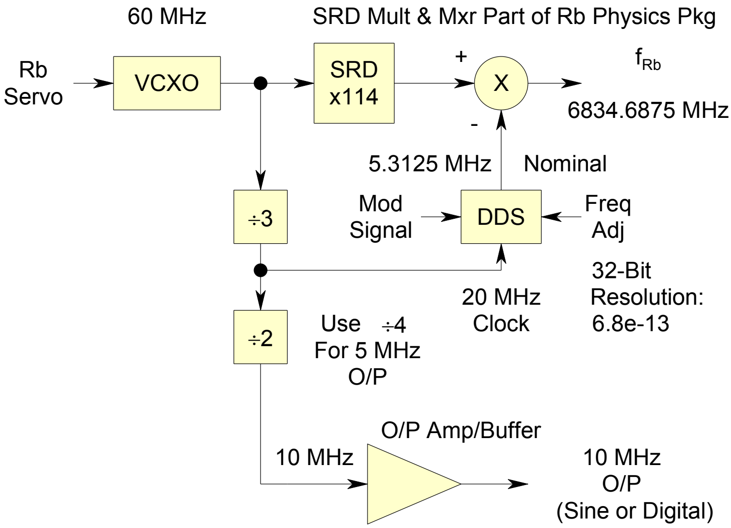

Figure 50. Modern Tactical RFS RF Chain

Another RFS RF chain arrangement is shown in Figure 51 which offers the advantage of a cleaner microwave spectrum by avoiding mixing in the SRD multiplier. A second crystal oscillator is used in a phase-locked loop (PLL) to generate a pure frequency near 90 MHz at a submultiple of the Rb resonance. In this scheme, the servo modulation is applied via the PLL. The x9 block is a simple diode harmonic mixer. Note that the fixed ÷ 143 divider could be replaced with a DDS synthesizer to apply FM and adjust for cell frequency tolerance but, because of the subsequent x76 multiplication, it would not have sufficient resolution for fine frequency adjustments.

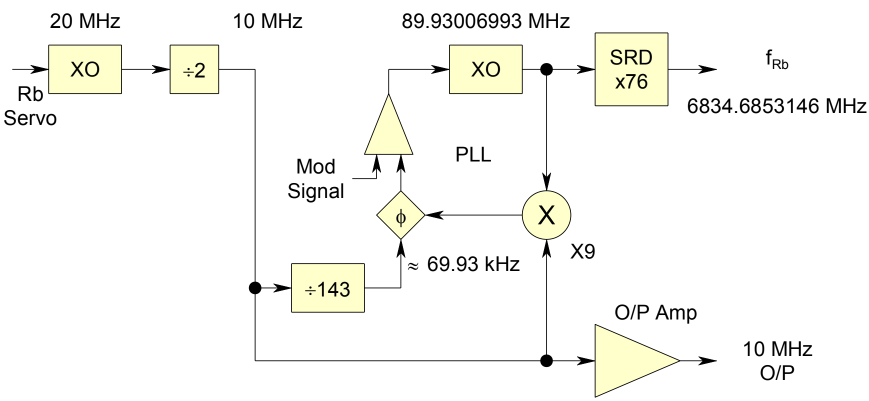

Figure 51. Another Tactical RFS RF Chain

An example of a non-synthesized RFS RF chain is shown in Figure 52, which shows the relative simplicity of this approach. This unit outputs a “natural frequency” of 13.40134393 MHz which is an exact sub-multiple of the Rb resonance. That frequency is used as the reference for the time-keeping system on board a GPS satellite, which provides conversion to 10.23 MHz and adjustments to correct for frequency offset and drift. If required, the RFS can utilize a divisor ratio of 2329/3051 to obtain 10.23 MHz in a secondary PLL.

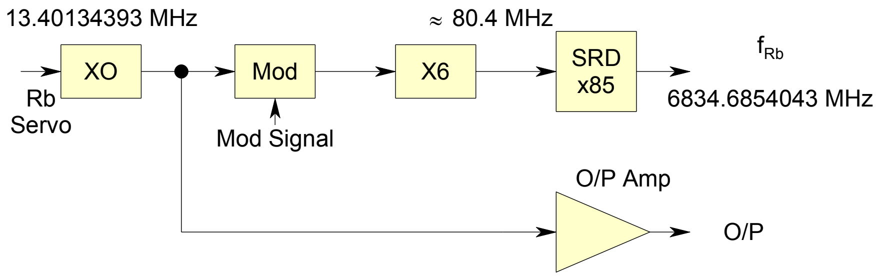

Figure 52. GPS RFS RF Chain

An especially simple synthesizer scheme suitable for timing applications is shown in Figure 53. Here a modulated and servo controlled 80.40806358 MHz VCXO at 1/85th of the Rb frequency is used as the clock for a DDS that produces a 10 MHz output. The DDS masks the servo modulation by spreading it into its noise sidebands, producing an output that is quite suitable for driving a clock.

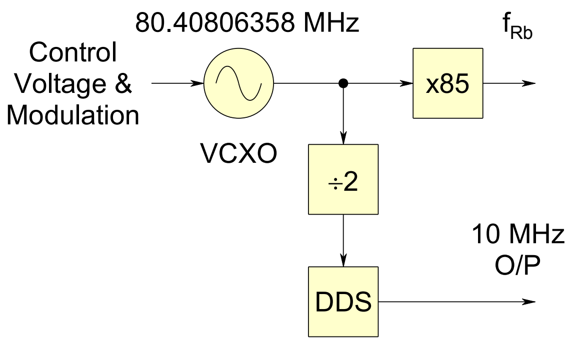

Figure 53 Simple Rb Clock RF Chain

As a final example, Figure 54 shows the RF chain of a modern commercial RFS that uses telcon RF ICs in its implementation. This design is noteworthy for the absence of a SRD multiplier. Instead an ≈ 2.3 GHz VCO, PLL and SSB mixer are used along with a simple diode tripler to generate a pure microwave interrogation signal that is tuned and modulated by a DDS.

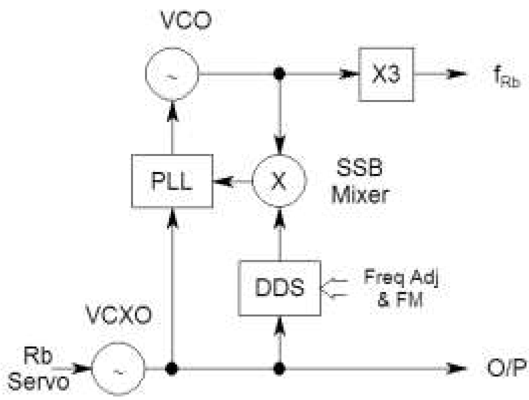

Figure 54. Modern Commercial RFS RF Chain

Output Amplifiers

Most rubidium frequency standards output a 5 or 10 MHz sinusoidal RF signal at a typical power level of +7 dBm into a 50 ohm load. Salient characteristics of the RF output include harmonic distortion (e.g., -30 dBc), non-harmonic spurious components (e.g., -80 dBc) and output impedance and VSWR (e.g., 50 ohms and 1.5:1). Other waveforms, frequencies, and multiple outputs may be available as an option. A sinusoidal waveform is generally preferable for distribution, a well-defined source and load impedance is required to avoid reflections, and reasonably low harmonic distortion is needed to avoid problems detecting zero-crossings. Spurious components can exist because of switching power supplies, synthesizer circuits and lamp exciter energy. The output is generally either AC-coupled or obtained from the secondary of an RF transformer. Tuned output stages are less common than wideband amplifiers with source resistors and low pass filters in modern designs. In either case, the output must be short circuit proof and immune to reasonable electrical transients. The output amplifier may include a level detector that is incorporated into the unit's monitoring and fault detection circuitry. It may also include a crystal filter, which can not only improve spectral purity but can also provide flywheeling to maintain a phase-continuous output under transient radiation. Such selectivity in the output path can, however, cause temperature dependent phase shift and frequency offset during temperature slew. Multiple outputs generally have specified inter-channel isolation. Unlike crystal oscillators, passive atomic frequency standards do not exhibit frequency pulling from reactive loads.

Harmonic Multipliers

Some RFS RF chain designs use a series of harmonic frequency multiplier stages to multiply the crystal oscillator frequency by small integer factors (typically x2 or x3) as part of the process to generate their microwave interrogation signal. These stages generally use Class C tuned amplifiers or diodes, often in push-push amplifier doubler, “full-wave rectifier” diode doubler, and Wenzel four diode squarer tripler configurations [106]. Their tank circuits must have sufficient selectivity to attenuate sub-harmonics but without excessive tuning sensitivity.

Modulation Distortion

Many subtle modulation distortion effects can occur in a harmonic multiplier chain. Each stage enhances the PM index while suppressing AM by limiting. AM-to-PM and PM-to-AM conversions can cause frequency sensitivity to RF stage tuning and level.

Amplitude modulation on the microwave interrogation signal at the fundamental or an odd-order multiple of the servo modulation rate will cause a frequency offset and potential instability because it produces a spurious component on the recovered signal that the servo nulls by changing the locked frequency. The frequency offset caused by AM at the servo modulation frequency is given by

$$\frac{\Delta f}{f} = \frac{\alpha_1}{2 \cdot Q_l}$$

where α_1 is the relative amount of AM and Q_l is the resonance line Q. Similar to 2^{nd} harmonic PM distortion, a -70 dB AM level with a line Q of 23 million causes a frequency offset of $7\text{x}10^{-12}$.

Sub-Harmonics

The spectrum of a harmonic multiplier chain contains sub-harmonic components that must be adequately suppressed (e.g., 50 dB or better) before further multiplication to avoid cyclic phase jitter that causes an interference pattern which can affect the microwave interrogation power according to the expression

$$\Delta P = 20log_{10}\left[\left|cos\left(2 \cdot 10^{\frac{S}{20}} \cdot N\right)\right|\right]$$

where ΔP is the change in microwave power in dB, S is the sub-harmonic level in the drive to the microwave multiplier in dBc and N is its multiplication factor [67].

Phase Modulators

The phase modulator of a traditional RFS RF chain (one that does not use a DDS to apply servo modulation) is a particularly critical circuit because any amplitude modulation and even-order distortion it introduces can cause frequency offsets and instability. Most RFS designs use squarewave FM as their modulation format, which in an analog RF chain, can be produced by applying triangular PM to a phase modulator, generally at the lowest frequency of the harmonic multiplier chain where the required deviation is least (a modulation index of ≈1 is required at the Rb frequency).

A simple R-C low-pass network, where a varactor diode is used as a variable capacitor, is commonly used, but, at the optimum 45° setting, produces as much AM as PM. Any such AM can be converted to PM by subsequent circuits, becoming a source of modulation distortion.

A better approach is to use an all-pass network like that shown in Figure 55. This all-pass phase modulator suppresses the AM while doubling the modulation sensitivity, and can therefore provide much better performance (immunity from subsequent AM-to-PM conversion and lower distortion). The varactor bias is adjusted for maximum phase sensitivity (≈ -90° where B = G).

.

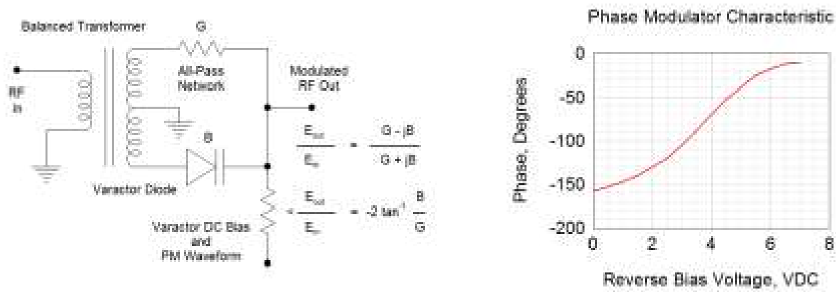

(a) Basic Circuit (b) Transfer Function

Figure 55. All-Pass Phase Modulator

Modulation in a phase-locked loop is another possibility but can have problems with coherent ripple that causes distortion.

Step Recovery Diode Multipliers

Many RFS designs use self-biased high-ratio step recovery diode (SRD) multipliers to multiply a frequency in the 50-120 MHz range up to the 6835 MHz Rb hyperfine frequency in one step. This is attractive because of their simplicity, and is feasible because little microwave interrogation power is needed (typically < 100µW). In many cases, the SRD multiplier is also used as a mixer. A common configuration is a 60 MHz to 6840 MHz (x114) multiplier combined with a 5.3125 MHz mixer to produce an interrogation frequency of 6834.6875 MHz, as shown in Figure 56.

The main 60 MHz drive power is coupled via C1 and the 5.3125 MHz offset via L1, while R1 sets the DC bias through L2. C2 and L3 form an input low-pass matching network and C3 and L4 are harmonic-generating components in series with the SRD D1.

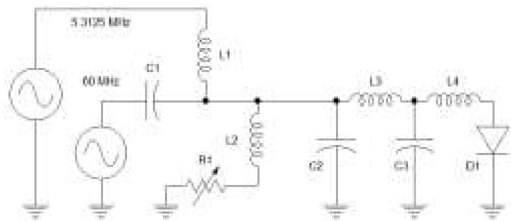

Figure 56. Typical SRD Multiplier Circuit

C3 is often a feedthrough capacitor in the microwave cavity and connects the multiplier to its external circuitry via a short coaxial cable, while L4 may be the SRD lead inductance, whose leads also serve as a coupling link.

Phase Locked Oscillator Multipliers

A microwave phase-locked oscillator multiplier (PLOM) is a more elaborate but higher-performance alternative to an SRD multiplier that eliminates subharmonics and has lower phase noise. The PLOM output can be produced by a dielectric resonator oscillator (DRO) at the Rb frequency or by a bulk wave quartz crystal or SAW resonator voltage-controlled oscillator (VCO) to produce a clean signal at a frequency between that of the primary RFS VCXO and the Rb resonance.

Frequency Synthesis

Frequency synthesis is required in most RFS designs to produce a standard (e.g., 10 MHz) output. Many techniques are available for frequency synthesis, including mixing, multiplying and dividing to perform frequency addition, subtraction, multiplication and division, often requiring filtration to obtain a satisfactory result. Many schemes have been devised to convert the Rb hyperfine frequency to a standard output (some of which were shown in the RF Chains section of this primer), and the choice depends on the design goals and the available components.

Direct Digital Synthesis

Direct digital synthesis (DDS) is a frequency synthesis technique made practical by modern high speed, low power integrated circuits. It is quite simple in concept: a phase accumulator is incremented by a programmable amount (the frequency setting) each clock cycle, and the phase values are converted into a sinusoidal analog waveform to obtain the output. This technique offers fast frequency switching along with high frequency resolution, a combination that is difficult to obtain with a phase locked loop synthesizer, along with reasonably good spectral purity. The high resolution is ideal for use in the synthesizer of an atomic clock.

Microwave Spectral Pulling

Spurious spectral components can pull the locked frequency by causing a shift in the center-of-gravity of the microwave interrogation power. The resulting fractional frequency change depends on the spurious level and its distance from the carrier according to the approximate expression [67]

$$\frac{\Delta f}{f} \cong \frac{\gamma^2 B^2}{8\pi^2 f_0 (f_0 - f)}$$

where γ is the gyromagnetic ratio, B is the spurious microwave induction at frequency f, and f_0 is the center frequency. The pulling can be estimated by scaling the measured pulling effect of applying a SSB interfering component equal to the carrier power at some frequency separation, for example, a sideband 5 MHz away might cause a frequency deviation of $5x10^{-13}$. That would then imply that a -30 dBc asymmetrical spur from a 25 kHz switching power supply would cause an offset of $1x10^{-13}$.

Oven Temperature Controllers

Oven temperature controllers are a necessary and important part of any RFS design. The Rb lamp and cells must be heated to obtain sufficient vapor pressure to operate, and their temperature must be tightly controlled to maintain their stability. These temperature controllers also influence the unit's warm-up and power characteristics.

RFS temperature controllers usually work at DC, but switching controllers are also used. DC temperature controllers can have their control element (e.g., transistor) either inside or outside the oven's thermal environment. The latter provides greater efficiency, but raises residual magnetic field issues. A switching power supply has good efficiency and dynamic range, but introduces EMI concerns.

Most RFS temperature controllers use thermistor temperature sensors because they are sensitive, small and have reasonably good stability. For good performance, they must have good thermal contact with their oven, and mechanical stresses must be avoided.

Some RFS designs use foil heaters with polyimide (Kapton®) insulation because they provide good, large-area thermal contact, can have low residual magnetic field and are very reliable. Two-layer foil heaters with matched meander patterns carrying opposite currents have very low magnetic field. They can be designed with irregular shapes and with contacts for thermistor leads. Transistor heaters are efficient and inexpensive, but have much larger residual field, and necessarily are exposed to high junction temperatures.

Oven thermal insulation can take many forms, but as RFS ovens have gotten smaller, there is less need for special insulating materials like urethane foam, and simple arrangements like thermally-isolated regions of a printed circuit board can be used. For space applications, the vacuum environment can be utilized to much advantage.

A typical RFS temperature controller circuit is shown in Figure 57. A DC thermistor bridge senses the oven temperature and drives a simple DC proportional controller comprising a bridge amplifier, voltage-to-current converter and heater transistor.

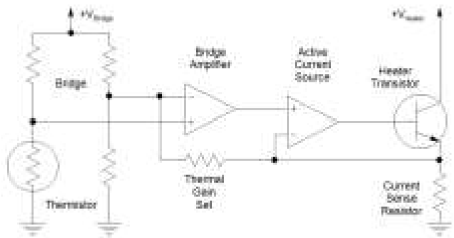

Figure 57. Basic Temperature Controller Circuit

Better performance can be obtained over a wide ambient range with a proportional-integrator (PI) controller, but it is harder to implement because of the long time constants that may be involved. Digital temperature controllers are becoming more common as RFS units include microcontrollers for other purposes. Besides offering easier implementation of a PI controller, they can also provide adaptive oven demand power.

The maximum supportable thermal gain can be estimated as the ratio of the oven thermal time constant to that of either the heater or sensor (whichever is larger). Thermal stability is improved by a larger oven mass, lower thermal loss, and better sensor and heater thermal coupling. Elaborate thermal modeling is seldom very helpful because of the difficulty in obtaining the various parameters, and its limited effectiveness in predicting gradients. The exact location of the sensor in relation to ambient is often critical and must be optimized by experiment. Shunting the heater with an external load to simulate a lower temperature will show the static proportional gain but tell nothing about the effect of gradients, which can be caused by asymmetry of the oven, its insulation and lead losses, its heater, and/or any internal dissipation.

Thermal runaway of an RFS oven is a rare but potentially catastrophic event. Open thermistor and over-temperature protection may be a wise precaution in some critical applications.

Mechanical Design

Mechanical design factors are clearly more important in an RFS design than most types of electronic equipment, mainly because of its physics package. It is useful to start at the inside of the physics package and consider some of the mechanical, thermal, structural and magnetic design considerations.

The microwave cavity tends to set the overall size, as well as the size of the absorption or resonance cell. A smaller cell must operate at a higher temperature to provide a usable Rb signal (i.e., a higher Rb vapor pressure is needed for a shorter optical length). That may be desirable to support operation in a high-temperature environment, but it also results in a wider resonance line, lower Q and lower stability. Nevertheless, very small gas cells work remarkably well, as has been demonstrated by the mm-sized cells used in chip-scale atomic clocks. For conventional microwave interrogation, a correspondingly small "cavity" is needed, which then must either be heavily dielectrically loaded or use a different principle to produce the required H-field configuration at 6.8 GHz.

For a small design, an integrated resonance cell is almost always used to avoid the need for a separate filter cell.

Next, one must consider the cell oven, which is also the microwave cavity, and, in particular the means that heat will be applied. Let us assume that the heating will be done with DC (AC heating is quite unusual and switching heaters, while offering good efficiency and dynamic range, create troublesome EMI). A foil heater has excellent thermal properties and minimal residual magnetic field, but is inefficient if the control element (e.g., transistor) is located outside the oven. A transistor heater has 100% efficiency, but applies the heat to a local spot, thus creating poorer temperature uniformity (gradients) and is likely to create an unacceptable magnetic field. This leads to the possibility that the cavity oven would be made of a high-permeability magnetic shielding material, plated for good electrical conductivity (but still having inferior thermal properties). In that case, the C-field must be inside the cavity, probably wound on the cell and close to the inner cavity wall.

So our cavity design tends to take one of two approaches, (a) an aluminum oven shell (copper could also be used for better thermal properties) with a foil heater and external control element with a C-field coil outside the cavity and magnetic shielding outside that, or (b) a plated mu-metal oven shell with a transistor heater/control element with a C-field coil on the cell and additional external magnetic shielding (perhaps the RFS case).

Let us now consider the lamp oven assembly. It must enclose the lamp and lamp coil plus its resonating capacitor, but the lamp exciter circuit can be either inside or outside the lamp oven. If it is inside, its operation is improved because of the short connections, its power dissipation contributes toward the oven heating, and its EMI is contained within the oven assembly. But it is a stressful thermal environment, and a high reliability design is likely to locate the exciter circuit outside the lamp oven. In that case, it should be as close as possible.

The physics package oven assemblies must be thermally isolated from their environment but nevertheless ruggedly supported. The performance of their temperature controllers depends on the oven thermal mass and its thermal loss to ambient. A space design can effectively utilize vacuum insulation and employ low emissivity coatings to minimize thermal loss, while a ground-based design can utilize small air gaps to minimize convective heat transfer. Conductive loss via leads, especially coaxial cables, must also be considered. Alloy wire and stainless steel coax can be used to minimize those losses.

Clearly, there are many interacting considerations that go into an RFS physics package mechanical design, and all the relevant concerns not have by any means been exhausted. The need for magnetic shielding must be satisfied by the physics package and overall structure. The C-field, which is influenced by the magnetic shielding, must be uniform over the length of the resonance cell to avoid inhomogeneity, as must thermal gradients be minimized for the same reason.

In a dynamic environment, relative motion between the lamp and cavity assemblies must be minimized in order to avoid mechanical modulation of the physics package light path. Mechanical vibration also affects the spectral purity of the crystal oscillator and thereby the microwave interrogation signal, and vibration isolation may be required. Fortunately, a wide bandwidth Rb servo can reduce vibration sensitivity at the lower vibration rates, so the vibration isolators need work only at higher, more practical, vibration frequencies. Cable isolators, although large, have been found to be particularly effective, but may inhibit thermal transfer.

RFS modules have few, if any, physical controls. Older units had accessible potentiometers for adjusting their frequency, but nowadays that is more likely to be accomplished with an external voltage or resistance, or an internal non-volatile digital memory. Some units have a lock indicator, and none have on-off switches. All RFS modules have a connector for DC power, analog monitor signals and, possibly, digital control lines. The same connector may contain the RF output signal, or otherwise it will have a separate coaxial connector. Dual RF outputs are sometimes available, possibly at different frequencies.

Complete RFS instruments are far less common, and have a larger complement of connectors, indicators and controls, and generally operate from the AC power mains.

Thermal Design

In general, conductive heat transfer is preferred, and is essential for vacuum operation. Temperature gradients should be minimized in the overall RFS chassis as well as in its physics package ovens, because, in air, they may cause frequency changes that depend on the orientation of the unit (otherwise an RFS frequency is not sensitive to static g forces or tip-over).

Small RFS units often dissipate enough power that they must be heat sunk in some way, making them not so small after all.

Baseplate Temperature Control

Baseplate temperature control can be used to stabilize the chassis temperature of an RFS against environmental temperature variations. For example, a GPS satellite Rb clock may have an integral baseplate temperature controller (BTC) comprising heaters and a thermistor temperature sensor inside the bottom of the RFS chassis, a thermal insulator between the chassis and the space vehicle (S/V) panel, and an electronic controller circuit. Besides improving the RFS stability, the BTC also has the advantage of allowing its performance testing and operation to be limited to a single temperature. Its main disadvantage is an increase in power consumption that depends on the difference between the BTC set point and S/V panel temperatures.

An example of BTC operation is shown in Figure 58, which plots its overall power consumption against the S/V panel temperature to which it is mounted.

The BTC set point is +45°C, where the total power is zero, but the hottest possible operating condition is when the S/V panel is at +25°C, where the BTC heater power is zero but the clock itself still dissipates 14 watts. Similarly, the coldest possible operating condition is when the S/V panel is at -11°C and the heater is at its maximum demand power. The slope of this operating characteristic is determined by the 0.7 W/°C thermal conductance of the thermal insulator.

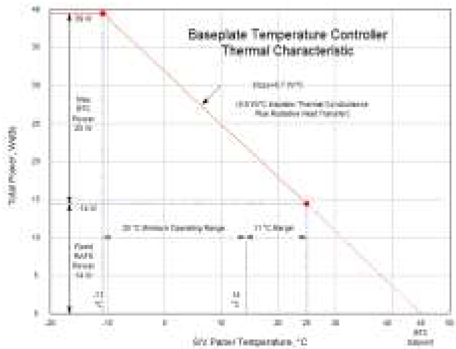

Figure 58. BTC Thermal Characteristic

An uncontrolled RFS with a temperature coefficient of 2×10^{-13}/°C, would show significant instability when exposed to 12-hour orbital S/V panel temperature variations of 3.5°C peak-peak, as shown in the Figure 59. The BTC reduces this instability about two orders-of-magnitude to below the $2\times10^{-12}\tau^{-1/2}+2\times10^{-14}$ noise level of this example.

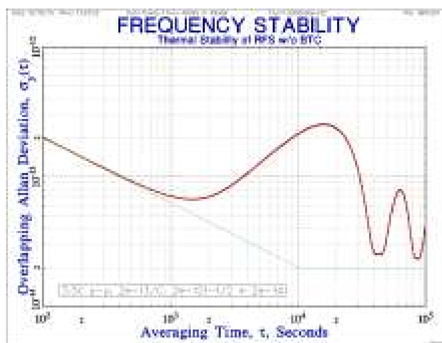

Figure 59. Stability Plot for RFS Under Temperature Cycling without BTC

Stability

Frequency stability is the main attribute of a rubidium frequency standard, so it naturally follows that it plays an important role in their design, specification and testing. RFS stability (actually *in*stability) is usually separated into its noise-like frequency fluctuations, its gradual frequency change over time, and the dependence of its frequency on environmental factors such as temperature and supply voltage. It is best that those sources of instability be examined separately. The noise-like frequency fluctuations are described by statistical stability measures, the frequency aging is usually described under constant environmental conditions, and the environmental sensitivity is expressed by a number of individual sensitivities. Note that aging refers to internal RFS mechanisms that cause its frequency to change while drift includes external factors and therefore depends on the unit's operating conditions. This primer section emphasizes the measurement and analysis of the noise-like frequency fluctuations, which are commonly described by power-law power spectral densities ranging from white PM to flicker FM noise. As we have seen previously, the dominant RFS noise type is white FM noise extending over averaging times from 1 second to several hours or more.

Stability Measures

The principal RFS time-domain stability measure is the Allan deviation which is a statistic similar to the ordinary standard deviation but is better able to handle the more divergent noise sources that are present in most frequency sources [255], [354]. In the frequency domain, the stability of an RFS can be described by its phase noise. Those two methodologies are complementary. Time domain measures are generally applied for analyzing stability at times of 1 second and longer while frequency domain measures are more often used for shorter averaging times. Conversions are possible between the two domains, but it is usually best to use the one that most closely resembles the requirements of a particular application.

Stability Measurements

RFS stability measurements generally require greater precision and accuracy than can be obtained from an ordinary frequency counter [358]. High precision can be achieved by a heterodyne process that enhances the measurement resolution, while high accuracy requires a suitable reference source such as a cesium beam instrument or a GPS time and frequency receiver. RFS stability is best performed by measuring its phase, from which data it is easy to also obtain its frequency record.

Stability Analysis

The stability of an RFS is usually analyzed in a series of steps designed to separate and describe both its deterministic and stochastic behavior, while dealing with any anomalies involving the measurements or unit under test.

One usually begins with a phase record, its time error versus a highly stable reference. Because an RFS has high stability (pp10^{13}) but is likely to have a rather large frequency offset (pp10^{10}) and significant frequency drift (pp10^{12}/day), the raw phase record may be a straight line whose slope corresponds to the frequency offset. So the next steps in the analysis process are to remove that frequency offset and drift, which we assume are deterministic parameters.

The following example (see Figures 60-67) shows the basic RFS stability analysis of a 1-week set of $\tau = 1$ second simulated phase data having a nominal frequency offset of $1x10^{-10}$, white FM noise at a level of $1x10^{-11}\tau^{-1/2}$, and linear frequency drift of $3x10^{-12}$/day.

The phase data are essentially a straight line whose slope represents the average frequency offset ($1.035x10^{-10}$), which can be determined by a least-squares linear fit. If that were removed from the phase data, one would see a quadratic representing the frequency drift as shown in Figure 61. If a quadratic fit were removed from the phase data, one would see phase residuals showing their noise fluctuations as shown in Figure 62.

Figure 60. Phase Data

Figure 61. Phase Residuals without Frequency Offset

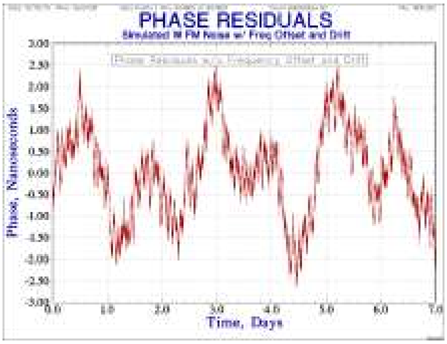

Figure 62. Phase Residuals without Frequency Offset Drift

Converting the original phase data to frequency data shows that there is linear frequency drift plus noise. Note that if there were outliers in the frequency data they would have to be removed before proceeding with the analysis. The drift can be made clearer by averaging the frequency data as shown in Figures 64 and 65 for averaging factors of 10 and 100 respectively.

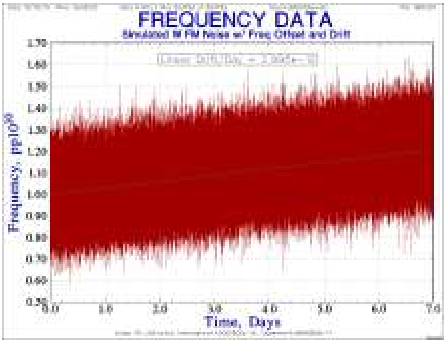

Figure 63. Frequency Data

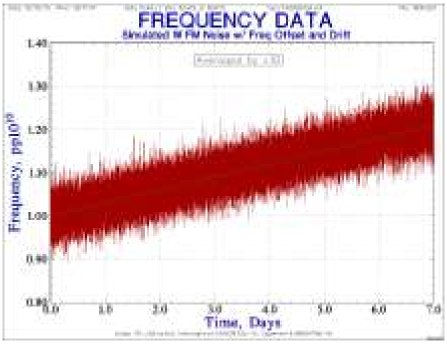

Figure 64. Frequency Data Averaged by Factor of 10

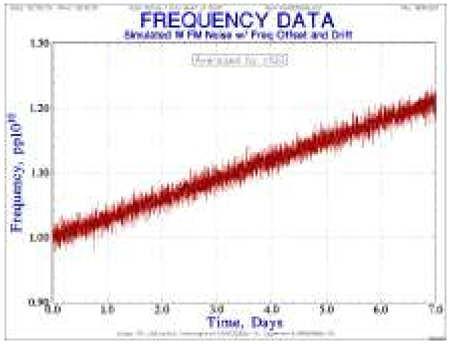

Figure 65. Frequency Data Averaged by Factor of 100

Removing a linear fit from the frequency data leaves the frequency residuals which can then be analyzed for their noise.

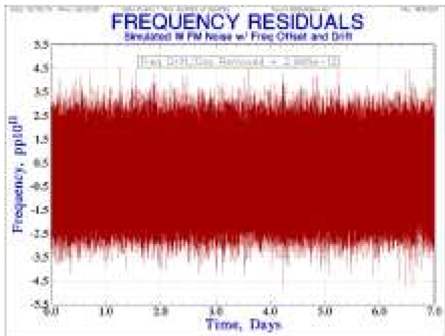

Figure 66. Frequency Residuals

An Allan deviation plot shows the frequency stability versus averaging time. The white FM noise has a slope of -0.5 on a log sigma versus log tau plot. Note that most RFS units would have flicker FM noise that would impose a noise floor before the stability reached 1×10^{-13}. Other statistics are available to analyze frequency stability for data having linear drift, with better confidence and at larger averaging factors [354].

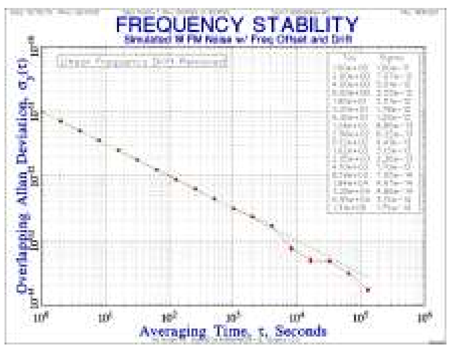

Figure 67. Frequency Stability

It is important to inspect the phase and frequency records for jumps and other anomalies. The source of a phase discontinuity is unlikely to be in the frequency standard, but rather a problem with the measuring system, but nevertheless should be explained. A frequency jump is potentially a serious problem for a frequency standard and requires careful investigation.

The frequency drift may be non-linear and better modeled by a logarithmic or diffusion fit. The principle is to separate any deterministic behavior from the stochastic noise before performing a stability analysis of the latter. Most importantly, always remember R.W. Hamming's advice that "the purpose of computing is insight, not numbers". One needs to keep in mind the purpose of the analysis and use appropriate methodologies to obtain a meaningful result.

Phase Noise

The phase noise of an RFS is determined mainly by its crystal oscillator. Close to the carrier, however, within the bandwidth of the servo loop, the noise becomes that of the Rb reference, thus taking advantage of the best performance of both. Analytical expressions for this relationship were shown in the section on frequency lock loops and can be used to calculate the overall RFS phase noise as a function of sideband frequency, or it can be found numerically using a spreadsheet. Figure 68 shows the results of such a calculation using measured values for the phase noise of the crystal oscillator and Rb reference, and the servo of Figure 45. The RFS phase noise follows that of the Rb reference at low sideband frequencies and the VCXO at high sideband frequencies, with some noise peaking at the transition between them near the servo closed-loop bandwidth.

The phase noise of the Rb reference is white FM noise that is quite simply related to its time domain stability, and has a -20dB/decade slope at a level that can be scaled from the value $\mathcal{L}(1\ \text{Hz}) = -80$ dBc/Hz at 10 MHz for a 1-second stability of $1\text{x}10^{-11}$.

Several parameters influence the overall RAFS output phase noise including (a) the VCXO white PM and flicker FM noise levels, (b) the Rb reference white FM noise level, and the frequency lock loop gain and bandwidth.

The VCXO white PM noise affects the RFS output dB per dB at the higher sideband frequencies. Similarly, the Rb reference stability at low sideband frequencies affects overall the close-in phase noise dB per dB. The VCXO flicker FM noise level is important for intermediate sideband frequencies (say 100 Hz to 1 kHz) where it largely determines the overall phase noise, again dB per dB. The most interesting region is between 10 to 100 Hz where the Rb reference white FM and VCXO flicker FM phase noise both affect the results depending on the servo response.

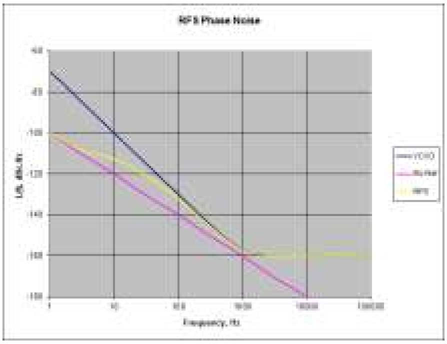

Figure 68. RFS Phase Noise

.

Note that this model does not include an explicit $S_y^N(f)$ term for the $2f_{mod}$ intermodulation noise because that is already included in the white FM noise values.

Signal Parameters

An RFS physics package is characterized by a number of parameters that describe the dependence of its linewidth, discriminator signal and light shift to such operating conditions as lamp, filter cell and absorption cell temperatures, RF interrogation power, modulation rate and deviation. Figure 69 shows some of these dependencies in the form of plots from research conducted during the development of the EG&G GPS Rb clocks [30]. While they apply to that particular hardware and its operating conditions, they also serve to show the general dependences of an RFS physics package using a discrete filter cell. The plots are not necessarily from the same cells or operating conditions, and should not be used for quantitative comparisons, but illustrate the sort of investigations that are performed during RFS development. The following notes describe some of the features of the individual plots:

A. The linewidth increases with modulation deviation and RF interrogation power due to line broadening
B. The linewidth increases with RF power and the signal peaks at a particular RF power. There is an optimum RF interrogation power as a tradeoff between signal strength and RF broadening.
C. The linewidth increases at higher temperatures due to an increase in Rb vapor pressure and a higher spin-spin collision rate.
D. The frequency decreases with filter cell temperature in the region where the signal is strongest. All RFS have a relatively large negative filter cell TC under their normal operating conditions.
E. The lamp TC is a light shift effect that can be nulled by adjusting the filter cell temperature (or length).
F. This shows the desired zero light shift condition at the optimum filter cell temperature.
G. This is the actual light shift coefficient, showing the null (flat line) at the optimum filter cell temperature, and that the lines converge at zero light intensity.
H. The signal peaks at a particular light intensity due to light broadening above that point, and at a higher than optimum filter cell temperature.
I. The cell TC is determined mainly by its buffer gas mixture (N_2/Ar=0.73 here) and is non-linear.
J. The lamp modes depend on both temperature and RF excitation power (lamp exciter supply voltage here). The two basic modes are called “ring” and “red” based on their appearance, and there is an oscillatory region between them, along with considerable hysteresis. Most RFS operate in the cooler ring mode, which avoids the oscillatory region, because, although the brighter red mode signal is stronger, the light shift is larger and the spectral lines are self-reversed.

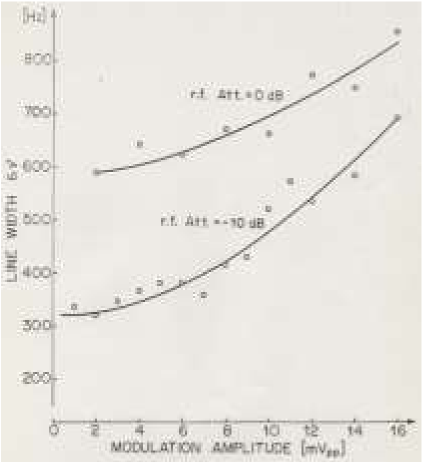

A. Linewidth vs. Modulation Deviation

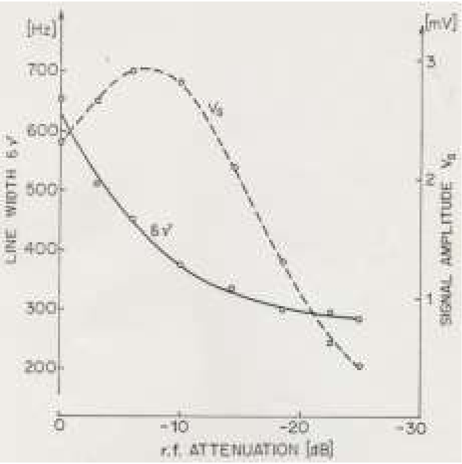

B. Linewidth and Signal vs. RF Power

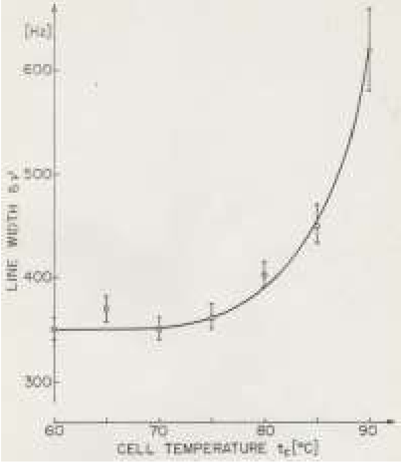

C. Linewidth vs. Cell Temperature

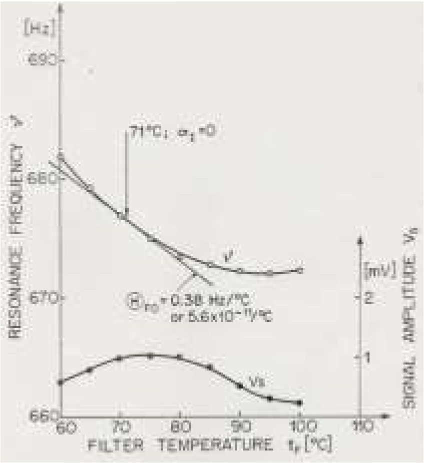

D. Frequency and Signal vs. Filter Temperature

Figure 69. RFS Signal Parameters

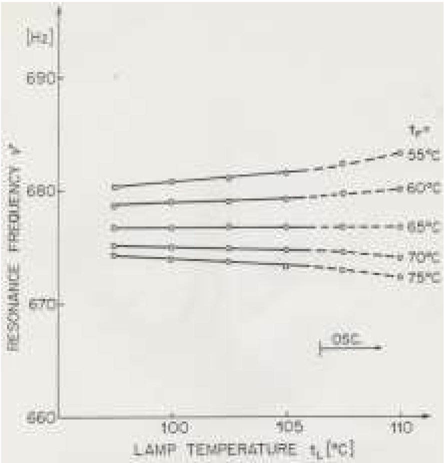

E. Frequency vs. Lamp Temperature

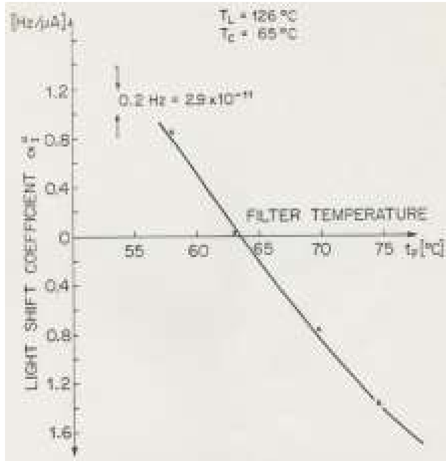

F. Light Shift Coefficient vs. Filter Temperature

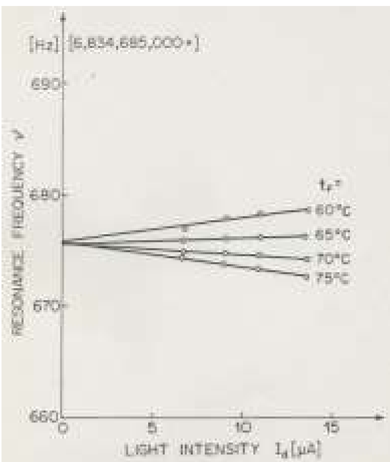

G. Frequency vs. Light Intensity

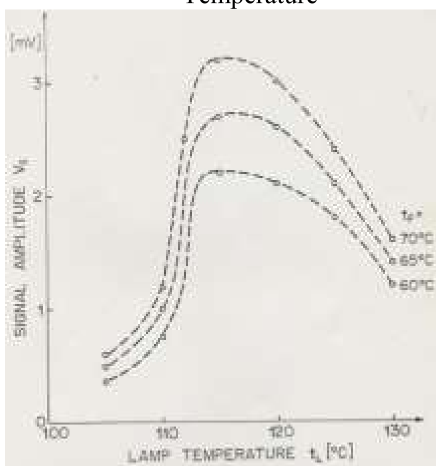

H. Signal vs. Lamp Temperature

Figure 69. RFS Signal Parameters (Cont.)

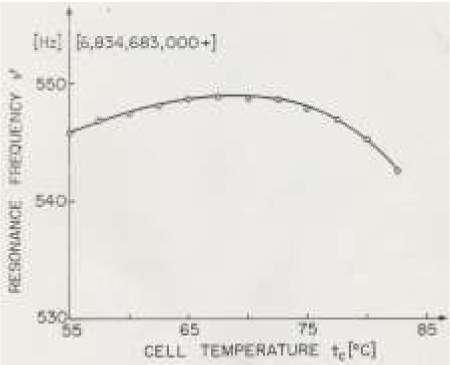

I. Frequency vs. Cell Temperature

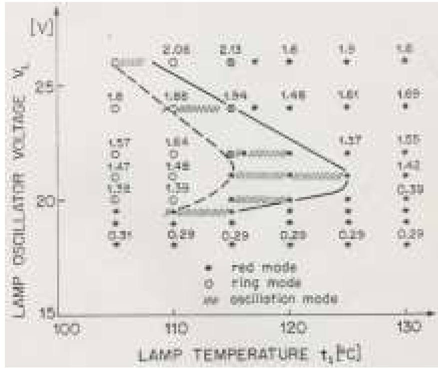

J. Lamp Modes

Figure 69. RFS Signal Parameters (Cont.)

RFS Internal Operating Adjustments

An RFS requires several of its operating parameters to be adjusted for best performance depending on its particular design and the degree to which it is to be individually optimized. Those adjustments and parameters may include some or all of the following:

1. Frequency calibration
2. RF interrogation power
3. Oven temperature set points
4. Modulation deviation
5. Synchronous detector phasing
6. Lamp exciter frequency
7. Internal temperature compensation
8. S/N and S/W version information

Commercial units generally minimize such adjustments to save manufacturing cost, militarized units are generally subjected to more extensive testing during which certain adjustments may be made, and space units generally emphasis performance and undergo extensive acceptance testing and optimization.

Frequency calibration is almost always done, either by adjusting the C-field or the setting of a frequency synthesizer. It is usually necessary to adjust the RF interrogation power, especially if a SRD multiplier is used whose DC bias very likely requires adjustment. Oven temperatures, which affect important operating parameters like light shift and TCs, may be individually set. Modulation deviation often requires adjustment if it is implemented with an analog phase modulator rather than a DDS. An adjustment of the lamp exciter frequency is generally not required, nor is adjustment of the synchronous detector phasing. If internal temperature compensation is used, it likely must be individually set. An RFS with digital control requires that its embedded software be loaded, and generally includes specific serial number and version information.

Internal Measurements

Several techniques have been found useful for measuring internal RFS operating parameters.

1. The physics package discriminator signal is its primary attribute, but is not directly observable during normal operation. The 2nd harmonic signal is therefore often used as a proxy for it while making internal adjustments and to judge the general health of a unit. Measuring the actual discriminator slope, the amount of fundamental recovered signal per unit of frequency deviation, can be done by injecting a small offset current into the servo integrator and measuring the amplitude of the resulting fundamental error signal (generally at the preamplifier output) and the corresponding frequency offset.
2. The RF interrogation power should be optimized for the largest discriminator signal. This is usually accomplished by observing the magnitude of the recovered 2nd harmonic signal and relating that to predetermined knowledge about the mutual dependence of both the 2nd harmonic and discriminator signals on RF interrogation power. For example, one might adjust the RF power slightly lower than for peak 2nd harmonic signal.
3. The servo modulation deviation is often set for a certain maximum fundamental-to-second harmonic signal ratio, again based of predetermined knowledge about the deviation that produces the best discriminator signal.
4. Servo-induced frequency offsets must be minimized. Integrator DC offset is one example of that. Pickup of stray fundamental synchronous detector reference signal at the input to the servo amplifier is another. Those errors can be assessed by removing the signal to the servo amplifier and observing the drift of integrator output.
5. Information can be obtained about residual magnetic fields by reversing the applied C-field. For example, frequency data versus temperature with both C-field polarities can measure the effect of residual cavity heater field.
6. The RF interrogation power can be related to the phase of the recovered 2nd harmonic signal (see Figure 18).

While some of these measurements relate to analog RFS servos they can also be applied to DSP implementations. It is possible to automate measurements of most RFS operating parameters, especially for a unit with a digital interface that supports control of oven temperatures and other settings.

PERFORMANCE

These primer sections cover the performance, testing and of rubidium frequency standards.

Performance

RFS stabilities span 1-2 decades depending on type of unit and typical versus specification values, as shown in Figure 70. Rubidium frequency standards have the widest range of stability (as well as design architecture, size, weight, power, other performance factors, and cost) of any of the commercially-available passive atomic frequency standards. This plot shows the approximate range between commercial RFS specifications and actual GPS RAFS performance.

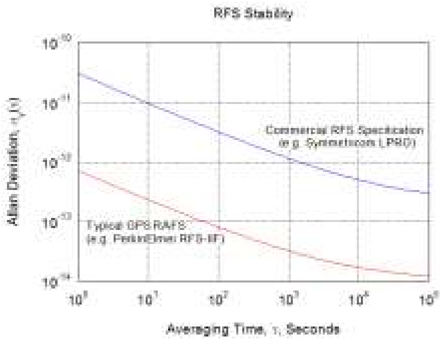

Figure 70. RFS Stability

Like any passive atomic frequency standard, the dominant short and medium term noise type is white FM noise set by basic physics package parameters (S/N, Q, etc.) that varies inversely as the square root of the averaging time. At longer averaging times, the stability reaches a "flicker floor" where flicker FM and other more-divergent noise and environmental sensitivity limit the stability. This ultimate stability is reached at about $1x10^{-13}$ at an hour or so for commercial RFS units, and below $1x10^{-14}$ at several days for the GPS RAFS. Frequency drift (mainly physics package aging mechanisms) also varies quite widely, from 10^{-11}/day for small commercial units to well below 10^{-13}/day for GPS RAFS. The aging rate also depends on how long a unit has stabilized. For commercial RFS units, a rule-of-thumb is that, after initial syntonization, in a constant environment, a unit will provide an accuracy of 10^{-11} per day, 10^{-10} per month, and 10^{-9} "forever". Experience has shown that RFS frequency on-off retrace is excellent ($\approx 10^{-11}$), and that the trend of its retrace is essentially the same as its continuous drift. Warm-up and retrace performance is much better than any crystal oscillator.

Rubidium frequency standards have a number of environmental sensitivities, including, in rough order of importance, temperature, barometric pressure, shock and vibration, magnetic field, EMI, voltage, humidity, and perhaps nuclear radiation [67]. Temperature sensitivity is on the order of several $pp10^{10}$ over the full operating temperature range. Barometric sensitivity (about 10^{-10}/atm) can dominate day-to-day instability in an otherwise well-controlled environment. Vibrational sensitivity is a complex issue, mainly related to the acceleration sensitivity of the quartz resonator used in the unit's crystal oscillator, causing degraded phase noise, discrete spurii, and interference with the frequency lock servo. Unlike crystal oscillators, an RFS has no static g-sensitivity. Tip-over and orientation sensitivity, if any, is caused by thermal redistribution and external magnetic field change. Voltage sensitivity is also mainly a thermal effect. The magnetic field sensitivity is largest along the axis of the internal C-field. The most severe EMI sensitivity is usually conducted power line ripple at the servo modulation rate and its harmonics. Thermal and power on-off cycling is not a problem for a well-designed unit, and is recommended as an applied stress for both design qualification and production quality screening. Nuclear radiation (total gamma dose, neutron fluence, and transient X-rays) is generally not a severe problem at tactical levels, but requires special analysis and testing.

Environmental Sensitivity

RFS environmental effects are determined mainly by internal sensitivities associated with the physics package and electronic circuits [67]. Most of those internal sensitivities have been described in previous sections of this primer. The physics package sensitivities include C-field, light shift, lamp and cell temperature coefficients, the cell barometric coefficient and the RF interrogation power coefficient, while the electronic sensitivities include RF chain modulation distortion, amplitude modulation, RF spurious components and sub-harmonics, and the voltage, temperature and radiation sensitivities of the various electronic components. Those sensitivities can be analyzed and summarized in the form of an error budget covering, for example, all the factors that contribute to a unit's overall temperature instability.

The external environmental effects include acceleration, supply voltage, humidity, EMI, magnetic field, pressure, radiation, shock, temperature, vibration. Those sensitivities are summarized in Figure 71 along with the RFS sections that they affect. Other factors include the response of a unit to power-off storage, power cycling, its retrace characteristics, and even the relativistic effects that affect any clock.

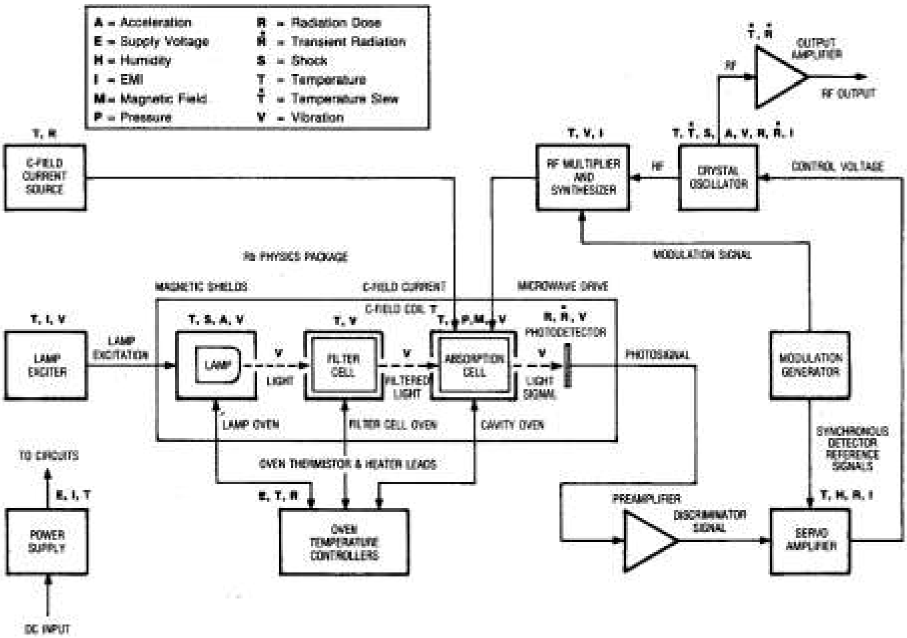

Figure 71. RFS Environmental Sensitivities

Temperature Compensation

It is quite common to improve the temperature stability of an RFS by applying some form of temperature compensation. That usually involves measuring the uncompensated frequency versus temperature characteristic of an individual unit and using that information to adjust its frequency as a function of a temperature sensor reading, but generic compensation can also be applied to reduce a consistent temperature dependence. RFS temperature compensation can be implemented either internally or externally, with the former done by the RFS manufacturer and the latter possibly added by the user (for example, by varying the speed of a cooling fan).

RFS temperature compensation requires not only a temperature sensor but also a means for storing the compensation information and a way to adjust the frequency. Classic analog RFS temperature compensation often used a thermistor network with a select-in-test resistor value to apply a correction to the unit's C-field current. While reasonably effective, the scheme had the disadvantages that the general shape of the compensation was fixed, and that it varied as the nominal C-field setting was changed. Modern RFS designs often employ a high-resolution DDS synthesizer and have internal digital frequency control, offering an effective way to implement temperature compensation by means of a lookup table or mathematical model. That also lends itself to automatic temperature compensation whereby the frequency of a unit can be measured as a function of temperature and the necessary compensation information stored in non-volatile memory, which also allows the compensation to be easily updated. Temperature compensation requires little or no additional hardware in these modern designs, but does need additional embedded software and more test effort.

An example of the latter form of temperature compensation is shown in Figure 72. In this case, the uncompensated unit had a nearly linear TC close to its specified limit, and compensation using a single value representing the average TC slope was able to effect a x7 improvement in the unit's overall frequency stability versus temperature.

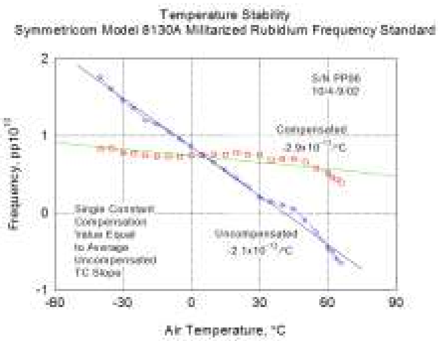

Figure 72. RFS TC Compensation

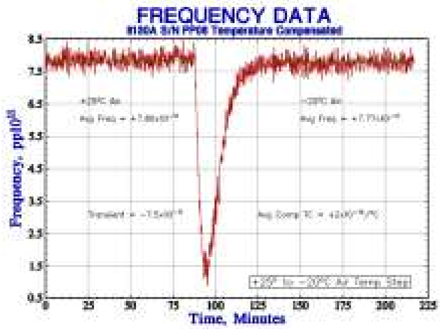

Figure 73. Temperature Compensated Transient Response

The main limitation to RFS temperature compensation is frequency transients in response to large temperature steps because of unmatched time constants between the temperature sensitive components and the temperature sensor. Figure 73 shows the response of the same RFS for an abrupt 45°C temperature step. While the steady-state frequency change is essentially zero, there is a large transient excursion (which is, nevertheless, much better than if uncompensated). Temperature compensation must also be implemented in a way that does not degrade short-term stability.

Pressure Sensitivity

The barometric sensitivity of a gas cell atomic frequency standard is determined primarily by the "oil-can" deflection of the cell windows, and the resultant buffer gas pressure change inside the cell, which scales with the buffer gas frequency offset [68]. While this effect is calculable, it is most easily measured, at least for a clock designed for vacuum operation by simply pumping it down in a thermovac chamber. A typical value for a large (1" diameter) glass cell is $1x10^{-10}$/atm. In air, an extreme weather-induced barometric change of (say) 10% would cause a frequency change of $1x10^{-11}$, a noticeable but probably tolerable effect for a small commercial or tactical military unit in comparison to other environmental sensitivities. During operation in an unpressurized aircraft, this could be the dominant environmental sensitivity. In ground operation under otherwise controlled (laboratory) conditions, barometric sensitivity often sets the "flicker floor" stability limit of such a unit. In a space application, barometric sensitivity is a non-issue as long as the (quite predictable and reproducible) air-to-vacuum offset is acceptable.

Radiation Sensitivity

The Kenschaft model of the Rb signal can be used to analyze the response of an RFS to transient radiation that causes a 5.3×10^{-9} frequency step, as shown in Figure 74A (simulated) and B (actual) [194].

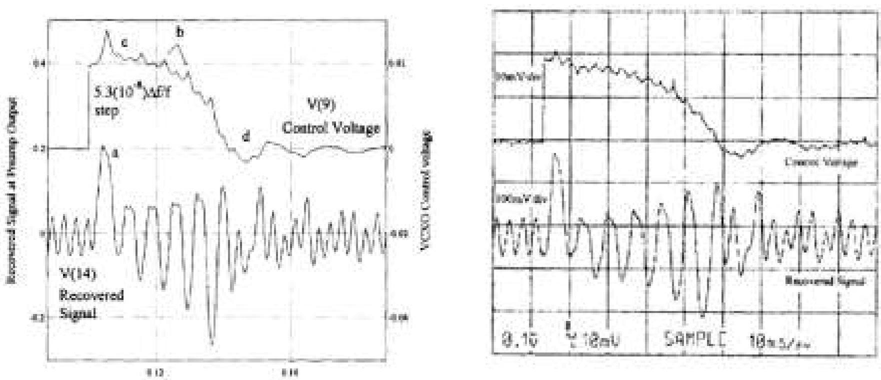

(A) Simulation (B) Actual

Figure 74. Servo Transient Response

Vibration Sensitivity

The vibration sensitivity of an RFS depends on the acceleration sensitivity of both its crystal oscillator and physics package, and the frequency lock loop that connects them.

Vibration can affect the performance of a rubidium frequency standard in several interacting ways [170], [219], causing dynamic degradation of its phase noise, spectral purity, short-term stability, and quasi-static or permanent frequency offset, as follows:

1. Direct vibrational modulation of the crystal oscillator that produces the RFS output will cause a degradation of its phase noise and spectral purity. Random vibration degrades the phase noise, while sinusoidal vibration produces discrete spurious sidebands on the RF output spectrum. These effects are possibly reduced by the frequency lock servo that locks the crystal oscillator to the

rubidium reference. Very high vibration levels can damage a quartz crystal resonator.

2. Crystal oscillator vibrational modulation also affects the microwave interrogation signal applied to the rubidium physics package. Random vibration causes noise on the Rb discriminator signal, sinusoidal vibration can cause a quasi-static frequency offset when its frequency is related to the servo modulation rate, and high levels of low frequency sinusoidal vibration can reduce the applied microwave interrogation power. Sinusoidal modulation of the microwave interrogation signal is particularly important when the vibration frequency is twice the servo modulation rate.

3. Vibration can also affect the Rb physics package itself, mainly due to modulation of its light throughput. Random vibration increases the noise on the discriminator signal, while sinusoidal vibration can cause a quasi-static frequency offset when its frequency is related to the servo modulation rate. The latter is particularly important when the vibration frequency is equal to the servo modulation rate. High levels of vibration can cause temporary frequency offsets due to rubidium redistribution in the Rb spectral lamp. Very high vibration levels can also induce mechanical damage to the physics package that can cause permanent frequency offsets and loss of discriminator signal.

Let us first consider Item 1, the direct vibrational modulation of the crystal oscillator that produces the RAFS output signal. The main effect of sinusoidal vibration is to cause spurious components at a sideband frequency equal to the vibration frequency on each side of the RF output spectrum because of the acceleration sensitivity of the quartz crystal oscillator. The level of the discrete spectral components is determined by the standard formula for sinusoidal FM modulation:

$$\text{Sideband Level (dBc)} = 20 \log_{10} (\Delta f / 2 \cdot f_{mod})$$

where Δf is the peak frequency deviation in Hz and f_{mod} is the modulation rate and sideband frequency.

For vibration, this formula for discrete FM is modified to use the peak $\Delta f = g \cdot \Gamma \cdot f_o$, where g is the peak applied g level, Γ is the acceleration sensitivity of the device (expressed as a fractional frequency per g), and f_o is the nominal carrier frequency:

$$\text{Sideband Level (dBc)} = 20 \log_{10} (g \cdot \Gamma \cdot f_o / 2 \cdot f_{vib})$$

Note that both the applied vibration and the vibration sensitivity are directional, and thus a detailed analysis of the crystal resonator’s orientation with respect to the vibration may be required. A typical quartz crystal resonator has an acceleration sensitivity of 1×10^{-9} per g along its most sensitive axis. Lower quartz crystal resonator acceleration sensitivity is possible, either by specification or screening, and

$5x10^{-10}/g$ is feasible, but a further reduction requires special compensation techniques.

While degrading the spectral purity, such crystal oscillator vibrational modulation does not cause a static or permanent frequency offset. Unless the vibration level is very high, the nominal resonant frequency of the quartz crystal is not changed, and, even if it were, the Rb frequency lock loop would correct it. The vibrational modulation will not affect the average RFS output frequency, and therefore will not affect its long term time error. Low frequency vibrational disturbance of the crystal oscillator can be corrected by the frequency lock loop to the extent that it has open loop gain at the vibration frequency.

Next, let us consider Item 2, the effect of crystal oscillator vibrational modulation on the microwave interrogation signal applied to the Rb physics package. Firstly, we can usually rule out a gross loss of carrier power because the vibration would have to be extremely large to cause a Bessel null.

But, if the vibration frequency is exactly equal to an even multiple of the RFS servo modulation rate, there exists an intermodulation mechanism that causes the lock point of the synchronously-detected frequency lock servo to be offset [189]. More probably, if the (incoherent) vibration frequency is near one of those multiples of the servo modulation rate, there will be "beats" that cause a low frequency disturbance of the locked frequency. This instability mechanism can be quite significant. A rough estimate for it can be based on its analogy with even-order modulation distortion, which leads to a frequency offset value of about $1x10^{-9}$ for a -30 dBc coherent $2 \cdot f_{mod}$ component. The effect can be very large, especially at the worse-case vibration level, orientation and crystal g sensitivity for vibration at exactly twice the modulation rate and coherent with it at a particular phasing, and it is possible for the RFS to actually lose lock. Otherwise, one would expect degraded short-term stability at the "beat" frequency, which would not appreciably affect the average frequency or long term time error.

Finally, consider Item 3, the effect of vibration on the Rb physics package itself. The moderate vibration levels under consideration are well below those imposed during qualification testing, so it is reasonable to rule out gross effects such as permanent damage or even Rb lamp disturbance. The main consideration is therefore interference on the discriminator signal due to vibrational modulation of the light beam. This depends critically on the mechanical design of the physics package, particularly the ruggedness of the mounting of the Rb lamp, the three ovens, and the various cells and optical elements.

EMI

RFS electronics are subject to several specific EMI considerations that are described in the following sections of this primer.

Conducted Susceptibility

An RFS has particular susceptibility to audio frequency ripple on its DC power supply at the servo modulation frequency and its second harmonic. For example, ripple at the fundamental modulation rate can disturb the RFS output frequency (a) by reaching the lamp exciter and impressing interference onto the light, (b) by appearing at the input of the servo amplifier, (c) or by affecting the amplitude of the RF interrogation signal, while ripple at the second harmonic of the servo modulation rate can disturb the RFS output frequency impressing PM on the RF interrogation signal. Such interference causes a false discriminator error signal that affects the frequency lock servo, especially if the interference is coherent or nearly coherent with the servo modulation. This susceptibility is difficult to completely eliminate.

Conducted Emissions

Conducted emissions from the power input of an RFS are usually associated with a switching power supply, while must utilize an effective ripple filter to avoid this problem. Conducted RF emission at the lamp exciter frequency is another potential issue.

Radiated Susceptibility

A properly packaged RFS should not have susceptibility problems from RF radiation.

Radiated Emissions

The most common radiated emission from an RFS is RF energy from its lamp exciter, but proper packaging should avoid this problem.

DC Power Interface

Several additional factors can impact an RFS DC power interface, including (a) reverse polarity protection, (b) over and under voltage protection, (c) voltage transient vulnerability, (d) input ripple current limits and (e) dynamic input impedance, and (e) ground isolation requirements. These requirements are particularly severe for vehicular power systems. Reverse polarity protection can be provided by a series input diode at the expense of some inefficiency; a polarity-sensitive relay is another possibility. Otherwise, it is wise to provide a fuse or other sacrificial circuit element along with a shunt diode. Over voltage protection can be provided in a similar way with a zener diode. Under voltage protection is particularly important with a switching power supply. Protection against voltage transients is often provided by a transient protective zener or varistor. It is sometimes necessary to avoid high ripple currents at the series resonant frequency of an input choke and filter capacitor, perhaps by allowing the choke to saturate and thereby reduce the circuit Q. An assessment of the dynamic input impedance may be necessary when the unit is powered by a switching power supply. DC ground isolation of the input power return is usually provided by an internal DC/DC converter, along with a balun transformer for better AC isolation.

Aging

RFS frequency aging is defined as a slow change in average frequency due to effects within the device (as compared with frequency drift which includes external environmental effects). There is a fairly long list of possible contributors to RFS aging, and, the better the design, the fewer of them are significant. The following factors are generally the most important:

1. Absorption cell buffer gas (partial pressure change)
2. Light intensity and spectrum (light shift)
3. Microwave power (RF power shift)
4. C-field (voltage reference)
5. Oven temperatures (lamp and cell TCs, thermistor instability)
6. Servo offset (static and dynamic)
7. Modulation distortion (even order)
8. Microwave spectral purity (spurs, CG pulling)

For most RFS units, the first two items are the dominant causes. The best such units show small, smooth, monotonically-stabilizing, highly-modelable and predictable aging where, at least after initial stabilization, the direction of the aging never reverses. Non-monotonic aging is an indication that there is more than one significant factor, and which makes modeling difficult.

Item (1), absorption cell buffer gas pressure, has very large leverage (the total buffer gas frequency offset which may be on the order of 1 ppm) and is subject to several aging mechanisms, including He permeation and physical and/or chemical reaction of the commonly-used N_2 with the cell envelope or Rb film. These effects are smooth, steady and consistent, and tend to slowly diminish with time. It is therefore the leading candidate for the cause of RFS drift. Loss of N_2 buffer gas by diffusion into the Rb film or by weak Rb-N_2 chemical reactions would cause negative aging, as is consistently observed for the lowest-aging GPS Rb clocks. The diffusion hypothesis is strengthened by the tendency of the aging of those units to be well-modeled as proportional to the square root of time.

Item (2), light shift, is a popular aging mechanism invoked because it can also have significant leverage and it is likely that the lamp output will change over time. It is undoubtedly a significant factor in the aging of most RFS, but probably not for the lowest-aging GPS Rb clocks that are carefully adjusted for a zero light shift (ZLS) condition by adjusting the temperature of their discrete filter cell

Item (3), microwave interrogation power, depends on the RF power sensitivity of the particular design, which is much larger for units employing an integrated resonance cell than those with separate filter and absorption cells. The lowest-aging GPS Rb clocks have an RF sensitivity of about $\pm 2\text{x}10^{-12}$/dB and highly-stabilized RF interrogation power, and their aging is not believed to be affected by this factor. Clearly there cannot be a large long-term RF power change because of the resulting unobserved effect that would have on the magnitude of the recovered 2nd harmonic signal. For example, a 1 dB change per year, more than would be inferred from the signal record, corresponds to an aging contribution of only $5x10^{-15}$/day.

Item (4), C-field, is an obvious but insignificant factor. One can estimate and exclude instability of the zener diode that controls the C-field. A 10 ppm/month voltage stability corresponds to an aging of only about $1x10^{-15}$/day for a unit operating at a low (50 mG) C-field.

Item (5), oven temperature change, is also very small. The thermistors that control the oven temperatures have ±0.05%/year stability, and, for the filter cell oven with the largest $-6x10^{-11}/^{o}C$ TC, this would cause an aging of under $3x10^{-15}$/day.

Items (6)-(8), electronic effects like servo offsets, modulation distortion and microwave spurs can be analyzed and shown to be OK.

Some more details about aging mechanisms in a rubidium gas cell frequency standard are as follows:

1. Permeation of helium through the walls of the absorption cell is a well-understood reason for negative RFS aging in vacuum. Helium has a high positive pressure shift coefficient (PC), +720 Hz/Torr. During storage in air, it can enter the cell by permeation through the glass envelope, thereby raising the frequency. Then, during subsequent operation in vacuum, the He would leak out, causing negative frequency aging with a long stabilization time. A glass type having low helium permeation (e.g., Corning 7056) should be used for the absorption cell envelope.

2. Loss of N_2 buffer gas partial pressure in the absorption cell is another potential drift mechanism. The PC of N_2 is +548 Hz/Torr, and change in its partial pressure of only $-1.25x10^{-6}$ Torr/day would cause a cell using that common buffer gas to drift $-1x10^{-13}$/day.

   Permeation is not a plausible mechanism for N_2 loss. Gross leaks are unlikely, and would show obvious signs of Rb oxidation while in air. But interaction between nitrogen and the rubidium film in the absorption cell is a possible way that N_2 could be lost. Such interactions could be chemical reactions or (more likely) physical adsorption. It is well known that large negative aging ($pp10^{10}$) takes place immediately after an absorption cell containing a pure or partial N_2 buffer gas is made, and that the aging of a cell is affected by disturbing the thin Rb film that forms on its inside walls. This film, although invisible, is electrically conductive, as indicated by the increase in the microwave loss of a cavity into which a freshly-chased cell is placed. A monolayer of N_2 on the absorption cell wall represents a frequency offset of $\approx 7x10^{-9}$, so an aging of $1x10^{-13}$ corresponds to a change of only about 14 ppm of a monolayer. The long aging time constant is consistent with slow Rb redistribution, which requires about 200 days to move the length of the absorption cell under the influence of a 0.1°C temperature gradient.

3. Much the same argument can be applied to N_2-glass reactions. A very small rate of N_2 partial pressure reduction due to reaction with the absorption cell glass envelope could account for gradually decreasing negative frequency aging

4. Hydrocarbon contamination, perhaps as a buffer gas trace constituent, could be a concern because it would likely have a very large pressure shift coefficient (e.g. heptane (C_7H_{16}) has a PC ≈ -4.5 kHz/Torr).

5. Changes in the intensity and spectrum of the Rb lamp used as the optical pumping light source, because of changes in the lamp exciter RF power, lamp oven temperature, lamp Rb distribution, lamp mounting thermal conductivity, light beam darkening, etc., can cause frequency changes due to the light shift effect. A classical RFS uses a "double-resonance" technique whereby the optical pumping (state selection) and microwave interrogation are performed simultaneously. This causes the frequency to depend on the optical pumping conditions, causing a so-called light shift coefficient (LSC). Most RFS operate at a condition of nominal zero. It is likely that a significant portion of the RFS flicker FM noise floor is determined by lamp intensity and spectral fluctuations via residual light shift effects, but there is no compelling reason to believe that lamp changes and residual LSC is the dominant cause of long-term RAFS drift, especially if it is always in the same direction.

6. Frequency drift could be caused by changes in the DC magnetic bias field caused by (a) drift of the reference zener and other electronic components associated with the C-field source, or (b) changes in the cavity oven residual heater field caused by changes in the thermal losses or external temperature producing a change in the heater power, or (c) changes in internal residual magnetism, or (d) changes in the external magnetic field environment

7. A change in the temperatures of the lamp, filter cell and cavity ovens because of aging of their control thermistors would cause frequency drift due to the temperature sensitivity of the Rb lamp, filter cell and absorption cell. Such an effect could cause frequency aging that would slowly stabilize with time.

8. A change in cavity RF magnetic field strength because of change in the RF drive level, the step-recovery diode multiplier conversion gain or the microwave cavity Q would cause frequency drift due to RF power sensitivity. An SRD multiplier output can change because of component variations and bias circuit changes. The cavity Q (which determines the relationship between the RF power and magnetic field strength) can vary because of Rb migration within the absorption cell. RFS RF power sensitivity is caused primarily by spatial inhomogeneity due to DC and RF magnetic field variations and temperature gradients within the absorption cell that cause the frequency to vary within the

cell volume. A change in RF level causes the place of optimum signal to move, thus changing the locked frequency. A typical RFS RF power sensitivity is a few pp10^{12}/dB for a unit having a discrete filter cell and an order-of-magnitude larger for an integrated cell, for which this effect could obviously be more significant.

One concludes that the absorption cell buffer gas and light shift factors are most likely to be the largest contributors to RFS aging.

RFS aging is often well-modeled by a logarithmic expression of the form:

$$y(t) = a \cdot \ln(bt + 1).$$

This is the recommended drift model of MIL-O-55310, and has been used successfully to describe the aging of rubidium frequency standards over time spans ranging from days to years. Physically, for *bt* >>1, the formula can be used to describe an Arrhenius Law chemisorption process with:

$$a = A \cdot e^{-E_a/kT}$$

where E_a= activation energy, eV, *k*=Boltzmann's constant, 8.616x10^{-5} eV/°K, *T*=absolute temperature, °K, and *A* is a constant.

Another way to model RFS drift that may offer physical insight into the drift mechanism is with the diffusion equation:

$$y(t) = a + b \cdot (t + c)^{1/2}$$

where *a* is a frequency offset term, *b* is a multiplicative scaling term, *t* is time, and *c* is a time offset term. This expression fits the aging of the highest-performance GPS Rb clocks extremely well, even better than the logarithmic model, as shown in Figure 75.

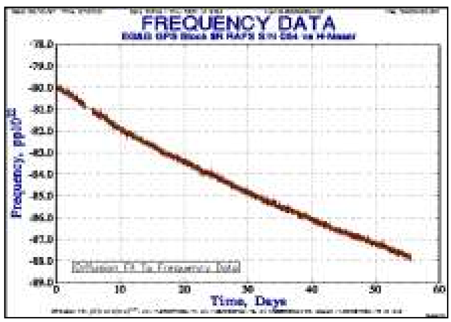

Figure 75. Diffusion Fit to RFS Aging

Since a √t dependence is associated with a diffusion process, this provides evidence of a diffusion aging mechanism (such as diffusion of N_2 buffer gas into the Rb film or glass cell envelope).

Flicker Floor

The drift-removed stability of most rubidium frequency standards improves as the square root of the observation time as its white FM noise is averaged until a so-called "flicker floor" is reached where the Allan deviation becomes constant versus averaging time. That region can therefore be characterized by flicker FM noise, but it is seldom clear whether it is actually caused by such a noise source or whether it is simply the result of environmental sensitivity and/or uncorrected aging. Medium-performance commercial RFS units generally "flicker out" at a stability floor around $1x10^{-13}$ depending on their operating environment. Under benign thermal conditions, barometric pressure can be an important factor. Some of the highest-performance space Rb clocks, with their aging well-stabilized, modeled and removed, have shown flicker floors at or even below the $pp10^{15}$ level [155].

One can speculate as to internal sources of RFS flicker noise, but there is little concrete evidence regarding it. Leading candidates are (a) lamp intensity and spectral changes along with residual light shift sensitivity, (b) lamp and cell oven temperature fluctuations, perhaps caused by thermistor flicker noise, and (c) microwave interrogation power instability.

Life and Reliability

The life of a rubidium frequency standard can be limited by the depletion of its Rb lamp due, but this does not have to be the case for a lamp with adequate Rb fill. The rubidium in a gas cell is reused indefinitely, and its reliability is therefore determined mainly by ordinary electronic failure rate factors, which is long enough that its practical life may be governed by its technological obsolescence. Many units have run for over 30 years, and the large number of commercial RFS on the surplus market testifies to their excellent life and reliability.

Warm-up

The typical several-minute RFS warm-up time is satisfactory for most usage. Slower warm-up can actually be preferable for some applications (e.g., GPS satellite clocks) which operate continuously, require the highest reliability or operate from a limited power source. But other applications (e.g., tactical or missile-borne units) may call for ultrafast warm-up, necessitating special design measures including (a) instantaneous lamp starting, (b) high oven heater demand power, (c) enhanced physics package thermal transfer, and (d) a fast acquisition servo. Those techniques have achieved a remarkable 7-second warm-up and lock-up time at +5°C [178].

Power and Thermal Cycling Endurance

It is important that an RFS be designed to withstand many power and thermal cycles without degradation or damage, especially a unit intended for an RbXO or tactical military application where such conditions are common. The physics package is especially vulnerable to warm-up stress, and design verification testing is needed to assure reliability. One particularly effective test is to expose the unit to several thousand on-off cycles while varying the temperature over its full operational range [184]. A plot of the frequency retrace versus temperature should describe a consistent pattern.

Storage

Long-term off storage is not a severe problem for RFS units, but there are several considerations that are worth keeping in mind. An RFS should be stored at room temperature and away from a source of helium. One generally assumes that the failure rate during storage is less (say one-half) of that during normal operation because there are no electrical stresses applied and internal temperatures are lower.

Periodic Turn-On

It is not necessary to periodically turn on an RFS during prolonged storage. Nevertheless, for critical applications, it is probably desirable to do so (say for 24 hours at 6-month intervals) to allow the physics package to re-stabilize.

Lamp Starting After Prolonged Storage

One concern regarding prolonged RFS storage is the possible failure of the Rb lamp to start. This concern is primarily associated with slow migration of excess rubidium from the tip of the lamp into the active region where the discharge is excited. The resulting Rb film on the inside surface of the glass lamp envelope could then load the lamp exciter circuit to such an extent that it would not oscillate, and the lamp would never start.

Excess rubidium (more than that needed to support a saturated vapor pressure at the operating temperature) is necessary to assure sufficient lamp life. This excess rubidium (about 100 µgrams, liquid at temperatures above 39°C) collects in the tip (cold spot) of the lamp during normal operation. When the RFS is off, the rubidium is "frozen" and nearly all of it remains in the tip. Nevertheless, it still has a finite vapor pressure, and under the influence of any temperature gradient, could migrate to another locating within the lamp. This is a very slow process, especially at relatively cool temperatures with the whole lamp at the same temperature, but, over a long period of time, can result in some rubidium condensed in the active region of the lamp.

The Rb lamp exciter is an RF power oscillator delivering about 0.5 watt at about 115 MHz to the lamp located inside its tank coil. The unlit lamp normally presents a very light load to the exciter, which then has excess loop gain and easily starts oscillating. The high RF voltage associated with the lightly-loaded tank circuit along with some initially-ionized buffer gas atoms lights a plasma discharge in the lamp. As the lamp oven heats, the Rb vapor pressure rises, and the lower ionization potential of Rb causes the lamp discharge to emit light at the two Rb "D" lines that provide optical pumping for the RFS.

The most essential aspect of this lamp starting process is that the RF exciter has sufficient loop gain to oscillate. If it does, even if loaded by condensed rubidium, the resulting RF induction heating will cause the rubidium to rapidly migrate away from the discharge region to the cooler lamp tip, the tank Q and RF voltage will increase, and the lamp will start. A successful lamp exciter design must recognize and overcome those issues by having sufficient RF exciter power, perhaps boosting it for lamp starting. It is relatively easy to provide adequate margin, and the failure of even a heavily-loaded lamp exciter circuit to oscillate is very unusual, thus assuring that the lamp will start after prolonged storage.

Helium Permeation into the Absorption Cell

Helium gas in the atmosphere can permeate through the walls of the glass absorption cell and thereby affect its buffer gas and frequency. For a unit stored and operated in air, this is not an important issue unless the unit is stored in a location with an atmosphere enhanced in helium. It will eventually each equilibrium with the atmospheric helium tension and the helium diffusion rate is lower when the cell is cool during off storage. But for a space Rb clock, the helium will diffuse out again in vacuum, so, if it has "breathed in" helium during ground storage the unit will show negative frequency aging as the helium diffuses out [126]. In that application, it is recommended that the unit be stored in a helium-free (e.g., dry nitrogen) atmosphere.

Applications

RFS applications can be divided into commercial, military and space sectors.

Commercial RFS units are distinguished primarily by their low cost, made feasible mainly by the economies of scale created by telecom usage. Those applications have also driven size reductions and extended their upper operating temperature range, with less emphasis on best stability and performance. Nevertheless, commercial RFS units have gotten smaller and cheaper with only modest reductions in performance, a result fundamentally enabled by the remarkable ability to achieve strong, narrow resonance line in a small gas cell utilizing buffer gas.

Military RFS units are distinguished by their ability to perform reliably from unconditioned power in harsh environments such as shock, acceleration and vibration, extreme temperatures, and exposure to moisture, humidity, EMI and radiation. In the past, such units were often developed specifically to satisfy the need of a particular program according to standard military specifications and employing special MIL-spec parts. Today, the RFS units used in most military equipment are based on ruggedized versions of commercial-off-the shelf (COTS) designs. That results in significant cost savings and faster development schedules, and is feasible in large part because of the improved reliability of commercial electronic parts. It is still necessary, however, to consider the demands of the military environment and to modify and qualify a commercial RFS design as necessary to satisfy those demands.

Phase noise and spectral purity under vibration is often a concern for a MIL RFS, and may require that the crystal oscillator and physics package be modified accordingly. Interestingly, smaller commercial physics packages are an advantage, as is their ability to operate at higher temperatures. Low temperature operation (below -40°C) may be an issue, however, for COTS plastic encapsulated microcircuits (PEMs).

Space RFS units emphasize performance, reliability and launch survival, and they have achieved extraordinary levels of those attributes. They must also be hardened against space radiation.

Most RFS are used as sources of precise timing rather than as frequency standards. Few applications require frequency accuracies at the pp10^{11} level, but that corresponds to nearly a microsecond per day, a very large timing error for many systems.

RFS with a GPS Receiver

An RFS coupled to a GPS time and frequency receiver makes an attractive arrangement for combining the best attributes of both devices. The RFS, especially if it uses a high quality crystal oscillator, is an excellent frequency source in the short and medium term, but its aging and lack of absolute accuracy limit its suitability as a standard of frequency, and it, of course, has no independent source of time. In contrast, a GPS receiver provides an absolute time and frequency reference, but has high noise. Thus, if an RFS is loosely locked to GPS, the combination provides good stability at all averaging times, plus absolute time and frequency. It is as if one has a primary time and frequency, traceable to GPS time which is steered to USNO and NIST.

Figure 76 shows the stability of a free-running Stanford Research PRS10 RFS (red), a GPS receiver (black) and the RFS loosely locked with a time constant of ≈ 1 day to GPS (blue). Clearly, the combination is better than either one by itself (except for a narrow range of intermediate averaging times), providing a consistent stability below $1x10^{-11}$ at low cost. There is little reason to invest in a cesium beam frequency standard for any application as long as a GPS signal is available, especially if an absolute time reference is required. One would have to advance to a much more expensive H-maser steered by a two-way satellite time and frequency transfer system to do significantly better.

It is clear why a GPS-disciplined RFS is so popular for telecom timing.

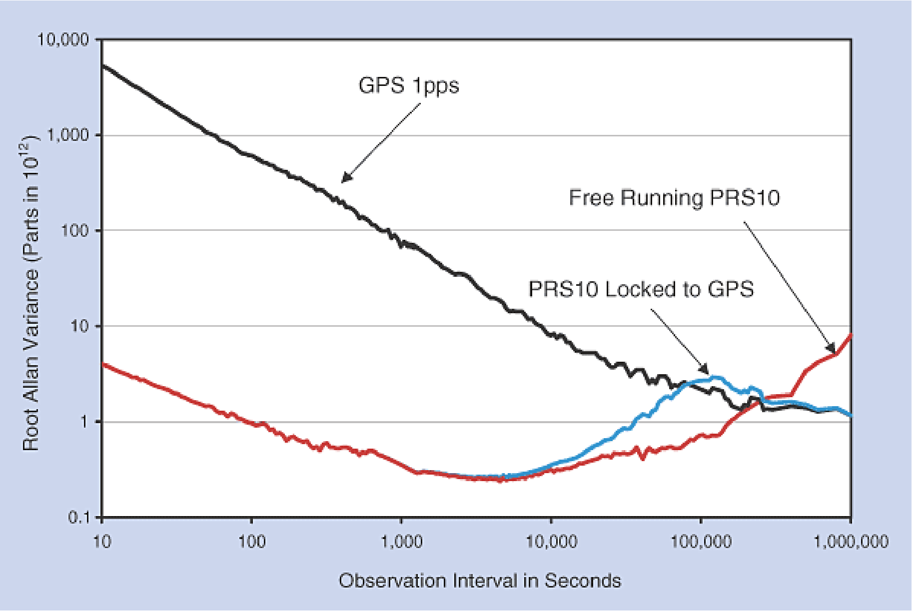

Figure 76. RFS and GPS Stability Plot

Specifications

An example of the condensed specification for a typical medium-performance RFS is shown in Table III [63]. Detailed specifications for a number of classic RFS products will be found in Reference [54], and the data sheets for current products should be consulted for more information.

Table III. Typical RFS Condensed Specifications

Parameter	Value
Output Frequency	5 or 10 MHz
Output Waveform	Sine
Output Level	+7 dBm nominal
Harmonics	≤ -40 dBc
Spurious	≤ -80 dBc
Phase Noise at 10 MHz	$\mathcal{L}$(100 Hz) ≤ -120 dBc $\mathcal{L}$ (1 kHz) ≤ -135 dBc
Allan Deviation	$\leq 1\text{x}10^{-11}\tau^{-1/2}$ for $1 \leq \tau \leq 100$ sec
Drift	$\leq 3\text{x}10^{-11}$/month (after 1 month)
Operating Temperature Range	-40 to +68°C
Temperature Sensitivity	$\leq 3\text{x}10^{-10}$ over op temp range

Parameter	Value
Supply Voltage	+22 to +32 VDC
Power	≤ 30 W (max), ≤ 12 W (SS, +25°C)
Warm-up Time	≤ 5 min to lock at +25°C
Voltage Sensitivity	≤ $1x10^{-11}$/10%
Magnetic Field Sensitivity	≤ $2x10^{-11}$/Gauss
Size (L, W, H)	3" x 3" x 4"

Testing

Environmental performance is critical for many applications of rubidium frequency standards. IEEE Standard 1193, *IEEE Guide for Measurement of Environmental Sensitivities of Standard Frequency Generators* [256] and Section 4.9 of MIL-O-55310B for crystal oscillators [253] provide guidelines for the testing of these devices, but a custom test plan and procedure is often required.

Rubidium frequency standards are, for the most part, tested similarly to other pieces of electronic equipment. Commercial RFS units are subject to their manufacturer's normal development tests, followed by those production tests deemed necessary to maintain product quality, while military and space clocks are subject to more stringent developmental, qualification and acceptance testing as dictated by program requirements and their specifications.

The main differences associated with RFS tests are (a) the need for an adequate frequency reference and specialized clock measuring facilities, and (b) the need to verify RFS long-term aging which requires that units be operated for an extended period of time. Space RFS testing imposes the additional requirement of conducting the tests under thermovac conditions. RFS testing is described comprehensively in Reference [69] in the context of military specification requirements.

Table IV. Military Specifications for the Testing of Electronic Equipment

RFS USAGE	GENERAL SPECIFICATION	TEST REQUIREMENTS	ENVIRONMENTAL TEST METHODS	EMI TEST METHODS
All	MIL-STD-454		MIL-STD-810	MIL-STD-461
Airborne	MIL-E-5400	MIL-T-5422		
Ship	MIL-E-16400			
Ground	MIL-E-4158			
Space	DOD-E-8983	MIL-STD-1540		MIL-STD-1541

Table V. RFS Environmental Tests						
Environmental Test	Critical Parameter	QTP	ATP	MIL-O-55310B PARAGRAPH	MIL-STD-202 METHOD	MIL-STD-810 METHOD
Acceleration/Orientation	Frequency	0	N/R	4.9.18,.41	212	513
Acoustic Noise	Phase Noise	N/R	N/R	4.9.39		515
Altitude/Pressure	Frequency	0	N/R	4.9.45-.46	105	500
Bench Handling	Function	R	N/R			516
EMI Susceptibility	Frequency	A/R	N/R	4.9.36	MIL-STD-461	
Explosive Atmosphere	Function	N/R	N/R	4.9.42	109	511
Fungus	Function	N/R	N/R	4.9.54		508
Humidity/Moisture	Function	0	N/R	4.9.49	103	507
Immersion	Function	A/R	N/R		104	512
Magnetic Field	Frequency	R	0	4.9.43	ASTM 346-64	
Radiation	Frequency	A/R	N/R	4.9.47		
Rain	Function	0	N/R	4.9.49	106	506
Salt Fog	Function	0	N/R	4.9.50	101	509
Sand and Dust	Function	N/R	N/R		110	510
Shock, Operating	Function	0	N/R	4.9.40	213	516
Temperature, Operating	Frequency	R	R	4.9.10-.12		
Temperature, Non Op.	Function	0	N/R	4.9.46		
Temperature/Altitude	Frequency	0	N/R			504
Temperature Cycling	Function	R	N/R		102	
Temperature Shock	Function	0	0	4.9.44	107	503
Vibration, Sine	Frequency	R	0	4.9.18-.38	201	514
Vibration, Random	Phase Noise	R	0	4.9.18-.38	214	514

<u>Test Setup</u>. A typical test setup for the environmental testing of an RFS is shown in Figure 77. The RFS under test is installed in an environmental chamber (which may be a temperature, humidity, altitude, or other such chamber, or a shaker, shock machine, flash X-ray or other such apparatus). It is powered from a dc supply and its current and monitors are measured by digital or analog meters, and its recovered signal is observed on an oscilloscope. Alternatively, a custom “monitor box” may be

used, especially if special control or monitor functions are involved. A stripchart record of the RFS dc supply current is often useful for evaluating performance and diagnosing problems. Besides warm-up and steady-state power, the current record shows lamp ignition and oven stability, and can be integrated to determine RbXO syntonization energy [184]. The primary measurements, however, are the RFS RF output level, frequency, and spectral purity. The frequency measuring system may be simply a vector voltmeter or analog frequency difference meter to measure RFS phase or frequency change, a frequency counter (perhaps the high resolution interpolating reciprocal type), or a very high resolution heterodyne arrangement (perhaps with computer control and data analysis). The frequency reference may be a crystal oscillator (for low noise), another rubidium standard (for stability, portability, and fast warm-up), or a cesium standard (for absolute frequency determination). The RFS spectral purity may be observed on an RF spectrum analyzer or on a wave or FFT analyzer (after down conversion). A phase noise measuring system may also be necessary (by using a double-balanced mixer and loose phase-locked crystal oscillator). The primary concern for this instrumentation is often its portability to an outside testing lab. In such a case, careful planning is critical and all the test instrumentation should be set up "at home" to confirm the test methodology and to avoid missing or malfunctioning items in the field.

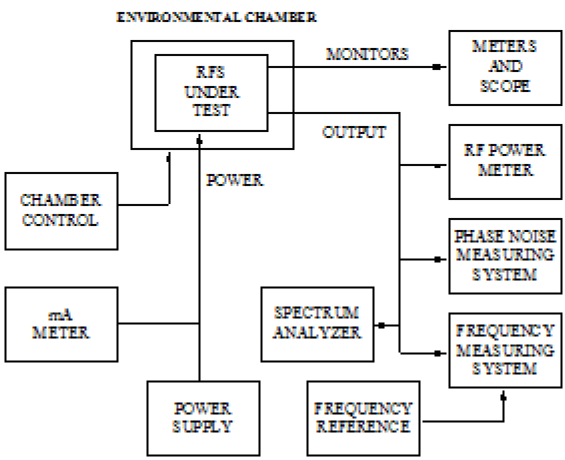

Figure 77. RFS Environmental Test Setup

Acceleration/Orientation. Unlike a quartz crystal oscillator, an RFS does not have any inherent static acceleration sensitivity (either "tip-over effect" or centrifuge). It is possible, however, for an RFS to show some frequency change due to acceleration and reorientation because of thermal effects. A test for RFS orientation sensitivity should therefore allow sufficient time (about five minutes) to reestablish thermal equilibrium. It is also possible to have some change in the physical distribution of the rubidium in the lamp under high static g-forces that can cause a small frequency change. This effect will occur if the acceleration forces liquid rubidium into the body of the lamp and will be reversed by acceleration in the opposite direction or by quiescent operation. It is possible, but not always easy, to make the precision frequency measurements necessary to see these effects via the slip rings of a centrifuge. Redundant slip rings should be used for both power and RFS output to reduce contract noise.

A separate “2g tip-over” test may be required for the crystal oscillator portion of an RbXO. The test results should be reported as the resultant of the g-sensitivity vector.

Dynamic acceleration can have a profound effect on the stability and purity of an RFS, and those tests are discussed in the Vibration section below.

Acoustic Noise. Acoustic noise is usually not a significant factor affecting RFS operation. The RFS is typically suspended on elastic cords during exposure; frequency and phase noise should be measured.

Altitude/Barometric Pressure. The main considerations for the sensitivity of an RFS to ambient pressure are; (a) frequency shift due to absorption cell buffer gas pressure change caused by deflection of the glass cell envelope (about $1x10^{-10}$/atm), (b) frequency shift due to thermal effects involving the physics package ovens and Rb lamp, and (c) thermal effects due to heat transfer of the electronic circuits. Effect (a) is proportional to the pressure change; effects (b) and (c) are small until the pressure is reduced to about 10 Torr (100,000 feet altitude). Oven power will be less and stabilization factor better in vacuum. The electronic circuits must be designed for adequate heat transfer without air, and temperature profiling may be necessary to ensure reliable operation in vacuum. The barometric sensitivity of an RFS can also be measured as part of a temperature-altitude test. Unlike a cesium beam frequency standard, an RFS does not use high voltages and can be safely operated throughout the full pressure range from sea level to hard vacuum without any corona discharge hazard.

Bench Handling. A bench handling shock test is perhaps the most severe yet realistic and practical way to check an RFS for ruggedness. The unit should be removed from its enclosure as it if were being serviced. After completing the test, the unit should be inspected for damage and operated to show any resulting frequency offset.

EMI Susceptibility. The most significant form of EMI susceptibility in an RFS is usually due to ripple (CS01) and transients (CS06) on the dc input power. This aspect of RFS design is covered by military and other standards [257], but specific requirements may also be imposed. Ripple susceptibility is generally worst at the RFS servo modulation rate; large frequency offsets are possible due to interference with the servo that locks the VCXO to the Rb reference. A phase comparator, vector voltmeter, or analog frequency difference meter is very useful for showing RFS EMI susceptibility, as is observation of the RFS recovered signal on an oscilloscope. Ripple susceptibility testing does not require a screen room or specialized EMI test instrumentation, and can be investigated with ordinary laboratory equipment. The EMI susceptibility test procedure must include a pass/fail criterion; a frequency change of 1×10^{-10} is a reasonable value for a tactical RFS. The radiated susceptibility test setup should pay particular attention to the shielding and grounding of the RFS power/monitor leads; this is often the primary path for interfering RF into the unit. It is also advisable to use a low-noise linear (rather than switching) dc supply to power the RFS during all EMI testing.

The requirements for transient protection vary depending on the degree of external power conditioning. Reverse and overvoltage protection is often necessary and must be tested. Applying a pre-charged capacitor across the dc input is one simple way to simulate voltage transients. RFS turn-on (inrush current) and turn-off (voltage spike) transients can be a problem for the host system. A manually tipped mercury relay and a digital storage oscilloscope is an effective means to simulate and observe these transients.

Explosive Atmosphere. An RFS does not use high voltages or mechanical relays and switches, and can be operated in an explosive atmosphere with minimal likelihood of causing an explosion. Since an RFS is not normally sealed, the outer cover should be removed or loosened during the test to facilitate the penetration of the explosive vapor.

Fungus. A fungus test is usually conducted “by analysis” to verify that the design uses only components and materials that are inherently fungus inert.

Humidity/Moisture. A typical humidity test consists of five, 48-hour temperature-humidity cycles with RFS operation near the end of each cycle. With an unsealed unit, the test results depend strongly on the adequacy of conformal coating and encapsulating processes, and these should closely represent the actual production processes for the test results to be valid. RFS moisture sensitivity is most often associated with the high impedance servo amplifier synchronous detector/integrator circuits.

Immersion. The capability to withstand immersion in water is seldom a requirement for an RFS. Immersibility requires a sealed case and connectors, but it otherwise does not affect RFS design or performance.

Intermittent Operation/Retrace. (See Power/ Temperature Cycling below.) A test for the frequency retrace of an RFS under intermittent operation should, by definition, return the unit to exactly the same operating conditions so as not to confuse retrace with environmental sensitivity. The main concern is that the retrace error be non-accumulative. The test must define; (a) operating conditions (temperature, etc.), (b) off time, (c) restabilization time, and (d) number of retrace cycles. A well-designed RFS should have an excellent retrace characteristic (pp10^{11}) that has little dependency on temperature, off time, or restabilization time.

The test emphasis should therefore be on performing enough cycles to verify that the retrace error does not accumulate.

Magnetic Field. An RFS has an inherent sensitivity to dc magnetic field and contains magnetic shielding to reduce this sensitivity. The largest magnetic sensitivity is along the physics package optical axis (the direction of the internal bias field), and has a quadratic dependence of frequency on dc magnetic field ($\Delta f/f = 8.38x10^{-8}$ H, Gauss^2). Since the magnetic sensitivity varies with C-field frequency adjustment, the test procedure must specify the RFS frequency setting (minimum, nominal, upper range, or maximum); nominal is usually used.

The test procedure must also define the magnetic field environment. The electrical reversal of a 3 Gauss field from a pair of 4 foot diameter Helmholtz coils [89] is recommended. This field is easy to produce yet considerably larger than the Earth's field of about 0.5 Gauss, and field reversal tends to eliminate offsets due to the Earth's field (a shielded room is impractical). Other considerations for the test field are; (a) uniformity using coils much larger than RFS and away from metallic objects, (b) calibration (measure field at center w/o RFS), and (c) magnitude which affects shielding factor and measurement resolution. Care should be exercised when de-energizing the Helmholtz coils; unplugging them can produce a hazardous high voltage.

Magnetic sensitivity is generally a qualification test, but variations in C-field and/or shield permeability and fit can require 100% testing for critical applications. AC magnetic field sensitivity is generally part of EMI susceptibility testing.

Radiation. The radiation sensitivity of an RFS is essentially that of its electronic circuits; the Rb physics package is inherently quite hard. RFS survivability can be a critical requirement for both transient and total dose radiation environments. Transient radiation testing usually requires a Flash X-Ray (FXR) facility to generate an intense gamma pulse. The RFS is operated during the exposure and may be required to "operate through" or to quickly recover frequency accuracy; in all cases, it must not suffer latch-up, burnout, or other permanent degradation. The test setup generally includes extensive recording of RFS output level, phase, frequency, light monitor, VCXO control voltage, and dc input current (as well as radiation dosimetry). Transient radiation testing is very desirable to verify analysis of the RFS circuits, and is meaningful even for a single sample having generic parts. The most critical parts causing latch-up are usually CMOS devices; all circuits may require resistors or other means for current limiting.

Total dose radiation testing requires a different methodology. Analysis based on piece-part test data is often preferable to a test of the entire RFS because a worst-case error budget can be done. The most critical devices are usually servo amplifier and temperature controller op amps and the C-field voltage reference. RFS testing, if done to confirm the analysis, must be done with hardened parts. Total dose testing is likely to damage the unit as it is exposed to a series of successively higher radiation levels. The test setup is usually quite simple if the unit does not have to be operated during the exposure; before and after frequency and perhaps monitor measurements are generally all that is required. Total gamma dose is usually done by placing the unit in a Co^{60} cell. Dose rate and annealing effects should be considered. If the unit is operating during exposure, the RFS photodetector will respond to the gamma irradiation. Neutron exposure is usually done by placing the unit in a reactor. The unit may become radioactive because of neutron activation of the magnetic shields and other high-Z materials. The most critical part for neutron fluence is usually the silicon photodetector, which loses output due to lattice damage.

No standard procedures apply to RFS radiation testing; each case requires careful planning and expert advice.

Rain. The test procedure should specify which sides of the RFS are to be exposed to rain. Typically, waterproof cables are attached throughout the test, and the unit is operated near the end of each exposure.

Salt Fog. Since the RFS is typically not operated during exposure, its connectors should be covered. The unit should not be washed after exposure (as allowed by MIL-STD-810). EMI testing should follow salt fog exposure since salt deposits and corrosion could affect grounding and shielding. This can be a very destructive test.

Sand and Dust. The test procedure should specify the RFS face to be exposed. Since the RFS is non-operating during exposure, connectors should be covered. Penetration of dust should not necessarily be considered a failure.

Shock. The RFS under test should be powered to best show intermittent failures under shock. Test cables should have strain relief and should be supported close to the unit to prevent whipping and damage which could affect RFS measurements. The RFS should be observed for timing error and permanent frequency offset. Rubidium motion in the lamp (as described under Acceleration) may occur.

Temperature, Operating. Temperature sensitivity is often the most significant environmental factor affecting the performance of an RFS. A stability of $3x10^{-10}$ is typical for a small tactical RFS over a military temperature range, whereas the unit will not have that much frequency aging over several years. Furthermore, there is considerable unit-to-unit variation of this important parameter which is not necessarily monotonic and which may have regions of high incremental sensitivity. The RFS temperature stability is usually specified as the maximum (peak-to-peak) variation in frequency anywhere within the operating temperature range. RFS operating temperature range is usually specified from a minimum ambient value to a maximum baseplate value. The distinction between ambient and baseplate temperatures is necessary because of the RFS internal dissipation unless the unit is attached to a large heat sink or is otherwise well coupled to the ambient. It is sometimes necessary to specify the thermal resistance of the heat sink (from ambient air to RFS baseplate).

RFS temperature stability should be measured as part of the ATP for every unit. It is best to make continuous frequency measurements on a stripchart recorder as the RFS is stepped or ramped over its full operating temperature range (rather than just measure the RFS frequency at a few discrete temperatures) so that a region of large sensitivity or anomalous behavior is detected. An averaging time should be chosen long enough to average the measurement noise while not masking rapid changes; 100 seconds is usually a good choice. Sufficient dwell time must be allowed, especially at the temperature extremes, and the record should be examined for noise, “glitches,” and retrace.

If the RFS uses C-field temperature compensation, it may exhibit disparate frequency-temperature characteristics at different frequency adjustments.

Temperature, Non-Operating. Sufficient soak time must be used to ensure that RFS internal temperatures reach the specified limits.

Temperature Cycling. (See Power/Temperature Cycling below).

Temperature Shock. Temperature shock testing is not as effective with an RFS as with small components because of the slow internal temperature response of the ovens. The severity of the test is indicated more by the internal temperature extremes than the rate of change of ambient temperature, which may be expensive to produce.

Temperature/Altitude. The Temperature/Altitude test has been deleted from the latest revision of MIL-STD-810. It is better to measure the effects of pressure (altitude) and temperature separately.

Vibration. The stability and purity of an RFS are affected by mechanical vibration primarily because of the acceleration sensitivity of the quartz crystal used in the VCXO that produces the output signal. Direct vibrational modulation of the crystal oscillator generally affects the RFS phase noise and spectral purity at vibration frequencies higher than the servo bandwidth without producing a frequency offset. Vibrational modulation of the VCXO at the 2nd harmonic of the servo modulation rate, however, can cause a frequency offset. Low frequency vibrational modulation of the crystal oscillator can cause a frequency offset due to loss of microwave power. These XO effects are reduced by a high modulation rate, a wide servo bandwidth, and a low crystal g-sensitivity.

RFS stability can also be affected by vibrational modulation of the physics package light beam at or near the servo modulation rate. This problem is reduced by rigid physics package construction. Circuit board and wiring microphonics can also affect RFS stability.

RFS vibration testing requires measurement of frequency offset, frequency stability (Allan deviation) and phase noise under dynamic conditions while the unit is on a shaker. It should also include before and after measurements to check for a permanent frequency offset. Phase noise is the primary parameter of concern during random vibration, and frequency stability is the most critical factor under sine vibration. Particular attention should be paid to frequency stability while the RFS is vibrated at the servo modulation rate and its harmonics. An analog frequency difference meter is an effective measurement tool; counter measurements are subject to beats due to coherence between the gate time and vibration frequency. The RFS recovered signal should also be observed, as should the lock detector output. Checks should be made for interference from the magnetic field of an electrodynamic shaker by holding the unit slightly above the top of the operating shaker. A slip table can help by allowing separation between the shaker and the RFS under test, and it also reduces cross-axis vibration. Ground insulation (rigid) or an isolation transformer in the RFS output can also help to avoid ground loops, hum and interference; sine dwell measurements should not be made at 60 Hz harmonics.

Power/Temperature Cycling

RFS units intended for frequent on-off and temperature cycling (in particular, the Rb reference of an RbXO [184]) should be subjected to a Design Verification Test (DVT) to prove their endurance under such cycling. The physics package of a fast-warm-up RFS turned on after a cold soak experiences severe thermal stresses; nevertheless, with proper design, a unit can survive such cycling and provide a stability comparable to a unit that operates continuously. A typical DVT would subject four RFS units to 20 on-off cycles per day while subjecting them to a -62 to +68°C temperature cycle each day for 180 days. The daily temperature cycles include a cold soak at the low temperature extreme. The internal temperature of the Rb physics package should decay essentially all the way to the air temperature between turn on. The 3600 on-off cycles and 180 temperature cycles of the DVT simulate 20 years of normal RFS operation.

The DVT should also include frequency measurement data after each turn-on cycle. A plot of RFS frequency vs. temperature should show a consistent pattern for each daily temperature cycle, similar to the static temperature stability characteristic. A plot of average daily frequency vs. time should show a retrace characteristic trend similar to the normal RFS aging behavior.

A DVT such as this should be performed on any basic Rb physics package design that is intended for an application that involves frequent on-off and temperature cycling, e.g., 7500 fast warm-up turn-on cycles over a period of 25 months without any sign of wear-out due to thermal fatigue stress. A cold soak and turn-on is also an effective means of environmental stress screening for production RFS units as discussed below.

Environmental Stress Screening

The purpose of Environmental Stress Screening (ESS) is different from other environmental tests. The latter are intended to verify the adequacy of the RFS design, construction, and performance under the anticipated environments. The purpose of ESS is to reduce the number of service failures by applying temperature and vibration screens to each production unit to precipitate latent manufacturing defects as detectable failures.

To devise a suitable ESS test, vibration and temperature surveys are performed to arrive at tailored levels which will show flaws without damaging a sound RFS unit. A typical tailored vibration screen is random vibration of 5 grms (0.028 g^2/Hz from 80 to 350 Hz, decreasing at 3 dB/octave to 20 Hz and 2000 Hz), applied for ten minutes in each of three axes with the RFS unit operating and the input current and lock monitor signal recorded. Wideband random vibration is far more effective than sine vibration because the random excites all vibrational modes simultaneously and for the full duration of the exposure. Single axis excitation is usually selected because of shaker limitations.

A typical tailored temperature screen consists of 12 temperature cycles with power applied after a cold soak of one hour. The cold soak is necessary to adequately stress the physics package ovens and temperature control circuitry in terms of temperature rates and excursions. The cold soak duration is determined by the thermal time constants of the physics package ovens. The effectiveness of temperature cycling in precipitating and detecting failures is greatly increased by operating and monitoring the test unit, and by recording the input current and the lock monitor signal. In particular, a cold soak and turn-on is much more effective than exposing a fast-warm-up RFS to an external temperature shock. A temperature rate of 5°C/minute is generally selected (rather than a faster rate which requires a higher performance test chamber) since the internal response of the RFS is not significantly different for the slower rate.

Experience has shown that a properly chosen ESS test is a cost-effective way to find latent defects and thereby ensure a lower failure rate in the field. An important part of the ESS process is to review the test records to refine both the RFS manufacturing processes and the effectiveness of the ESS test.

Embedded Software

Many modern RFS units employ embedded software (“firmware”) to support their operation, and this presents unique test requirements. Of particular concern is the possibility of encountering an unexpected operating condition that causes a failure that could otherwise be undetected. Careful code review and testing under a wide range of circumstances is recommended.

Analog Control and Monitoring

A typical analog C-field tuning circuit is shown in Figure 78. The op amp serves as an active current source whose nominal current is equal to the reference voltage at its non-inverting input divided by the resistance from its inverting input to ground. That current is adjustable by applying an external tuning voltage or by connecting a variable resistor from the tuning voltage input to ground. The tuning voltage pin also serves as a monitor point for the reference voltage. Circuits to linearize the C-field tuning characteristic are feasible, but are seldom used.

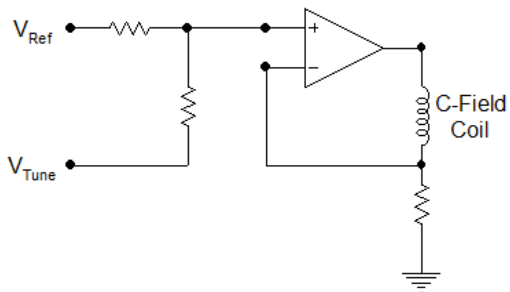

Figure 78. Typical C-Field Circuit

Digital Control and Monitoring

Most modern RFS units have provisions for external digital control and monitoring via a serial communications interface, most often a 9600-baud RS-232 interface that supplemented by a PC user interface program.

Calibration

An RFS is a secondary frequency standard and, as such, requires frequency calibration (syntonization) to obtain full accuracy. RFS calibration must be done with respect to a NIST or USNO traceable frequency reference such as a cesium beam tube instrument or a GPS time and frequency receiver using a high-resolution frequency measuring system. The specific means for performing the frequency adjustment depends on the particular unit, but it should be done at the expected operating temperature after allowing sufficient measurement time to provide the desired precision. It is possible to make this process automatic [315]. A typical adjustment tolerance is $1pp10^{11}$, which is adequate in relation to the usual RFS TC and drift performance, and requires a measurement time of only about 100 seconds of noise averaging time. Recalibration should be performed at least annually since the aging rate of a mature unit is typically $1x10^{-11}$/month, $1x10^{-10}$/year and $1x10^{-9}$ “forever”.

PRODUCTS

These primer sections cover rubidium frequency standard manufacturers and their products.

Manufacturers

There are currently four major RFS manufacturers in the United States and several in other countries, as shown in Table VI. Those companies tend to have rather long technological heritages from prior organizations, often involving the same key people. In addition, there are many other companies that build products that contain RFS modules, sold either as time and frequency products or as some other instrument (e.g., counter, synthesizer, radio, time server) that needs a precise time or frequency reference. Some of the RFS manufacturers offer a complete line of time and frequency products such as quartz crystal oscillators, distribution amplifiers and GPS time and frequency receivers.

Table VI. Major RFS Manufacturers

Country	Company	Heritage	Types
United States	Excelitas	Varian, General Radio, EG&G, PerkinElmer	c, M, S
	Symmetricom	Efratom, Ball, Datum	C, M, s
	Frequency Electronics	Litton	C, m, s
	Stanford Research		C
UK	Quartzlock		C, m
Switzerland	Spectratime	Neuchatel Observatory, Temex	C, S
Israel	Accubeat	Tadiran, Time & Freq. Ltd.	C, M
Others: Aqtron, CJI Technology, Darlington, Fujitsu, NEC			
Type code: C=Commercial, M=Military, S=Space Emphasis code: Lower case=Minor, Upper Case=Major, Red=Emphasis			

This information is obviously subject to change, and one should read ads, conduct web searches, attend trade shows and use other means to obtain current information about RFS manufacturers and their products.

Gallery of RFS Products

The following pictures show a collection of commercial, military and space RFS units in Figures 79, 80 and 81 respectively.

Varian Associates V-4700, c. 1961. The first commercially available rubidium vapor frequency standard.

Examining a V-4700A instruction manual shows a design that is very similar to today's units, albeit implemented with discrete transistors and a vacuum tube lamp exciter instead of integrated circuits or firmware, and its specifications are quite competitive with today's RFS products (a 1-second short-term stability of 1×10^{-11} and a long-term stability of 5×10^{-11} per year). But it's a lot bigger and heavier!

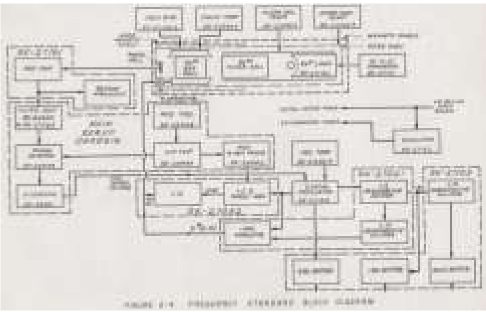

General Technology 304-B, c. 1965. This lineage began at Space Technology Laboratories, moved to Clauser Technology (c. 1960), then General Technology (c. 1962) and finally Tracor.

The General Technology 304-B Rb physics package shown in this c. 1962 drawing from a c. 1967 Tracor service manual is typical of those early assemblies. The discrete filter cell appears to share the same cavity thermal environment as the absorption cell, similar to the approach taken in the first General Radio designs.

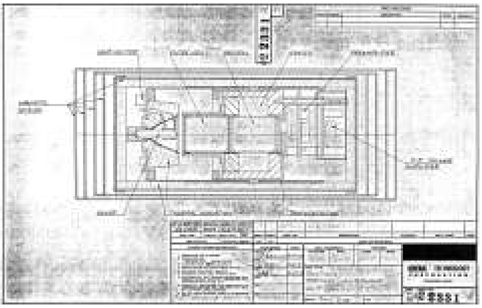

Hewlett Packard 5065, c. 1968. Classic high performance RFS laboratory instrument.

Efratom, Ball Efratom FRK-L. Original miniature RFS, c. 1971.

Efraton FRS, c. 1985. Smaller than FRK

Stanford Research PRS10, c. 1995. Very good performance, excellent phase noise

Frequency Electronics 5680, c. 1998. Low profile.

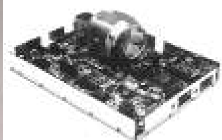

Efratom LPRO (Low Profile Rubidium Oscillator), c. 1995. Good performance, manufactured in large volumes for commercial telecom applications.

Symmetricom X72, c. 2000. Small size, high temperature op, modest performance, for telecom apps.

Figure 79. Gallery of Commercial RFS Products

PRODUCTS

Collins Radio (later Rockwell Collins) AFS-81 Airborne RFS for Verdin VLF Communications system, c. 1970. Physics package built by General Radio. High performance, rugged.

Efratom (later Ball Efratom, Datum and Symmetricom) M100 general purpose (e.g., ground anti-jam and troposcatter radio) MIL RFS, c. 1980. Similar RFS-10-7 made by EG&G.

Efratom (later Ball Efratom) M3000 airborne tactical RFS, c. 1985. Similar units were built by EG&G and FEI. Probably the most environment-tally hardened RFS units ever made.

EG&G (later PerkinElmer and Excelitas) RFS-10 general purpose MIL RFS, c. 1985. Smaller version of M100 and RFS-10-7.

Symmetricom 8130A modern MIL-spec RFS, c. 2002. Re-placement for M100. Has DDS and digital control interface, screened PEMs.

Symmetricom 8100 general purpose MIL RFS, c. 2000. Ruggedized version of LPRO.

Symmetricom 8122 ruggedized airborne version of X72, c. 2005.

Figure 80. Gallery of Tactical Military RFS Products

PRODUCTS

General Radio SATS (Spacecraft Atomic Timing System), c. 1970. First space qualified RFS. Rb frequency standard and digital clock.

Rockwell GPS II Rb Clock, c. 1980. First GPS atomic clock. Uses Efratom physics package.

EG&G GPS Block IIR RAFS, c. 1990. About 100 built. Very high performance and reliability.

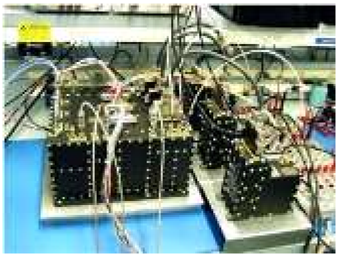

Frequency Electronics Advanced EHF triple redundant Rb and quartz clocks, c. 2000. Similar to FEI Milstar RFS c. 1990.

Temex Galileo RAFS, c. 2000.
Moderately high performance.
Backup to passive H-maser.

PerkinElmer GPS IIF RAFS, c. 1995. Includes 10.23 MHz secondary loop synthesizer. Enhanced performance.

Figure 81. Gallery of Space Rb Clocks

RbXO

The RbXO [184] is the combination of a rubidium frequency reference and a low-powered crystal oscillator configured so that the Rb reference is only occasionally turned on to briefly syntonize the crystal oscillator and thereby minimizing the overall energy consumption. The continuously-running crystal oscillator may be the same one used in the Rb reference, or a separate low power crystal oscillator. It must, of course, have a non-volatile memory to maintain its last syntonized tuning condition. The main differences for the Rb reference requirements are fast warm-up and re-stabilization, good frequency retrace, and robust power-cycling endurance. An RbXO contains logic to adapt its syntonization duration to the minimum necessary for adequate Rb reference re-stabilization versus ambient temperature. A photograph of an RbXO is shown in Figure 82 [238]. This unit could, for example, serve as an accurate battery-powered portable timing reference in an application where GPS independence was needed. The optimum syntonization interval depends on the standby clock's aging and temperature stability, its operating environment, and the system's timing requirements. More recently, the RbXO concept has been revisited using a chip-scale atomic clock as the atomic frequency reference [262].

Figure 82. Photograph of EG&G RbXO

Laser-Pumped Gas Cell Frequency Standards

Optical pumping with diode lasers instead on spectral lamps offers the advantage of smaller size and lower power, along with the possibility of higher S/N ratio. Laser pumping eliminates the need for isotopic filtration and thus allows the use of Cs rather than Rb cells, which has higher vapor pressure at a given temperature and requires no isotopic separation. The main issues are laser diode availability, noise and reliability, along with their difficult wavelength and intensity stabilization requirements. Laser pumping can be effectively combined with pulsed light operation to reduce light shift.

An innovative miniature Cs resonator, using conventional microwave interrogation, was developed by Westinghouse (later Northrop-Grumman) around 1995 (see Figure 83). It used a 1.2 cm^3 highly dielectrically loaded TE_{201} rectangular 9.2 GHz cavity in a 1.6 cm^3 overall resonator assembly with a 0.1 cm^3 cell. This scales to a 3.0 cm^3 cavity for Rb at 6.8 GHz. This technology has been supplanted by CPT interrogation in chip-scale atomic clocks.

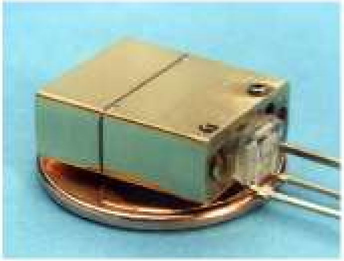

Figure 83. Northrop-Grumman Miniature Cs Resonator

Chip Scale Atomic Clocks

Chip scale atomic clocks (CSAC) are a new class of atomic frequency standards currently undergoing intensive development [258]-[263]. Their goals are (a) very small size (≈1 cm^3), (b) very low power (≈30 mW), (c) moderate stability (≈$1x10^{-11}$) and, ultimately, (d) very low cost. Several technologies are being explored, but the leading approach strongly resembles that of rubidium gas cell devices.

A fundamental factor is that tiny (≈1 mm long) cesium and rubidium gas cells with buffer gas can produce narrow (≈1 kHz) resonances. Other enabling factors are the use of diode lasers and coherent population trapping (CPT) interrogation, along with MEMS (micro electro-mechanical systems) technology to batch-fabricate cells using semiconductor technology. Coupled with low power RF and microcontroller electronics, many of the CSAC goals have already been realized as shown in Figure 84 for the 16 cc, 120 mW Symmetricom SA.45s CSAC.

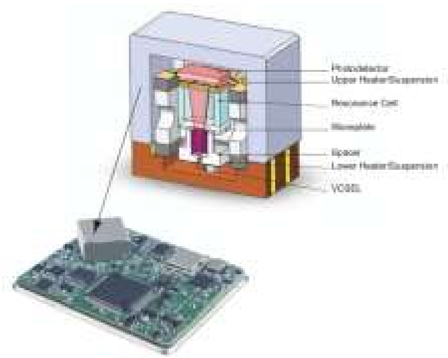

Figure 84. Symmetricom SA.45s Chip Scale Atomic Clock

CPT Interrogation

CPT interrogation avoids the requirement for a large microwave cavity by modulating a diode laser tuned to one of the Cs or Rb D lines with RF at one-half of the hyperfine frequency. That produces an optical field with coherent sidebands separated by the atomic resonance that interacts with the atoms such that the transmitted light is a maximum when the RF frequency is at the center of the atomic line. A frequency lock servo locks the RF frequency as in a conventional RFS, while other digital servo loops control the cell and laser diode temperatures and the laser wavelength and intensity.

Chip scale atomic clocks and coherent population trapping interrogation offer attractive new opportunities for wider deployment of atomic clocks, opening up entirely new applications for precise timing, especially in portable equipment. An example of a commercial CPT rubidium clock is described in Reference [264].

Advanced Rubidium Clocks

The mature RFS technologies covered in this primer have a 50-year record of improvement, and, because of their combination of performance and practicality, will continue to be the most common form of atomic clock for the foreseeable future. Opportunities also continue for further improvements, including the use of laser pumping, a better understanding of aging and noise floor mechanisms, more effective use of digital control, and the availability of new electronic components.

BIBLIOGRAPHY

These primer sections include a glossary and list of acronyms, and a bibliography with references about rubidium frequency standards.

Glossary and Acronyms

ADC	Analog to Digital Converter
ADEV	Allan Deviation, a frequency stability statistic
AFS	Generic atomic frequency standard or “atomic clock”
ATP	Acceptance Test Procedure
BTC	Baseplate Temperature Controller
Buffer Gas	Inert gas used in Rb lamps and cells
C-Field	Static magnetic bias field applied to Rb physics package
CPT	Coherent Population Trapping
CSAC	Chip Scale Atomic Clock
DAC	Digital to Analog Converter
DDS	Direct Digital Synthesizer
DSP	Digital Signal Processing
DVT	Design Verification Test
EMI	Electromagnetic Interference
ESS	Environmental Stress Screening
FXR	Flash X-Ray
GPS	Global Positioning System
LSC	Light Shift Coefficient
NIST	National Institute of Standards and Technology
OCVCXO	Oven Controlled Voltage Controlled Crystal Oscillator
PC	Pressure Shift Coefficient
QTP	Qualification Test Procedure
Rabi Rate	Physics package parameter related to the RF interrogation power
RAFS	Rubidium Atomic Frequency Standard, often a GPS clock
Rb	Chemical symbol for rubidium
^{85}Rb	Most abundant Rb isotope, used for hyperfine filter
^{87}Rb	Other common Rb isotope, used as hyperfine frequency reference
RbXO	Rubidium - Crystal Oscillator hybrid
RF	Radio Frequency
RFS	Generic rubidium frequency standard
S/N	Signal-to-Noise Ratio
SSB	Single Sideband
S/V	Space Vehicle
SRD	Step Recovery Diode, used in microwave multiplier circuits
Synchronization	Adjustment to same phase
Syntonization	Adjustment to same frequency
TC	Temperature Coefficient
USNO	United States Naval Observatory
VCXO	Voltage Controlled Crystal Oscillator
XO	Crystal Oscillator
ZLS	Zero Light Shift

Bibliography

Note: This bibliography is organized by topic, sorted by date, and numbered consecutively. Some of these items are also referenced by number in the main text.

General Atomic Clocks

[1] C. Steiner, “Atomic Clocks”, Parts I-III, *Frequency*, March-May 1968.
[2] H. Hellwig, “Areas of Promise for the Development of Future Primary Frequency Standards”, *Proceedings of the 24th Annual Symposium on Frequency Control*, pp. 246-258, April 1970.
[3] C. Audoin and J. Vanier, “Atomic Frequency Standards and Clocks”, *J. Phys. E.*, Vol. 9, pp. 697-720, 1976.
[4] H. Hellwig, K.M. Evenson and D.J. Wineland, “Time, Frequency and Physical Measurement”, *Physics Today*, pp. 23-30, December 1978.
[5] C. Audoin and J. Vanier, “Atomic Frequency Standards, a Critical Review”, c. 1980.
[6] J. Vanier and C. Audoin, *The Quantum Physics of Atomic Frequency Standards*, Adam Hilger, Bristol and Philadelphia, Volume 2, Chapter 7, ISBN 0-85274-433-1, 1989.
[7] D.B Sullivan, D.W Allan, D.A. Howe and F.L.Walls (Editors), "Characterization of Clocks and Oscillators", *NIST Technical Note 1337*, U.S. Department of Commerce, National Institute of Standards and Technology, March 1990.
[8] A.O. McCoubrey, “History of Atomic Frequency Standards: A Trip Through 20th Century Physics”, *Proceedings of the 1996 IEEE International Frequency Control Symposium*, pp. 12251241, June 1996.
[9] C. Audoin and B. Guinot, *The Measurement of Time*, Cambridge University Press, Cambridge, U.K., ISBN 0-521-80080-3, 2001.
[10] F.G. Major, *The Quantum Beat: Principles and Applications of Atomic Clocks*, 2nd Edition, Springer-Science, 2007, ISBN 978-0-387-69533-4.

History

[11] N.F. Ramsey, “History of Early Atomic Clocks”, *Metrologia*, Vol. 42 S1, 2005.
[12] P. Forman, “Atomic Clocks: Preview of an Exhibit at the Smithsonian, *Proceedings of the 36th Annual Symposium on Frequency Control*, pp. 220-222, June 1982.

Early Scientific Papers

[13] Bitter, *Physical Review*, Vol. 76, pp. 883-885, 1949.
[14] Brossel and A. Kastler, *C.R. Acad. Sci.* (Paris), Vol. 229, p.1213, 1949.
[15] R.H. Dicke, *Physical Review*, Vol. 89, pp. 472-473, 1953.
[16] R.H. Dicke, “Atomic and Molecular Frequency Standards, *Proceedings of the 10th Annual Symposium on Frequency Control*, p. 259, 1956.

[17] P.L. Bender, E.C. Beaty and A.R. Chi, "Optical Detection of Narrow Rb87 Hyperfine Absorption Lines", *Physical Review Letters*, Vol. 1, No. 9, pp. 311-313, November 1958.

General RFS Theory

[18] A.L. Bloom, "Optical Pumping", *Scientific American*, pp. 72-80, XXX 1960.
[19] M. Arditi and T.R. Carver, "Pressure, Light and Temperature Shifts in Optical Detection of 0-0 Hyperfine Resonance of Alkali Metals", *Physical Review*, Vol. 124, No. 3, pp. 800-809. November 1961.
[20] A. Kastler, "Displacement of Energy Levels of Atoms by Light", *J. Op. Soc. Am.*, Vol. 53, No. 8, pp. 902-910, August 1963.
[21] M. Arditi and T.R. Carver, "Hyperfine Relaxation of Optically Pumped Rb^{87} Atoms in Buffer Gases", *Physical Review*, Vol. 136, pp. A643-A649, November 1964.
[22] R. Bernheim, *Optical Pumping*, W.A. Benjamin, New York, 1965.
[23] R.W. Frank, R.P. Kenschaft, R.A. Mortenson, W.J. Riley and H.P. Stratemeyer, "Design Concepts Study for an Aerospace Rubidium Standard", General Radio Company, Bolton, MA 01740, October 1969.
[24] B.E. Blair, Editor, *Time and Frequency: Theory and Fundamentals*, NBS Monograph 140, U.S. Department of Commerce, May 1974.
[25] G. Missout and J. Vanier, "Some Aspects of the Theory of Passive Rubidium Frequency Standards", *Canadian Journal of Physics*, Vol. 53, No. 11, pp. 1030-1043, 1975.
[26] A. Risley and G. Busca, "Effect of Line Inhomogeneity on the Frequency of Passive Rb^{87} Frequency Standards", *Proceedings of the 32nd Annual Symposium on Frequency Control*, pp. 506-513, June 1978.
[27] A.S. Risley. "Final Report on the Microwave Power and Lamp Temperature Dependence of the Frequency of a Passive Rb^{87} Frequency Standard", National Bureau of Standards, Boulder, CO, c. 1977.
[28] T.C. English, E. Jechart and T.M. Kwon, "Elimination of the Light Shift in Rubidium Gas Cell Frequency Standards Using Pulsed Optical Pumping", *Proceedings of the 10th Annual Precise Time and Time Interval (PTTI) Applications and Planning Meeting*, Greenbelt, MD, pp. 147-168, November 1978.
[29] J. Vanier and L. Bernier, "On the Signal to Noise Ratio and Short Term Stability of Passive Rubidium Frequency Standards", Laboratorire D'Electronique Quantique, Departement de Genie Electrique, Universite Laval, February 1981.
[30] J. Vanier, "Light Shifts in Passive Rubidium Frequency Standards Using Hyperfine Filtering", Final Report, Universite Laval, April 1981.
[31] J. Vanier, R. Kunski, P. Paulin, J.V. Savard, M. Tetu and N. Cyr, "On the Light Shift and Buffer Gas Shift in Passive Rubidium Frequency Standards", *Proceedings of the 36th Annual Symposium on Frequency Control*, pp. 348-354, June 1982.

[32] C. Audoin, J. Viennet, N. Cyr and J. Vanier, "Influence of Modulation Frequency in Rubidium Cell Frequency Standards", *Proceedings of the 14th Annual Precise Time and Time Interval (PTTI) Applications and Planning Meeting*, Greenbelt, MD, pp. 87-110, November-December 1982.

[33] P. Tremblay, N. Cyr and Michel Tetu, "Evaluation of the Performance of Passive Rubidium Frequency Standards Using Cavity Operated in Mode TE_{011}, TE_{111}, and TE_{101}", *Proceedings of the 38th Annual Symposium on Frequency Control*, pp. 406-415, June 1984.

[34] P. Tremblay, N. Cyr and Michel Tetu, "Pumping Light Intensity Transmitted through an Inhomogeneously Broadened Line System: Application to Passive Rubidium Frequency Standards", *Can. J. Physics*, Vol. 63, No. 12, December 1985.

Early RFS Research and Development

[35] T.R. Carver, "Rubidium Oscillator Experiments", *Proceedings of the 11th Annual Symposium on Frequency Control*, pp. 307-XXX, XXX 1957.

[36] M. Arditi, "Gas Cell Atomic Clocks Using Buffer Gases and Optical Orientation", *Proceedings of the 12th Annual Symposium on Frequency Control*, pp. 606-622, April 1958.

[37] J.M. Andres, D.J. Farmer and G.T. Inouye, "Design Studies for a Rubidium Gas Cell Frequency Standard", *IRE Trans. Mil. Electron*., MIL-3, pp. 178-183, October 1959.

[38] M. Arditi, "Evaluation of ITT Breadboard Gas Cell Frequency Standard", *Proceedings of the 13th Annual Symposium on Frequency Control*, pp. 655-667, May 1959.

[39] M. Arditi, *IRE Trans. Mil. Electron*., MIL-4, pp. 22-XX, 1960.

[40] R.J. Carpenter, E.C. Beaty, P.L. Bender, S. Saito and R.O. Stone, "A Prototype Rubidium Vapor Frequency Standard", *IRE Trans. Instrum*., Vol. I-9, pp. 132-135, September 1960.

[41] M. Arditi, "Frequency Control by Gas Cell Standards – Fundamental Problems in the Light of Recent Experimental Results", *Proceedings of the 15th Annual Symposium on Frequency Control*, pp. 181-202, April 1961.

[42] M. Arditi and T.R. Carver, "The Principles of the Double Resonance Method Applied to Gas Cell Frequency Standards", *Proc. IEEE*, pp. 190-202, January 1963.

[43] D.J. Farmer, "Performance and Application of Gas Cell frequency Standards", *Proceedings of the 17th Annual Symposium on Frequency Control*, pp. 449-XXX, April 1963.

[44] M.E. Packard and B.E. Swartz, "The Optically Pumped Rubidium Vapor Frequency Standard", *IRE Trans. Instrum*., I-11, pp. 215-223, December 1962.

[45] A.R. Chi, J.H. Roeder, S.C. Wardrip and B. Kruger, "Long-Term Stability Frequency Stability Measurement of Rubidium Gas Cell Frequency Standards", *Proceedings of the 22nd Annual Symposium on Frequency Control*, pp. 592-604, XXXX 1968.

RFS Products

[46] D.H. Throne, “A Rubidium Vapor Frequency Standard for Systems Requiring Superior Frequency Stability”, *Hewlett-Packard Journal*, Vol. 19, No. 11, pp. 8-16, July 1968.
[47] D.H. Throne, “A Report on the Performance of a New Rubidium Vapor Frequency Standard, *Proceedings of the 23rd Annual Symposium on Frequency Control*, pp. 274-278, May 1969.
[48] K. Chiba and T. Hashi, “An Ultra-Miniature Rubidium Frequency Standard”, *Proceedings of the 35th Annual Symposium on Frequency Control*, pp. 646-650, May 1981.
[49] T. Hashi, K. Chiba and C. Takeuchi, “A Miniature, High-Performance Rubidium Frequency Standard”, *Proceedings of the 39th Annual Symposium on Frequency Control*, pp. 54-58, May 1985.
[50] G.M. Saxena, A. Chatterjee, D.S. Sachdeve and B.S. Mathur, “Evaluation of the Rubidium Atomic Frequency Standard Developed in India”, *Proceedings of the 39th Annual Symposium on Frequency Control*, pp. 59-63, May 1985.
[51] W. Weidemann, “Subminiature Rubidium Oscillator Model FRS”, *Proceedings of the 40th Annual Symposium on Frequency Control*, pp. 470-473, May 1986.
[52] A. Stern, M. Golosovsky, Y. Elbaz, A. Hertz and A. Lepek, “TF-4000A, TFL’s High Performance Ruggedized Rubidium Frequency Standard”, *Proceedings of the 43rd Annual Symposium on Frequency Control*, pp. 124-129, May-June 1989.
[53] A. Stern, B. Levy, M. Bootnik, E. Detoma and G. Pedrotto, “Rubidium Frequency Standard with a High Resolution Digital Synthesizer”, *Proceedings of the 43rd Annual Symposium on Frequency Control*, pp. 108-113, May 1992.
[54] Ball Corporation, Efratom Time and Frequency Products, Irvine, CA, *Precision Time and Frequency Handbook*, Ninth Edition, 1993.
[55] M. Bloch, I. Pascaru, C. Stone and T. McClelland, “Subminiature Rubidium Frequency Standard for Commercial Applications”, *Proceedings of the 1993 IEEE International Frequency Control Symposium*, pp. 164-177, June 1993.
[56] P. Rochat, H. Schweda, G. Mileti and G. Busca, “Developments of Rubidium Frequency Standards at Neuchatel Observatory”, *Proceedings of the 1994 IEEE International Frequency Control Symposium*, pp. 716-723, June 1994.
[57] Y. Koyama, H. Matsuura, K. Aysumi, Y. Nakajima and K. Chiba, “An Ultra-Miniature Rubidium Frequency Standard with Two-Cell Scheme”, *Proceedings of the 1995 IEEE International Frequency Control Symposium*, pp. 33-38, May-June 1995.
[58] T. McClelland, I. Pascaru, I. Shtaerman, C. Stone, C. Szekely, J. Zacharski and N.D. Bhaskar, “Subminiature Rubidium Frequency Standard: Manufacturability and Performance Results from Production Units”, *Proceedings of the 1995 IEEE International Frequency Control Symposium*, pp. 39-52, May-June 1995.
[59] C. Couplet, P. Rochat, G. Mileti, H. Schweda, P. Thomann and G. Busca, “Miniaturized Rubidium Clocks for Space and Industrial Applications”,

Proceedings of the 1995 IEEE International Frequency Control Symposium, pp. 53-59, May-June 1995.

[60] T. McClelland, I. Pascaru, I. Shtaerman, C. Stone, C. Szekely, J. Zacharski and N.D. Bhaskar, "Subminiature Rubidium Frequency Standard: Performance Improvements", *Proceedings of the 1996 IEEE International Frequency Control Symposium*, pp. 1011-1016, June 1996.

[61] K. Suzuki, Y. Abe, N. Ishihara, H. Kudoh and S. Fukugawa, "Small-Sized Rubidium Oscillator", *Proceedings of the 1998 IEEE International Frequency Control Symposium*, pp. 73-79, May 1998.

[62] J. Ho, I. Pascaru, C. Stone and T. McClelland, "New Rubidium Frequency Standard Designa for Telecommunications Applications", *Proceedings of the 1998 IEEE International Frequency Control Symposium*, pp. 80-83, May 1998.

[63] W. J. Riley, "A Modern Militarized Rubidium Frequency Standard", *Microwave Journal*, May 2002.

[64] Y. Koyama, H. Matsuura, K. Atsumi, K. Nakamuta, M. Sakai and I. Maruyama, An Ultra-Miniature Rubidium Frequency Standard", *Proceedings of the 2000 IEEE International Frequency Control Symposium*, pp. 694-699, June 2000.

Rubidium

[65] Daniel A. Steck. "Rubidium-87 D Line Data", Los Alamos National Laboratory Technical report LA-UR-03-8638, September 2001.

[66] It has been reported that a lack of the mineral rubidium may cause: depression, decreased cancer resistance, decreased cell PH, cell dehydration, increased enzyme toxicity, decreased glucose tolerance, decreased peroxides elimination. See http://www.4alw.com/liquid-minerals/rubidium.

RFS Environmental Sensitivity

[67] W. J. Riley, "The Physics of the Environmental Sensitivity of Rubidium Gas Cell Atomic Frequency Standards", *IEEE Transactions on Ultrasonics, Ferroelectrics and Frequency Control*, Vol. 39, No. 2, pp. 232-240, March 1992.

[68] M. Huang, C. M. Klimcak, and J. C. Camparo, "Vapor-Cell Clock Frequency and Environmental Pressure: Resonance-Cell Volume Changes", Proceedings of the 2010 IEEE International Frequency Control Symposium, pp. 208-211, June 2010.

RFS Testing

[69] T. J. Lynch, W. J. Riley and J. R. Vaccaro, "The Testing of Rubidium Frequency Standards", *Proceedings of the 43rd Annual Symposium on Frequency Control*, pp. 257-262, May 1989.

[70] J. Vanier, et. al., "Aging, Warm-up Time and Retrace: Important Characteristics of Standard Frequency Generators", *Proceedings of the 1992 IEEE Frequency Control Symposium*, pp. 807-XXX, June 1992.

[71] T. Lynch and W. Riley, "Tactical Rubidium Frequency Standard (TRFS)", RADC-TR-87-166, Final Technical Report, Oct. 1987.
[72] MIL-STD-454, "Standard General Requirements for Electronic Equipment".
[73] MIL-STD-810, "Environmental Test Methods".
[74] MIL-STD-461, "Electromagnetic Interference Characteristics, Requirements For Equipment".
[75] MIL-E-5400, "Electronic Equipment, Airborne, General Specification For."
[76] MIL-T-5422, "Testing, Environmental, Airborne Electronic And Associated Equipment."
[77] MIL-E-16400, "Electronic Equipment, Naval Ship and Shore, General Specification".
[78] MIL-E-4158, "Electronic Equipment, Ground, General Requirements For".
[79] DOD-E-8983, "Electronic Equipment, Aerospace, Extended Space Environment, General Specification For".
[80] MIL-STD-1540, "Test Requirements for Space Vehicles.
[81] MIL-STD-1541, "Electromagnetic Compatibility Requirements for Space Systems".
[82] MIL-C-45662, "Calibration System Requirements".
[83] MIL-O-55310B, "Military Specification, Oscillators, Crystal, General Specification For," 10 May 1988.
[84] MIL-STD-202, "Test Methods for Electronic and Electrical Component Parts."
[85] MIL-STD-462, "Electromagnetic Interference Characteristics, Measurement of".
[86] MIL-STD-704, "Platform Electrical Power Characteristics".
[87] MIL-STD-1275, "Characteristics of 28VDC Electrical System in Military Vehicles".
[88] ARNIC Report 413, "Guidance for Aircraft and Electrical Power Utilization and Transient Protection." Aeronautical Radio, Inc., Dec. 1976.
[89] ASTM 346-64, "Standard Methods of Test of Magnetic Shielding." American Society for Testing and Materials.
[90] W. Riley and J. Vaccaro, "Rubidium-Crystal Oscillator (RbXO) Development Program," *U.S. Army LABCOM R&D Technical Report SLCET-TR-84-0410F*, April 1986.
[91] MIL-STD-2164(EC), "Environmental Stress Screening Process for Electronic Equipment".
[92] NAVMAT P-9492, "Navy Manufacturing Screening Program".
[93] A.J. Curtis and R.D. McKain, "A Quantitative Method of Tailoring Input Spectra for Random Vibration Screens," *J. Env. Sci*., Sept. - Oct. 1987.
[94] R.G. Lambert, "Case Histories of Selection Criteria for Random Vibration Screening", *Inst. Env. Sci. Workshop Proc*., Sept. 1984.
[95] W. Weidemann, "Application Critical Parameters for Rubidium Standards", *Proceedings of the 1998 IEEE International Frequency Control Symposium*, pp. 84-87, May 1998.
[96] D. Watts, F. Li, F. Vu, W.F. Cashin and T.C. English, "Specifying Commercial Atomic Frequency Standards Using Statistics", *Proceedings of the 1996 IEEE International Frequency Control Symposium*, pp. 1023-1031, June 1996.

Rb Lamps

[97] W.E. Bell, A.L. Bloom and J. Lynch, “Alkali Metal Vapor Spectral Lamps”, *Review of Scientific Instruments*, Vol. 32, No. 6, pp. 688-692, June 1961.
[98] R.G. Brewer, “High Intensity Low Noise Rubidium Light Source”, *Review of Scientific Instruments*, Vol. 32, No. 12, pp. 1356-1358, December 1961.
[99] N. Oura, N. Kuramochi, S. Naritsuka and T. Hayashi, :Composite-Type 87Rb Optical Pumping Light Source for the Rubidium Frequency Standard”, *Proceedings of the 13th Annual Precise Time and Time Interval (PTTI) Applications and Planning Meeting*, Washington, DC, pp. 803-815, December 1981.
[100] C. H. Volk, R.P. Frueholtz, T.C. English, T.J. Lynch and W.J. Riley, “Lifetime and Reliability of Rubidium Discharge Lamps for Use in Atomic Frequency Standards”, *Proceedings of the 38th Annual Frequency Control Symposium*, Philadelphia, PA, pp. 387-400, May 1984.
[101] R.A. Cook and R.P. Frueholtz, “An Improved Rubidium Consumption Model for Discharge Lamps Used in Rubidium Frequency Standards”, *Proceedings of the 42th Annual Frequency Control Symposium*, Baltimore, MD, pp. 525-531, June 1988.
[102] J. Comparo and R. Mackay, “A Mechanism of Rubidium Clock Degradation: Ring-Mode to Red-Mode Transition in RF-Discharge Lamps”, *Proceedings of the 2007 IEEE International Frequency Control Symposium*, Geneva, pp. 45-48, May-June 2007.

Lamp Exciters

[103] R. Shaw, “Spontaneously Generated Ion Acoustic Waves in a Weakly Ionized Plasma”, MS Thesis, Cornell University, Ithaca, NY, September 1964. .
[104] W.J. Riley, “Power Supply Circuit for an Alkali Vapor Spectral Lamp” U.S. Patent No. 4,721,890, January 1988.
[105] Performance Analysis, Lamp Exciter, FP0034, EG&G Frequency Products, August 1990.

Harmonic Multipliers

[106] C. Wenzel, “New Topology Multiplier Generates Odd Harmonics”, RF Design, Vol. 10, No. 7, pp. 31-34, July 1987.
[107] B. Sadowski, “Low Additive Noise Frequency Tripler”, RF Design, pp. 32-35, May 2007.

SRD Multipliers

[108] H.T. Friis, “Analysis of Harmonic Generator Circuits for Step Recovery Diodes” *Proceedings of the IEEE*, Vol. 55, No. 7, pp. 1192-1194, July 1967.
[109] A. Shipow, “Harmonic Generators”, *Microwave Journal*, February 1978.
[110] “Harmonic Generation Using Step Recovery Diodes and SRD Modules”, *Application Note 920*, Hewlett-Packard Company.

GPS Rb Clocks

[111] D.E. Ringer, J. Gandy and E. Jechart, "Spaceborne Rubidium Frequency Standard for NAVSTAR GPS", *Proceedings of the 7th Annual Precise Time and Time Interval (PTTI) Applications and Planning Meeting*, pp. 671-696, December 1975.
[112] *Final Report*, "Design for a Rubidium Frequency Standard", General Radio Company, Bolton, MA 01740 , February, 1976.
[113] "Design for a Rubidium Frequency Standard for the GPS Program", Final Report, Rockwell Contract No. M5N3DGS-649024D, February 1976.
[114] *Progress Report*, "GPS Rubidium Frequency Standard", EG&G Electronic Components, Salem MA 01970, February 1980.
[115] "Preliminary Design Concept Review, Contract No. MOJ3BGR-484107E", EG&G Electronic Components, Salem MA 01970, May 1980.
[116] *Technical Report*, "Program Progress Review #2, Phase 1 Breadboard Development, Rubidium Frequency Standard", EG&G Electronic Components, Salem MA 01970, September 1980.
[117] *Technical Report*, "Program Progress Review #3, Phase 1 Breadboard Development, Rubidium Frequency Standard", EG&G Electronic Components, Salem MA 01970, November 1980.
[118] *Technical Report*, "Program Progress Review #4, Phase 1 Breadboard Development, Rubidium Frequency Standard", EG&G Electronic Components, Salem MA 01970, January 1981.
[119] *Performance Analysis*, "GPS Rubidium Frequency Standard", EG&G Electronic Components, Salem, MA 01970, October 1981.
[120] W. J. Riley, "A Rubidium Clock for GPS", *Proceedings of the 13th Annual Precise Time and Time Interval (PTTI) Applications and Planning Meeting*, Washington, DC, pp. 609-630, December 1981.
[121] *Technical Report*, "Critical Design Review, GPS Rubidium Frequency Standard", EG&G Electronic Components, Salem MA 01970, May 1982.
[122] T. J. Lynch and W. J. Riley, "Test Results for Prototype GPS Rubidium Clocks, *Proceedings of the 15th Annual Precise Time and Time Interval (PTTI) Applications and Planning Meeting*, Washington, DC, pp. 269-280, December 1983.
[123] *Final Report*, "140 Day Stability Test, EG&G GPS RFS Prototype #1", NBS Test No. 801590, EG&G Electronic Components, Salem MA 01970, February 1983.
[124] *Qualification Level Test Report*, "GPS RFS", EG&G Frequency Products, Salem, MA 01970, March 1983.
[125] *Final Technical Report*, "EG&G GPS RFS Continuation Program", EG&G Electronic Components, Salem MA 01970, June 1985.
[126] S. Goldberg, T. J. Lynch and W. J. Riley, "Further Test Results for Prototype GPS Rubidium Clocks, *Proceedings of the 17th Annual Precise Time and Time Interval (PTTI) Applications and Planning Meeting*, Washington, DC, pp. 145-155, December 1985.

[127] F. Danzy and W. J. Riley, "Stability Test Results for GPS Rubidium Clocks, *Proceedings of the 19th Annual Precise Time and Time Interval (PTTI) Applications and Planning Meeting*, Redondo Beach, CA, pp. 267-274, December 1987.

[128] *Acceptance Test Report*, "GE GPS Rubidium Frequency Standards S/N 3 & 4", EG&G Frequency Products, Salem, MA 01970, August 1989.

[129] W. J. Riley, "Rubidium Atomic Frequency Standards for GPS Block IIR, *Proceedings of the 22nd Annual Precise Time and Time Interval (PTTI) Applications and Planning Meeting*, Vienna, VA, pp. 221-230, December 1990.

[130] "Input Current Time Profile Analysis, Dynamic Input Impedance, GPS Block IIR RAFS", EG&G Frequency Products, Salem, MA 01970, March 1990.

[131] *Test Report*, "Transient Radiation Test, Crystal Oscillator, GPS Block IIR RAFS", EG&G Frequency Products, Salem, MA 01970, April 1990.

[132] *Test Report*, "Transient Radiation Test, Output Amplifier, GPS Block IIR RAFS", EG&G Frequency Products, Salem, MA 01970, April 1990.

[133] *Critical Design Review, GPS Block IIR Phase 2*, "Rubidium Atomic Frequency Standard", EG&G Frequency Products, Salem, MA 01970, June 1990.

[134] *Manufacturing Readiness Review, GPS Block IIR Phase 2*, "Rubidium Atomic Frequency Standard", EG&G Frequency Products, Salem, MA 01970, August 1990.*EG&G No. FP0043,* "Qualification-Level Test Report, GPS Block IIR RAFS", EG&G Frequency Products, Salem, MA 01970, June 1991.

[135] W. J. Riley, "Rubidium Atomic Frequency Standards for GPS Block IIR, *Proceedings of the 6th European Frequency and Time Forum*, Noordwijk, NL, pp. 231-238, March 1992.

[136] W. J. Riley, "Rubidium Atomic Frequency Standards for GPS Block IIR, *Proceedings of the 5th Technical Meeting of the Satellite Division of the Institute of Navigation*, Albuquerque, NM, pp. 537-545, September 1992.

[137] *Qualification Test Report*, "GPS Block IIR Rubidium Atomic Frequency Standard", EG&G Rubidium Products, Salem, MA 01970, May 1994.

[138] *Test Report*, "Frequency Retrace Test of GPS Block IIR RAFS EDM1", EG&G Rubidium, Salem, MA 01970, September 1994.

[139] W. J. Riley, "Early Stability Test Results for GPS Block IIR Rubidium Clocks, *Proceedings of the 5th Symposium on Frequency Standards & Metrology*, Woods Hole, MA, October 1995, pp. 403-405.

[140] *Technical Interchange Meeting*, "RAFS Frequency Jumps", EG&G Frequency Products, Salem, MA 01970, August 1995.

[141] "Interpretation of GPS Block IIR RAFS Monitor Signals", EG&G Rubidium, Salem, MA 01970, March 1996.

[142] *Design Concept*, GPS Block IIF Rubidium Frequency Standard, EG&G Frequency Products, Salem, MA 01970, September 1996.

[143] *Test Report*, RAFS Warm-up Test, EG&G Frequency Products, Salem, MA 01970, November 1996.

[144] *Operations Manual*, GPS Block IIR Rubidium Atomic Frequency Standard, EG&G Frequency Products, Salem, MA 01970, November 1996.

[145] *Breadboard Report*, "RFS-IIF Rubidium Frequency Standard", EG&G Frequency Products, Salem, MA 01970, December 1996.
[146] *Test Report*, "RFS-IIF Secondary Loop Synthesizer Flash X-Ray Test", EG&G Frequency Products, Salem, MA 01970, March 1997.
[147] *Test Report*, "RFS-IIF Prototype Evaluation", EG&G Frequency Products, Salem, MA 01970, June 1997.
[148] *Test Report*, "RFS-IIF Prototype Radiation Test", EG&G Frequency Products, Salem, MA 01970, September 1997.
[149] *Test Report*, "RFS-IIF EDU Initial Functional Test", EG&G Frequency Products, Salem, MA 01970, September 1997.
[150] *Critical Design Review, GPS Block IIF*, "Rubidium Frequency Standard", EG&G Frequency Products, Salem, MA 01970, November 1997.
[151] W.J. Riley, "Early In-Orbit Performance of GPS Block IIR Rubidium Clocks, *Proceedings of the 29th Annual Precise Time and Time Interval (PTTI) Applications and Planning Meeting*, Long Beach, CA, pp. 213-220, November 1997.
[152] *Qualification Test Report*, "AFTR RFS, EG&G P/N 603-9598", EG&G Optoelectronics, Salem MA 01970, July 1998.
[153] *Final Report*, "SVN43 TKS Event Investigation", EG*G Frequency Products, Salem, MA 01970, July 1998.
[154] T.J. Lynch, K.D. Lyon, W.J. Riley and J.R. Vaccaro, "A Rubidium Clock for GPS Block IIF", April 1999 (unpublished).
[155] R.F. Dupuis, T.J. Lynch and J.R. Vaccaro, "Rubidium Frequency Standard for the GPS IIF Program and Modifications for the RAFSMOD Program", *Proceedings of the 2008 IEEE International Frequency Control Symposium*, Honolulu, HI, pp. 655-660, May 2008.

Space RFS (Non-GPS)

[156] R.W. Frank, R.P. Kenschaft, R.A Mortenson, W.J. Riley and H.P. Stratemeyer, "Design Concepts for an Aerospace Rubidium Standard", General Radio Company, October 1969.
[157] *Final Report*, *NASA Contract NAS 9-5425, Part II*, "Rubidium Spacecraft Atomic Timing System", General Radio Company, W. Concord, MA 01742, December, 1969.
[158] *Design Study*, "Milstar Feasibility Study, Rubidium Interface Unit", EG&G Frequency Products, Salem, MA 01970, January 1998.

MIL (Tactical) RFS

[159] M.E. Frerking and D.E. Johnson, "Rubidium Frequency and Time Standard for Military Environment", *Proceedings of the 26th Annual Symposium on Frequency Control*, pp. 216-222, June 1972.
[160] *Final Technical Report, Rome Air Development Center, Contract No. F19628-82-C-0055*, "Phase 2A Bench Model Development, Tactical Rubidium Frequency Standard", EG&G Frequency Products, Salem, MA 01970, December 1982.

[161] W.J. Riley, "A Rubidium Clock for Seek-Talk", *Proceedings of the 14th Annual Precise Time and Time Interval (PTTI) Applications and Planning Meeting*, pp. 141-154, December 1982.

[162] *Final Technical Report, Rome Air Development Center, Contract No. F19628-82-C-0055*, "Phase 2B Prototype Redesign, Tactical Rubidium Frequency Standard", EG&G Frequency Products, Salem, MA 01970, January 1983.

[163] T.M. Kwon, B.C. Grover and H.E. Williams, "Rubidium Frequency Standard Study", *RADC-TR-83-230*, Final Technical Report, Rome Air Development Center, October 1983.

[164] T.M Kwon, R. Dagle, W. Debley, H. Dellamano, T. Hahn, J. Horste, L.K. Lam, R. Magnuson and T. McClellan, *Proceedings of the 16th Annual Precise Time and Time Interval (PTTI) Applications and Planning Meeting*, pp. 143-155, November 1984.

[165] *Instruction Manual*, "Model RFS-10 Rubidium Frequency Standard", EG&G Frequency Products, Salem MA 01970, January 1985.

[166] H. Fruehauf, W. Weidemann, C. Colson, S. Stein, T. English, H. Vorwerk, and R. Paul, "Militarized Rubidium Oscillator", *RADC-TR-85-23*, Final Technical Report, Rome Air Development Center, April 1985.

[167] *Qualification Test Report*, "EG&G Model RFS-10-7 Rubidium Frequency Standard", EG&G Frequency Products, Salem, MA 01970, December 1985.

[168] *Final Technical Report, Hanscom Air Force Base Contract No. F19628-83-0175*, "Tactical Rubidium Frequency Standard (TRFS)", EG&G Frequency Products, Salem, MA 01970, December 1986.

[169] T.M Kwon, T. Hahn, R. Dagle, J. Horste, and T. McClellan, *RADC-TR-87-140*, Final Technical Report, Rome Air Development Center, September 1987.

[170] T.J. Lynch and W.J. Riley, *RADC-TR-87-166*, Final Technical Report, "Tactical Rubidium Frequency Standard", Rome Air Development Center, EG&G Frequency Products, Salem, MA 01970, October 1987.

[171] *Reliability Prediction*, "SCOTT RFS-20 Rubidium Frequency Standard", EG&G Frequency Products, Salem MA 01970, August 1988.

[172] *Radiation Test Report*, "EG&G Model RFS-10-102, Regency Net Rubidium Frequency Standard", EG&G Frequency Products, Salem MA 01970, April 1988.

[173] *Qualification Test Report*, "SCOTT RFS-20 Rubidium Frequency Standard", EG&G Frequency Products, Salem MA 01970, August 1988.

[174] *Technical Information*, "Model RFS-10-7 Rubidium Frequency Standard", EG&G Frequency Products, Salem MA 01970, June 1989.

[175] *Test Report*, "Environmental Stress Screening (ESS), EG&G Model RFS-10-7 Rubidium Frequency Standard", EG&G Frequency Products, Salem, MA 01970, September 1989.

[176] *User Manual*, "Modular Intelligent Frequency, Time and Time Interval (MIFTTI) Subsystem", EG&G Frequency Products, Salem, MA 01970, March 1990.

[177] *Test Report*, "Vibration Testing of RFS-10 Rubidium Frequency Standard", EG&G Rubidium Products, Salem, MA 01970, October 1994.

[178] T.J. Lynch and J.R. Vaccaro, "Ultrafast Warm-up Rubidium Reference", *Proceedings of the 1996 IEEE International Frequency Control Symposium*, Honolulu, HI, pp. 993-1001, June 1996.

[179] *Qualification Test Report*, "RFS-10-7 LN Combat Direction Finder Rubidium Frequency Standard", EG&G Optoelectronics, Salem MA 01970, September 1998.

RbXO

[180] J.R. Vig and V.J. Rosati, "The Rubidium-Crystal Oscillator Hybrid Development Program", *Proceedings of the 16th Annual Precise Time and Time Interval (PTTI) Applications and Planning Meeting*, pp. 157-165, November 1984.

[181] *Instruction Manual*, "RbXO Demonstrator Unit", EG&G Frequency Products, Salem, MA 01970, December 1985.

[182] *Research and Development Technical Report, US Army Laboratory Command, Contract No. SLCET-TR-84-0410-F*, "Rubidium-Crystal Oscillator (RbXO) Development Program", EG&G Electronic Components, Salem, MA 01970, April 1986.

[183] W. J. Riley and J. R. Vaccaro, "A Rubidium-Crystal Oscillator (RbXO)", *Proceedings of the 40th Annual Frequency Control Symposium*, Philadelphia, PA, pp. 452-464, May 1986.

[184] W. J. Riley and J. R. Vaccaro, "A Rubidium-Crystal Oscillator (RbXO)", *IEEE Transactions on Ultrasonics, Ferroelectrics and Frequency Control*, Vol. UFFC-34, No. 6, pp. 612-618, November 1987.

[185] *Semiannual Progress Report #1*, Chip-Scale Atomic Clock, Defense Advanced Research Projects Agency (DARPA) Contract No. NBCHC020050, March 2003.

[186] *Semiannual Progress Report #2*,Chip-Scale Atomic Clock, Defense Advanced Research Projects Agency (DARPA) Contract No. NBCHC020050, August 2003.

[187] R. Lutwak, D. Emmons, T. English, W. Riley, A. Duwel, M. Varghese, D. K. Serkland and G. M. Peake, "The Chip-Scale Atomic Clock - Recent Development Progress", *Proceedings of the 35th Annual Precise Time and Time Interval (PTTI) Applications and Planning Meeting*, San Diego, CA, December 2003.

[188] *Semiannual Progress Report #3*,Chip-Scale Atomic Clock, Defense Advanced Research Projects Agency (DARPA) Contract No. NBCHC020050, February 2004.

Rb Signal Parameters

[189] Claude Audoin, Vincent Candelier, and Noel Dimarcq's, "A Limit to the Frequency Stability of Passive Frequency Standards Due to an

Intermodulation Effect," *IEEE Transactions on Instrumentation and Measurement*, Volume 40, No. 2, April 1991.

[190] J. Q. Deng, A. DeMarchi, F. L. Walls, and R. E. Drullinger, "Frequency Stability of Cell-Based Passive Frequency Standards: Reducing the Effects of Local-Oscillator PM Noise", *Proceedings of the 1998 IEEE International Frequency Control Symposium*, pp. 95-98, May 1998.

[191] Jacques Vanier and Laurent-Guy Bernier, "On the Signal-to-Noise Ratio and Short-Term Stability of Passive Rubidium Frequency Standards," *IEEE Transactions on Instrumentation and Measurement*, Volume IM-30, No. 4, December 1981.

[192] J. Vanier, "Light Shifts in Passive Rubidium Frequency Standards Using Hyperfine Filtering", Laboratorire D'Electronique Quantique, Departement de Genie Electrique, Universite Laval, April 1981.

Kenschaft Model

[193] R.P. Kenschaft, "Response of Quantum-Mechanical Resonances to Modulated Radio Frequency Signals", Ph. D. Thesis, University of Pennsylvania, 1969.

[194] K.D. Lyon and W.J. Riley, "Application of the Kenschaft Model to the Analysis of the Rubidium Gas Cell Frequency Standard", *Proceedings of the 1996 IEEE International Frequency Control Symposium*, pp. 1032-1040, June 1996.

[195] R.P. Kenschaft, "Mixed Modulation Signal and Noise Analysis and Simulation of the Rubidium Gas Cell Atomic Frequency Standard", *Proceedings of the 1996 IEEE International Frequency Control Symposium*, pp. 1041-1050, June 1996.

C-Field

[196] *Technical Report*, "Advantages of Fixed Minimum C-Field Operation of the EG&G GPS Rubidium Frequency Standard", EG&G Electronic Components, Salem MA 01970, July 1982.

[197] A. Stern, A. Hertz, Y. Zarfaty and A. Lepek, "A Novel Compact Rubidium Frequency Standard with a Low Sensitivity to Magnetic and Vibrational Disturbances", *Proceedings of the 42nd Frequency Control Symposium*, pp. 519-524, June 1988.

Magnetic Shielding

[198] W.G. Wadey, "Magnetic Shielding with Multiple Cylindrical Shells", *Review of Scientific Instruments*, Vol. 27, No. 11, pp. 910-916, November 1956.

[199] A. J. Mager, "Magnetic Shields", *IEEE Transactions on Magnetics*, Vol. MAG-6, No. 1, pp. 67-75, March 1970.

[200] S.M. Freake and T.L. Thorp, "Shielding of Low Magnetic Fields with Multiple Cylindrical Shells, *Review of Scientific Instruments*, Vol. 42, No. 10, pp. 1411-1413, October 1971.

[201] S.A. Wolf, D.U. Gubser and J.E.Cox, "Shielding of Longitudinal Magnetic Fields with Thin, Closely-Spaced, Concentric Cylindrical Shells with Applications to Atomic Clocks", *Proceedings of the 10th Annual Precise Time and Time Interval (PTTI) Applications and Planning Meeting*, Greenbelt, MD, pp. 131-146, November 1978.

[202] S.A. Wolf, D.U. Gubser and J.E.Cox, "Shielding of Longitudinal Magnetic Fields with Thin, Closely-Spaced, Concentric Cylinders of High Permeability Material", *Review of Scientific Instruments*, Vol. 50, No. 6, pp. 751-756, June 1979.

[203] Magnetic shielding formulae are available at: http:/www.amuneal.com/ magnetic-shielding/theory-design/formulas-calculations.

Microwave Cavities

[204] J. Viennet, C. Audoin and M. Desainfuscien, "Cavity Pulling in Passive Frequency Standards", *IEEE Transactions on Instrumentation and Measurement*, Volume IM-21, No. 3, pp. 204-209, August 1972.

[205] H.E. William, T.M. Kwon and T. McClelland, "Compact Rectangular Cavity for Rubidium Vapor Cell Frequency Standards", *Proceedings of the 37th Annual Frequency Control Symposium*, Philadelphia, PA, pp. 12-17, June 1983.

[206] T. Sphicopoulos, "Cavites Compacte Pour Etalons De Frequence Atomiques", Ecole Polythehnique Federale De Lausanne, 1986.

[207] G.H. Mei and J.T. Liu, "A Miniaturized Microwave Resonator for Rubidium Frequency Standards", *Proceedings of the 1999 IEEE International Frequency Control Symposium*, Besancon, p. 601, April 1999.

[208] J. Deng, "Subminiature Microwave Cavity for Atomic Frequency Standards", *Proceedings of the 2001 IEEE International Frequency Control Symposium*, pp. 85-88, June 2001.

[209] X. Huang, B. Xia, D. Zhong, S. An, X. Zhu and G. Mei, "A Microwave Cavity with Low Temperature Coefficient for Passive Rubidium Frequency Standards", *Proceedings of the 2001 IEEE International Frequency Control Symposium*, pp. 105-107, June 2001.

[210] J. Hu, et. al., "A Subminiature Microwave Cavity for Rubidium Atomic Frequency Standards", *Proceedings of the 2007 IEEE International Frequency Control Symposium*, Geneva, pp. 599-601, May-June 2007.

[211] Y. Wang, et. al., "A Downsized Microwave Cavity for the Rubidium Vapor Cell Frequency Standard", *Proceedings of the 2007 IEEE International Frequency Control Symposium*, Geneva, pp. 595-598, May-June 2007.

[212] S.S. Raghuwanshi, "Development & Analysis of Microwave Cavity and Magnetic Shielding for Rubidium Atomic Clock", M. Eng Thesis, Electrical and Instrumentation Engineering Department, Thapar University, New Delhi, July 2009.

Phase Noise

[213] J. Vanier, M. Tetu and L. Bernier, "Transfer of Frequency Stability from an Atomic Frequency Reference to a Quartz Crystal Oscillator", Proceedings of the 32nd Annual Symposium on Frequency Control, June 1978, pp. 520-526.
[214] F. Walls, "Stability of Frequency Locked Loops", Appendix in *Time Domain Frequency Stability Calculated from the Frequency Domain Description*, NIST Publication NISTIR 89-3916, September 1989.
[215] J. Vaccaro, "Derivation of RAFS Open Loop VCXO Phase Noise Specification", PerkinElmer, Salem, MA 01970, April 16, 2009.
[216] AFS Performance Specification, ITT Space Systems Division Document No. 1660027, Rev. A of October 21, 2008.
[217] Section 5.40 Servo Amplifier, GPS III RAFS WCCA, AEi Systems, LLC, Los Angeles, CA 90045.

Acceleration, Vibration and G-Sensitivity

[218] *Research and Development Technical Report, US Army Laboratory Command, Contract No. SLCET-TR-91-3*, "The Effects of Acceleration on Precision Frequency Sources", Electronics Technology and Devices Laboratory, Ft. Monmouth, NJ 07703, July 1992.
[219] R.L. Filler, "The Acceleration Sensitivity of Quartz Crystal Oscillators: A Review", *IEEE Transactions on Ultrasonics, Ferroelectrics and Frequency Control*, Vol. 35, No. 3, pp.297-305, May 1988.

Buffer Gas

[220] P. Bender, et al, 12th FCS 1958, pp.593-605
[221] M. Arditi, U.S. Patent No. 2955262, Oct. 1960.
[222] G. Missout and J. Vanier, "Pressure and Temperature Coefficients of the More Commonly Used Bufer Gases in Rubidium Vapor Frequency Standards", *IEEE Transactions on Instrumentation and Measurement*, Vol. 24, No. 2, pp. 180-184, June 1975.
[223] J. Vanier, R. Kunski, J.Y.Savard and M. Tetu, "On the Pressure and Temperature Coefficients of Buffer Gases Used in Optically Pumped Passive Rubidium Frequency Standards", Laboratoire D'Electronique Quantique, Universite Laval, July 1981.
[224] Beer & Bernheim, Phys. Rev. A 13, 1052-1057, March 1976
[225] F. Strumia, et al, 30th FSC 1976, pp. 468-472
[226] J. Vanier, 36th FCS 1982, pp.348-354
[227] W. Riley, Letter to J. Vanier, 6/3/75
[228] S. Goldberg. EG&G NB III, p.57
[229] P. Chantry, et al, 46th FCS "92, pp.114-122
[230] J. Vanier, Tech Note EV-19, May 1981.
[231] W. Stern and R. Novick, 26th FCS 1972, pp. 223-224.
[232] E. Beaty, et al, 13th FCS 1959, pp.668-675
[233] M Arditi and T. Carver, Phys. Rev. 124, No. 3, Nov. 1961, pp. 800-809.

[234] F. Gong, Y. Jau, and W. Happer, "Nonlinear Pressure Shifts of Alkali-Metal Atoms in Inert Gases", *Phys. Rev. Lett.*, Vol. 100, 233002, June 2008.

Relativity

[235] N. Ashby, “A Tutorial on Relativistic Effects in the Global Positioning System”, NIST Contract No. 40RANB9B8112, February 1990.
[236] P. Kline, “An Experimental Investigation of Relativistic Effects in GPS”, *Navigation*, Vol. 48, No. 4, pp. 297-305, Winter 1988-1999.
[237] N. Ashby, “Relativity and the Global Positioning System”, *Physics Today*, pp. 41-47, May 2002.

Crystal Oscillators

[238] J. R. Vig, “Quartz Crystal Resonators and Oscillators for Frequency Control and Timing Applications”, U.S. Army Communications-Electronics Command, Fort Monmouth, NJ 07703, USA, SLCET-TR-88-1 (Rev. 8.5.1.4), December 2001.

Baseplate Temperature Controllers

[239] PerkinElmer, Inc, “Improved Baseplate Temperature Controller (BTC) for GPS III RAFS”, July 2009.

Radiation Hardening

[240] T.M. Flanagan and R.E. Leadon, “Radiation Effects in Crystal and Atomic Frequency Standards”, *Proceedings of the 7th Annual Precise Time and Time Interval (PTTI) Applications and Planning Meeting*, Greenbelt, MD, pp. 125-135, December 1975.
[241] “Radiation hardening of EG&G Rb Frequency Standard”, *Final Report No. ED-7875*, U.S. Naval Research Laboratory, June 1982.
[242] J. Bell, “Radiation Tests on the GPS-RFS Silicon Photodetector”, EG&G Salem, September 10, 1982
[243] T. English, “Radiation Hardness of Efratom M-100 Rubidium Frequency Standard”, Proceedings of the 14th PTTI Meeting, December 1982, pp. 547-575.
[244] “Preliminary Test Report, Neutron Irradiation Test of EG&G # 316735 Silicon Photodetectors”, EG&G, Inc. Salem, MA 01970, April 26, 1984.
[245] T.C. English, G.L. Malley and R. Korde, “Neutron Hardness of Photodiodes for Use in Passive Rubidium Frequency Standards”, *Proceedings of the 42nd Frequency Control Symposium*, pp. 532-539, June 1988.
[246] M. Faltas, “Neutron Radiation Testing of uV444B Photodiodes, EG&G Canada, July 24, 1997.
[247] “Irradiation Report for MITRE-EGG”, Radiation Laboratory University of Massachusetts Lowell, December 1997.

[248] R. Tetreault, “Pre and Post-Radiation Test Data”, EG&G Canada, 1/20/98, and other related memos of 1/6/98, 1/7/98 and 1/16/98.
[249] W. Riley, “Rad Hardness of Si Photodiodes in RFS”, EG&G Salem, October 9, 1998.

Reliability

[250] MIL-HDBK-217F, Notice 2, “Military Handbook for Reliability Prediction of Electronic Equipment", February 1995.
[251] SR-332, Issue 2, Reliability Prediction Procedure for Electronic Equipment, Telcordia, September 2006.
[252] Telcordia (Bellcore) Reliability Prediction Software.

Standards

[253] MIL-O-55310B, “Military Specification, Oscillators, Crystal, General Specification For”, May 1988.
[254] IEEE Standard 1139-1988, “Standard Definitions of Physical Quantities for Fundamental Frequency and Time Metrology”.
[255] IEEE Standard 1139-1999, “IEEE Standard Definitions for Physical Quantities for Fundamental Frequency and Time Metrology – Random Instabilities”.
[256] IEEE Standard 1193-2000, “IEEE Guide for Measurement of Environmental Sensitivities of Standard Frequency Generators”.
[257] MIL-STD-461E, “Requirements for the Control of Electromagnetic Interference Characteristics of Subsystems and Equipment”.

Chip Scale Atomic Clocks

[258] R. Lutwak, D. Emmons, W. Riley, and R.M. Garvey, “The Chip-Scale Atomic Clock – Coherent Population Trapping vs. Conventional Interrogation”, *Proceedings of the 34th Annual Precise Time and Time Interval (PTTI) Systems and Applications Meeting*, December 3-5, 2002, Reston, VA, pp. 539-550.
[259] R. Lutwak, D. Emmons, T. English, W. Riley, A. Duwel, M. Varghese, D.K. Serkland and G.M. Peake, “The Chip-Scale Atomic Clock – Recent Development Progress”, *Proceedings of the 35th Annual Precise Time and Time Interval (PTTI) Systems and Applications Meeting*, December 2-4, 2003, San Diego, CA, pp. 467-478.
[260] R. Lutwak, J. Deng, W. Riley, M. Varghese, J. Leblanc, G. Tepolt, M. Mescher, D.K. Serkland, K.M. Geib and G.M. Peake, “The Chip-Scale Atomic Clock – Low-Power Physics Package”, *Proceedings of the 36th Annual Precise Time and Time Interval (PTTI) Systems and Applications Meeting*, December 7-9, 2004, Washington, DC, pp. 339-354.
[261] R. Lutwak, P. Vlitas, M. Varghese, M. Mescher, D.K Serkland and G.M. Peake, “The MAC – a Miniature Atomic Clock”, *Proceedings of the 2005*

IEEE International Frequency Control Symposium, Vancouver, BC, pp. 752-757, August 2005.
[262] R. Lutwak, A. Rashed, M. Varghese, G. Tepolt, J. Leblanc, M. Mescher, D.K. Serkland and G.M. Peake, “The Miniature Atomic Clock – Pre-Production Results”, *Proceedings of the 2007Joint Meeting of the European Frequency and Time Forum and the IEEE International Frequency Control Symposium*, Geneva, CH, pp. 1327-1333, May-June 2007.
[263] R. Lutwak, “The Chip-Scale Atomic Clock – Recent Developments”, *Proceedings of the 2009 IEEE International Frequency Control Symposium*, Besancon, FR, pp. 573-577, April 2009.

CPT Rubidium Clocks

[264] J. Deng, P. Vlitas, D. Taylor, L. Perletz and R. Lutwak, “A Commercial CPT Rubidium Clock”, *Proceedings of the 2008 European Frequency and Time Forum*, Toulouse, FR, April 2008.

Patents

[265] U.S. Patent No. 2,836,722, 05/27/1958, R.H. Dicke et al, “Atomic or Molecular Oscillator Circuit”.
[266] U.S. Patent No. 2,882,493, 04/14/1959, R.H. Dicke, “Gas Cells for Microwave Spectroscopy and Frequency Stabilization”.
[267] U.S. Patent No. 2,884,524, 04/28/1959, R.H. Dicke, “Method and System Employing Photon Absorption by a Microwave Resonant Medium”.
[268] U.S. Patent No. 2,927,278, 03/01/1960, R.H. Dicke, “Stable Oscillator”.
[269] U.S. Patent No. 2,951,992, 09/06/1960, M. Arditi, “Atomic Frequency Standard”.
[270] U.S. Patent No. 2,955,262, 10/04/1960, M. Arditi, “Gas Cell for Frequency Selective System”.
[271] U.S. Patent No. 2,975,330, 03/14/1961, A.L. Bloom, “Electrodeless Discharge Method and Apparatus”.
[272] U.S. Patent No. 3,038,126, 06/05/1962, P.C. Robison, “Tuning Arrangement Utilizing Optical Pumping”.
[273] U.S. Patent No. 3,071,721, 01/01/1963, H.G. Dehmelt, “Optical Absorption Monitoring of Oriented or Aligned Quantum Systems”.
[274] U.S. Patent No. 3,109,960, 11/05/1963, W.E. Bell et al, “Electrodeless Discharge Lamp Apparatus”.
[275] U.S. Patent No. 3,129,389, 04/14/1964, M.E. Packard et al, “Quantum Resonance Stabilized Frequency Source’.
[276] U.S. Patent No. 3,150,313, 09/22/1964, H.G. Dehmelt, “Modulation of a Light Beam by Absorbing Quantum Systems Exhibiting a Periodically Varying Alignment”.
[277] U.S. Patent No. 3,159,797, 12/01/1964, R.M. Whitehorn, “Atomic Frequency Standard”.
[278] U.S. Patent No. 3,165,705, 01/12/1965, R.H. Dicke, “Gas Cell Frequency Stabilization”.

[279] U.S. Patent No. 3,170,086, 02/16/1965, W.E. Bell, “Electrodeless Discharge Lamp Apparatus”.
[280] U.S. Patent No. 3,174,114, 03/16/1965, M. Arditi, “Atomic Clock”.
[281] U.S. Patent No. 3,187,251, 06/01/1965, W.E. Bell, “Quantum Oscillators’.
[282] U.S. Patent No. 3,192,472, 06/29/1965, P.L. Bender et al, “Alkali Vapor Frequency Standard Utilizing Optical Pumping”.
[283] U.S. Patent No. 3,196,312, 07/20/1965, W.A. Marrison, “Electrodeless Vapor Discharge Lamp with Auxiliary Voltage Triggering Means”.
[284] U.S. Patent No. 3,222,449, 12/07/1965, E.L. Garwin et al, “Magnetic Shield Arrangements”.
[285] 3,227,923 01/04/1966, W.A. Marrison, “Electrodeless Vapor Discharge Lamp with Auxiliary Radiation Triggering Means’.
[286] U.S. Patent No. 3,242,423, 03/22/1966, L. Malnar, ‘Resonance Cells for Optical Pumping’.
[287] U.S. Patent No. 3,246,254, 04/12/1966, W.E. Bell, “Atomic Stabilized Frequency Source’.
[288] U.S. Patent No. 3,248,666, 04/26/1966, D.J. Farmer, “Optically Pumped Combination Gas Cell and Microwave Resonating Cavity”.
[289] U.S. Patent No. 3,256,478, 06/14/1966, H.G. Dehmelt, “Optical Pumping of Hyperfine States by Light at the Zeeman Frequency”.
[290] U.S. Patent No. 3,267,360, 08/16/1966, H.G. Dehmelt, “Optical Absorption Monitoring of Aligned Alkali Atoms”.
[291] U.S. Patent No. 3,281,709, 10/25/1966, H.G. Dehmelt, “Apparatus for Optical Alignment and Detection of Atomic Energy States”.
[292] U.S. Patent No. 3,304,516, 02/14/1967, R. Novick et al, “Optically Pumped Atomic Resonance Apparatus with Improved Optical Pumping Means”.
[293] U.S. Patent No. 3,348,165, 10/17/1967, G.T. Inouye et al, “Gas Cell Frequency Standard”.
[294] U.S. Patent No. 3,363,193, 01/09/1968, J.T. Arnold, “Adjustable Frequency Atomic Frequency Standard”.
[295] U.S. Patent No. 3,364,438, 01/16/1968, R.J. Rorden, “Automatic Search Sweep for Atomic Frequency Standard”.
[296] U.S. Patent No. 3,382,452, 05/07/1968, R.C. Rempel et al, “Frequency Stabilization Apparatus”.
[297] U.S. Patent No. 3,388,339, 06/11/1968, L. Malnar et al, “Atomic Clocks with Spin Exchange Collision”.
[298] U.S. Patent No. 3,390,350, 06/25/1968, P. Davidovits et al, “Atomic Resonance Apparatus Utilizing an Improved Buffer Gas Cell”.
[299] U.S. Patent No. 3,403,349, 09/24/1968, I. Wieder, “Optically Pumped Maser and Solid State Light Source for Use Therein”.
[300] U.S. Patent No. 3,418,565, 12/24/1968, G. Broussaud et al, “Optical Resonance Cells”.
[301] U.S. Patent No. 3,510,758, 05/05/1970, G.R. Huggett, “Atomic Resonance Gas Cell having an Evacuated Double End Wall Structure”.
[302] U.S. Patent No. 3,513,381, 05/19/1970, W. Happer, Jr., “Off-Resonant Light as a Probe of Optically Pumped Alkali Vapors”.

[303] U.S. Patent No. 3,575,655, 04/20/1971, H.G. Dehmelt, "Apparatus for Optically Monitoring the Gyromagnetic Resonance of Quantum Systems".
[304] U.S. Patent No. 3,584,292, 06/08/1971, H.G. Dehmelt, "Apparatus for Optically Monitoring the Gyromagnetic Resonance of Quantum Systems".
[305] U.S. Patent No. 3,798,565, 12/14/1972, E. Jechart, "Gas Cell Atomic Frequency Standard of Compact Design".
[306] U.S. Patent No. 3,873,884, 02/11/1974, F.C. Gabriel, "Electrodeless Discharge Lamp and Power Coupler Therefor".
[307] U.S. Patent No. 3,903,481, 03/27/1974, E. Jechart, "Gas Cell Atomic frequency Standard Having Selected Alkali Vapor Isotopic Ratios".
[308] U.S. Patent No. 4,095,142, 06/13/1978, S. Murayama et al, "High Frequency Discharge Lamp for a Spectral Line Source".
[309] U.S. Patent No. 4,349,798, 09/14/1982, A. F. Podell et al, "Compact Microwave Resonant Cavity for Use in Atomic Frequency Standards".
[310] U.S. Patent No. 4,405,905, 09/20/1983, G. Busca et al, "Atomic Frequency Standard Having Microwave Loop Around Absorption Cell".
[311] U.S. Patent No. 4,434,406, 02/28/1984, W.R. Fowks, "Lamp Housing Assembly Primarily for the Lamp of a Rubidium Frequency Standard'.
[312] U.S. Patent No. 4,446,446, 05/01/1984, W.R. Fowks, "Programmable Frequency Synthesizer Primarily for Use in an Atomic Clock".
[313] U.S. Patent No. 4,456,891, 06/26/1984, W.R. Fowks, "Radio Frequency Source Circuit Primarily for Igniting the Lamp of a Rubidium Frequency Standard".
[314] U.S. Patent No. 4,462,006, 07/24/1984, W.R. Fowks, "Method for Stabilizing the Resonance Frequency of a Rubidium Frequency Standard".
[315] U.S. Patent No. 4,476,445, 10/09/1984, W.J. Riley, Jr., "Methods and Apparatus for Rapid and Accurate Frequency Syntonization of an Atomic Clock".
[316] U.S. Patent No. 4,485,333, 11/27/1984, S. Goldberg, "Vapor Discharge Lamp Assembly".
[317] U.S. Patent No. 4,494,085, 01/15/1985, S. Goldberg, "Miniaturized Atomic Frequency Standard Having Both Filter Cell and Absorption Cell in Resonator Cavity".
[318] U.S. Patent No. 4,495,478, 01/22/1985, T.M. Kwon et al, "Cavity Resonator for Atomic Frequency Standard'.
[319] U.S. Patent No. 4,661,782, 04/28/1987, W. Weidemann, "Integrated Microwave Cavity Resonator and Magnetic Shield for an Atomic Frequency Standard".
[320] U.S. Patent No. 4,692,716, 09/08/1987, A. De Marchi et al, "Method and a Device for the Frequency Control of an Atomic or Molecular Beam Frequency Standard".
[321] U.S. Patent No. 4,721,890, 01/26/1988, W.J. Riley, Jr., "Power Supply Circuit for an Alkali Vapor Spectral Lamp".
[322] U.S. Patent No. 4,953,148, 08/28/1990, A. Lepek et al, "Elimination of Magnetic Influence on Atomic Clocks".

[323] U.S. Patent No. 5,136,261, 08/04/1992, L. Lewis, "Saturated Absorption Double Resonance System and Apparatus".
[324] U.S. Patent No. 5,146,185, 09/08/1992, L. Lewis, "Compact Optically Pumped Resonance System and Apparatus".
[325] U.S. Patent No. 5,148,437, 09/15/1992, M. Ohtsu, "Laser Pumped Atomic Frequency Standard with High Frequency Stability".
[326] U.S. Patent No. 5,192,921, 03/09/1993, P.J. Chantry et al, "Miniaturized Atomic Frequency Standard".
[327] U.S. Patent No. 5,327,105, 07/05/1994, I. Liberman, "Gas Cell for a Miniaturized Atomic Frequency Standard".
[328] U.S. Patent No. 5,387,881, 02/07/1995, H.S. Schweda et al, "Atomic Frequency Standard".
[329] U.S. Patent No. 5,442,326, 08/15/1995, I. Liberman, "Atomic Time Standard with Piezoelectric Stabilization of Diode Laser Light Source'.
[330] U.S. Patent No. 5,457,430, 10/10/1995, T.C. English et al, "Method and Apparatus for Reduction of Light Intensity Decay in Optical Pumping Devices".
[331] U.S. Patent No. 5,489,821, 02/06/1996, J.D. Crockett, "Lamp Oscillator for Atomic Frequency Standards".
[332] U.S. Patent No. 5,491,451, 02/13/1996, T.C. English, "Method and Apparatus for Reduction of Atomic Frequency Standard Phase Noise".
[333] U.S. Patent No. 5,517,157, 05/14/1996, T.C. English, "Evanescent Field Interrogation for Atomic Frequency Standards".
[334] U.S. Patent No. 5,553,087, 09/03/1996, H.H. Telle, "Frequency Stabilized Laser Source".
[335] U.S. Patent No. 5,606,291, 02/25/1997, W.R. Verbanets, 'Miniature Atomic Frequency Standard Controlled by a Digital Processor'.
[336] U.S. Patent No. 5,627,497, 05/06/1997, G. Skoczen, 'Resonator Package for Atomic Frequency Standard'.
[337] U.S. Patent No. 5,656,189, 08/12/1997, J.D. Crockett et al, "Heater Controller for Atomic Frequency Standards".
[338] U.S. Patent No. 5,656,974, 08/12/1997, P. Thomann et al, "Atomic Frequency Oscillator".
[339] U.S. Patent No. 5,657,340, 08/12/1997, J.C. Camparo et al, "Rubidium Atomic Clock with Fluorescence Optical Pumping and Method Using Same".
[340] U.S. Patent No. 5,670,914, 09/23/1997, I. Liberman et al, "Miniature Atomic Frequency Standard".
[341] U.S. Patent No. 5,712,597, 01/27/1998, K. Atsumi et al, "Rubidium Atom Oscillator with Temperature Stabilized Frequency Output".
[342] U.S. Patent No. 5,714,910, 02/03/1998, G.L.Skoczen, "Methods and Apparatus for Digital Frequency Generation in Atomic Frequency Standards".
[343] U.S. Patent No. 5,721,514, 02/24/1998, J.D. Crockett et al, "Digital Frequency Generation in Atomic Frequency Standards Using Digital Phase Shifting".
[344] U.S. Patent No. 5,751,193, 05/12/1998, Y. Nakajima et al, "Rubidium Atomic Oscillator with Laser Diode Wavelength Adjustment".

[345] U.S. Patent No. 5,852,386, 12/22/1998, P.J. Chantry et al, "Apparatus and Method for Microwave Field Strength Stabilization in Cell Type Atomic Clocks".
[346] U.S. Patent No. 6,130,583, 10/10/2000, A. Stern et al, "Atomic Frequency Standard Using Digital Processing in its Frequency Lock Loop".
[347] U.S. Patent No. 6,133,800, 10/17/2000, J. Deng, "Subminiature Microwave Cavity".
[348] U.S. Patent No. 6,172,570, 01/09/2001, J. Deng, "Laser Light Quantum System".
[349] U.S. Patent No. 6,215,366, 04/10/2001, R.H. Kern, "Metallic Cell for Optically Activated Atomic Frequency Standards".
[350] U.S. Patent No. 6,225,870, 05/01/2001, G. Mei et al, "Miniaturized Microwave Cavity for Atomic Frequency Standard".
[351] U.S. Patent No. 6,255,647, 07/03/2001, J. Vanier, "Atomic Frequency Standard Based on Coherent State Preparation".
[352] U.S. Patent No. 6,265,945, 07/24/2001, M.J. Delaney et al, "Atomic Frequency Standard Based upon Coherent Population Trapping".
[353] U.S. Patent No. 6,426,679, 07/30/2002, T.A. Oblak et al, "Miniature Low Power Atomic Frequency Standard with Improved RF Frequency Synthesizer".

Frequency Stability

[354] W. Riley, *Handbook of Frequency Stability Analysis*, NIST Special Publication 1065, July 2008.

Tutorials

[355] L.S. Cutler, "Passive Atomic Frequency Standards", Tutorial at the 2002 IEEE International Frequency Control Symposium, New Orleans, LA, June 1, 2002.
[356] W.J. Riley, "Recent Trends in Rubidium Frequency Standard Technology", Tutorial at the 2002 Precise Time and Time Interval Meeting, Reston, VA, December 2, 2002.
[357] W.J. Riley, "Passive Atomic Frequency Standards", Tutorial at the 2006 IEEE International Frequency Control Symposium, Miami, FL, June 4, 2006.
[358] W. Riley, "Techniques for Frequency Stability Analysis", Tutorial at the IEEE International Frequency Control Symposium, May 2003.

Credits

It has been my pleasure to work on rubidium frequency standards with many outstanding colleagues in several organizations, including (but not only) Bill Cashin, Don Emmons, Tom English, Dick Frank, Mike Garvey, Sy Goldberg, Ken Kenschaft, Robert Lutwak, Tom Lynch, Ken Lyon, Herb Stratemeyer, John Vaccaro, and Jacques Vanier.

The material in this primer comes mainly from my personal archive of notes, papers, reports, tutorials, etc. from my work on rubidium frequency standards at General Radio/GenRad, EG&G and Datum/Symmetricom. Most of it has been previously published or otherwise distributed, and has been edited extensively for this book. Two of my tutorials from the 2002 PTTI meeting [356] and the 2006 Frequency Control Symposium [357] were major sources, as was briefing material I developed for intensive training sessions I conduct on this subject. Product photos come from their manufacturer or other undocumented web sources. Other material comes from sources either specifically referenced in the bibliography or credited in Table VII below.

I especially wish to thank David Howe of NIST for his thorough and thoughtful review of this primer; any remaining errors are mine alone.

Table VII. Miscellaneous Credits

Figure	Page	Content	Credit
-	Cover	Cover Photograph	Symmetricom, Inc.
1	5	Rb Ampoule Photograph	http://commons.wikimedia.org/wiki/File:RbH.JPG
20	22	Tanden Cell Cross-Section and Photo	EG&G Frequency Products (now Excelitas)
22	23	LPRO Cavity Photograph	Symmetricom, Inc.
23	24	Rb Lamp Photograph	PerkinElmer (now Excelitas)
25	27	RFS Cutaway Photograph	Temex (now Spectratime)
29	36	Rb Cells Photograph	Corby Dawson: http://www.leapsecond.com/pages/rb-c
33	41	Pulling Off Lamps Photo	EG&G *Monitor*, Issue No. 5, 1982
37	50	Photodiode Responsivity	Wikipedia web site: http://en.wikipedia.org/wiki/Photodiode
76	99	RFS Stability with GPS Receiver Plot	Stanford Research web site (PRS-10)
79-81	112-118	Product Gallery Photos	Product manufacturers and as noted below
79	112	V-4700A Photo & Dwg	Varian Associates instruction manual
79	112	General Technology 304-B Photograph	http://www.physics.uq.edu.au/physics_museum/tour/metrology.html
		Tracor 304B Drawing	Tracor service manual
83	119	Miniature Cs Resonator	Northrop-Grumman
84	120	SA.45s CSAC	Symmetricom, Inc.

Index

NOTES